arXiv:1408.0376v3 [physics.flu-dyn] 16 Apr 2016

Multi-scale turbulence modeling and maximum information principle. Part 3

L. Tao*

We investigate three-dimensional homogeneous shear turbulence within the framework of optimal control and optimization. In the physical and Fourier wave-number spaces, three models are formulated in detail or outlined: The first is the second-order model in which the second order correlation components are the state variables and certain linear combinations of the degenerated third order correlation components act as the control variables; The second is the third-order model with the second order correlation as the state variables and the degenerated third order correlation as the control variables; The third is the fourth-order model containing the correlations up to the fourth order with the degenerated fourth order correlation as the control variables. The sources of the constraints are discussed. The models take the turbulent energy per unit volume as the objective function to be maximized and are argued as the second-order cone programming problems in their discretized forms. The advantages and disadvantages of the models are addressed. It is proved that the non-negativity of turbulent energy spectra guarantees the satisfaction of the constraints for the second order correlation in the physical space that are constructed by the application of the Cauchy-Schwarz inequality to the correlation and the structure functions. The study focuses on the asymptotic states characterized by the dimensionless exponential time rate of growth σ; The rate has the upper bound of $\max \sigma = 0$, required by the variance of products being non-negative, which is more restrictive than those suggested by some experimental data. The optimal asymptotic state solution of the second-order model under $\sigma = 0$ has been obtained numerically and the predicted value of the anisotropy tensor is much more anisotropic than the experimental, which may be attributed to the model's incapacity to include constraints involving pressure fluctuations. This anisotropy is expected to be reduced in the third-order model, since the model includes the fluctuation pressure-velocity correlation constraint $\overline{q(\mathbf{x})\, w_{k,k}(\mathbf{y})} = 0$ which supposedly plays the role of redistributing energy among the diagonal components of the Reynolds stress tensor and making turbulent fluctuations more isotropic. The numerical simulation of the asymptotic state solution of the third-order model is under way.

1 Introduction

To test the multi-scale turbulence modeling framework proposed in [13], we have applied it to the two-dimensional homogeneous shear turbulence [14] (referred to as PART II hereafter)

*Department of Aerospace Engineering, Indian Institute of Technology Madras, Chennai 600 036, India. Email: luoyitao@iitm.ac.in; taoluoyi@gmail.com

and obtained certain analytical results. The focus of that study is to better understand mathematical and computational issues involved. One major limitation of the study is the assumed two-dimensionality of fluctuations against the three-dimensional nature of physical turbulence. In the present work, we remove this restriction by studying the problem of three-dimensional homogeneous shear turbulence.

To determine the possible internal structure of three-dimensional homogeneous shear turbulence, we start with the intrinsic mathematical relations resulting from the Navier-Stokes equations and the ensemble average operation itself. These relations concern the dynamical equations of evolution for the multi-point correlations up to the third order and the constraints of equality and inequality for the multi-point correlations up to the fourth order. The equations of evolution are derived as conventionally done. The equality constraints come from the self-consistency of the definition of the correlations and the divergence-free fluctuating velocity field because of the supposed incompressibility. The constraints of inequality are constructed on the basis of the following considerations. The first comes from the positive semi-definiteness of the Reynolds stress tensor, the non-negativity of the viscous dissipation and so on, as the realizability conditions. The second comes from the application of the Cauchy-Schwarz inequality to the correlations and the structure functions up to the fourth order in the physical space. The third is from the requirement of the non-negativity of the variance of products, applied to the second order correlation and the related structure functions. The fourth is from the non-negativity of the turbulent energy spectra. These inequalities are, to a large extent, neglected by or even unenforcible within the conventional schemes of turbulence modeling, except the limited implementation of realizability. We include and impose these relations through an optimal control scheme with the turbulent energy per unit volume as the objective function to be maximized; Such a scheme has the capacity to satisfy the intrinsic constraints without any parameters to be fitted, except the objective function itself introduced externally. If this strategy can be demonstrated to provide reasonable predictions against the experimental, it may be applicable, in principle, to the turbulence of some other fluids.

Taking into account the complexity of the flow problem and the exploratory nature of the present work, we discuss three models of low orders and formulate them in the physical and the Fourier wave-number spaces. Being the simplest, the second-order model takes the second order correlation as the state variables and three linear combinations of the spatially degenerated third order correlation components as the control variables; the forms of the combinations are dictated by the structures of the primary dynamical equations of evolution for the second order correlation. As implied by the control variables taken, this model cannot account for any constraints related to the pressure fluctuations, it can reveal, however, the direct impact of the mean sharing on the turbulent energy distributions among the diagonal components of the Reynolds stress tensor $U_{ij}(\mathbf{0})$, as indicated by the numerical results obtained. Also, the model provides us an easier way to test numerically whether the strategy of turbulence modeling through optimal controls can produce sensible results. As a straight-forward extension of the the second-order model, the third-order model takes the second order correlation as the state variables and the degenerated third order correlation as the control variables. Relatively speaking, this model has two advantages: (i) it satisfies the divergence-free condition for the lowest order correlation involving the pressure fluctuations, $\overline{q(\mathbf{x})\, w_{k,k}(\mathbf{y})} = 0$, which supposedly plays the role of redistributing the energy among the diagonal components of $U_{ij}(\mathbf{0})$; (ii) it is computationally feasible at present, though more demanding than the second-order model.

Both the second-order and the third-order models can accommodate the constraints produced by the application of the Cauchy-Schwarz inequality to the second order correlation and the related structure functions, they cannot, however, deal with the variance of products, which makes them inapplicable to the transient states of the turbulence concerned, as to be shown.

The fourth-order model contains the correlations up to the fourth order, with the spatially degenerated fourth order correlation as the control variables. It extends the second-order and the third-order models; It can resolve the lower order correlations involving pressure fluctuations and it can satisfy the constraints for the third and fourth order correlations produced by the Cauchy-Schwarz inequality and the lowest order inequalities produced by the variance of products being non-negative. The challenge is how to make it computationally feasible, since the model involves a tremendously great number of variables and constraints and the higher dimensional integrals, when discretized.

A few main and specific results of the present work obtained so far are summarized and commented below.

We argue that, if discretized, the three models are essentially the second-order cone programming (SOCP) problems. Consequently, we can take advantage of the SOCP theory and especially the software packages 'CVX' and 'MOSEK' ([4], [6]) to find numerical solutions. With the help of the packages, we have solved the second-order model, and we will carry out the simulation for the third-order model. In the case of the fourth-order model, more studies and developments may be needed in order to see whether it is computationally feasible at present, both from the aspect of algorithms and from the aspect of computer resources. In order to obtain explicit representations of the state variables and the relations in terms of the control variables as done in the theory of optimization, we formulate the models in the Fourier wave-number spaces. Additionally, such a formulation makes it possible to use a small set of inequalities in the wave-number space to replace many constraints of inequality in the physical space for the second order correlations related to the fluctuation fields of velocity, velocity gradient, vorticity and so on. The negative impact of such a formulation is the introduction of higher dimensional integrations and the necessity to compute them numerically. We use the open source code 'CUBA' ([7], [8], [9]) to accomplish the task of integration, which is computationally time-consuming for finer meshes. It is yet to be studied whether the SOCP problems can be formulated in the physical space in a computationally feasible fashion so as to bypass such higher dimensional integrations.

On the basis of the Cauchy-Schwarz inequality, a great number of constraints of inequality can be generated for the second order correlation in the physical space. These constraints involve the fluctuating velocity, velocity gradient and vorticity fields, in the forms of the simple correlations and the structure functions. We demonstrate the existence of six elementary inequalities in the wave-number space that are sufficient for the satisfaction of all these constraints in the physical space; The basis for the elementary inequalities is the supposed non-negativity of the turbulent energy spectra along the axes of the wave-number space. This result reduces greatly the complexity and makes many higher-dimensional integrals unnecessary in the determination of the optimal solutions. The question unsolved is whether such reductions are possible for the constraints involving the third and fourth order correlations.

There is a specific consequence of the constraints of inequality from the variance of products being non-negative. These variance constraints have the mathematical form of $\overline{XXYY} \geq \left(\overline{XY}\right)^2$, where X and Y represent the velocity and pressure fluctuations, their spatial deriva-

tives, their products or linear combinations, etc. It then follows that the second-order and the third-order models cannot take into account any such constraints, while the fourth-order model can include such constraints of the lowest order. In the case of the asymptotic states, we have $\psi = \psi^{(\infty)} \exp(\sigma t)$ with ψ representing any correlation and $\psi^{(\infty)}$ the part of ψ independent of time, the time-dependent form of $\exp(\sigma t)$ common to all the correlations in the models reflects both the mean shearing and the linear structures of the evolution equations, the value of σ denotes the exponential growth rate. The combination of both the variance constraints and the asymptotic form gives that $\sigma \leq 0$. We notice that this upper bound value of $\max \sigma = 0$ is more restrictive than those suggested by some experiments (where $\sigma > 0$ is inferred in some cases) (see the summaries in [11], [12]). Next, the enforceability of such variance inequalities in the fourth-order model expectedly leads to the natural emergence of an asymptotic state of $\sigma \leq 0$ out of a transient state within the model. However, for the second-order and the third-order models, such constraints are not enforceable, this causes the possibility that the models allow asymptotic state solutions of $\sigma > 0$ to occur. We show analytically that $\sigma < 1$ holds within the two models. For the second-order model, we have obtained numerically feasible solutions of σ slightly larger than zero. Therefore, the second-order and the third-order models should not be applied to the transient states of the homogeneous shear turbulence, they should be restricted to the asymptotic states where the specific values of $\sigma \leq 0$ can be imposed directly. For an inhomogeneous turbulent flow, if generalized appropriately, the second-order and the third-order models themselves may guarantee $\sigma \leq 0$ and produce steady state solutions, caused by the nonlinear two-way coupling between the averaged Navier-Stokes equations and the differential equations for the evolution of $\overline{w_i(\mathbf{x}) w_j(\mathbf{y})}$. In the special case of homogeneous shear turbulence, this two-way coupling degenerates into one-way and the differential equations for the correlation become linear since the mean velocity and pressure field is supposedly fixed.

As a preliminary test of the present optimal control framework for turbulence modeling, we have obtained numerically the optimal asymptotic state solution of the second-order model under $\sigma = 0$. Regarding the values of the anisotropy tensor $b_{ij}^{(\infty)}$, certain comparisons can be made between the theoretical and the experimental. First, for the non-trivial off-diagonal component, $b_{12}^{(\infty)} = -0.164$ (Theory) is compatible with $b_{12}^{(\infty)} = -0.156$ (Experiment). Second, the numerical order of the diagonal components is the same, $b_{11}^{(\infty)} = 0.364 > b_{33}^{(\infty)} = -0.126 > b_{22}^{(\infty)} = -0.238$ (Theory) against $b_{11}^{(\infty)} = 0.203 > b_{33}^{(\infty)} = -0.06 > b_{22}^{(\infty)} = -0.143$ (Experiment). The predicted values are much more anisotropic than the experimental, and this difference reflects the intrinsic inadequacy of the second-order model itself — the model may account for the effect of the mean shearing on the distributions among the diagonal components of the Reynolds stress $U_{ij}(\mathbf{0})$, it does not enforce any constraint involving the pressure fluctuations, especially the constraint of $\overline{q(\mathbf{x})\, w_{k,k}(\mathbf{y})} = 0$ which supposedly plays the role of redistributing the energy among the diagonal components of $U_{ij}(\mathbf{0})$ and making the turbulent fluctuations more isotropic. We then infer that the third-order model may improve the prediction against the experimental data since it takes into account this very constraint of equality, and the numerical simulation of the model is under way in order to examine the issue further.

The present report is organized as follows. In Section 2, we develop the differential and integro-differential equations, the constraints of equality and inequality and the objective function in the physical and Fourier wave-number spaces for the turbulence concerned. We also define the second-order, the third-order and the fourth-order models. In Section 3, without

enforcing the maximization of the objective function and the constraints, we present the formal solutions of the primary integro-differential equations for the asymptotic states; these formal solutions simplify the setup of the optimization problems. The upper bound for the exponential growth rate, $\max \sigma = 0$, is obtained with the help of the variance constraints. Also, discussed are certain limits for the correlations. In Section 4, we focus on the asymptotic states of the second-order model whose discretized solutions are shown to be a SOCP problem. The discretized third-order and the fourth-order models are argued as SOCP problems too. The other upper bound for the exponential growth rate is obtained on the basis of the constraints within the second-order model (and the third-order model). The finite support estimates are obtained for the control and the state variables, and these results provide a valuable ground for the numerical simulations. We then discuss and implement the numerical scheme and carry out the simulations of both feasible and optimal solutions within the second-order model. Detailed information is presented about the discretization, the computational schemes and the software packages. Also, presented are the numerical results of a feasible solution and certain dimensionless quantities of an optimal solution that can be evaluated against the experimental data.

2 Basic Formulation

Let us consider homogeneous shear turbulence in $\mathbb{R}^3$ with the mean velocity field of

$$V_i = \delta_{i1}\, S\, x_2 \tag{2.1}$$

where δ_{ij} is the Kronecker delta and S is a nontrivial positive constant. The fluctuation fields of velocity $w_i(\mathbf{x}, t)$ and scaled pressure $q(\mathbf{x}, t) := p(\mathbf{x}, t)/\rho$ are governed by

$$\frac{\partial w_k}{\partial x_k} = 0 \tag{2.2}$$

$$\frac{\partial w_i}{\partial t} + S\, x_2\, \frac{\partial w_i}{\partial x_1} + S\, \delta_{i1} w_2 + \frac{\partial (w_i\, w_k)}{\partial x_k} = -\frac{\partial q}{\partial x_i} + \nu\, \frac{\partial^2 w_i}{\partial x_k \partial x_k} \tag{2.3}$$

and

$$\frac{\partial^2 q}{\partial x_k \partial x_k} = -2\, S\, \frac{\partial w_2}{\partial x_1} - \frac{\partial^2 (w_l\, w_k)}{\partial x_k \partial x_l} \tag{2.4}$$

which can be easily derived from the Navier-Stokes equations for incompressible flows under (2.1). Next, we introduce the dimensionless quantities (indicated by the accent $'$) through

$$t = \frac{t'}{S}, \quad x_i = \left(\frac{\nu}{S}\right)^{1/2} x_i', \quad w_i = (\nu\, S)^{1/2}\, w_i', \quad q = \nu\, S\, q' \tag{2.5}$$

and non-dimensionalize the above equations of motion to obtain

$$\frac{\partial w_k}{\partial x_k} = 0 \tag{2.6}$$

$$\frac{\partial w_i}{\partial t} + x_2 \frac{\partial w_i}{\partial x_1} + \delta_{i1} w_2 + \frac{\partial (w_i\, w_k)}{\partial x_k} = -\frac{\partial q}{\partial x_i} + \frac{\partial^2 w_i}{\partial x_k \partial x_k} \tag{2.7}$$

and

$$\frac{\partial^2 q}{\partial x_k \partial x_k} = -2 \frac{\partial w_2}{\partial x_1} - \frac{\partial^2 (w_l\, w_k)}{\partial x_k \partial x_l} \tag{2.8}$$

Here, we have removed the accent $'$ for the sake of brevity.

2.1 Homogeneity

To simplify the mathematical treatment, we adopt the conventional supposition of homogeneity. To this end, we construct, on the basis of (2.6) through (2.8), the following equations for the evolution of the multi-point correlations up to the third/fourth order,

$$\begin{aligned}
&\frac{\partial}{\partial x_k} \overline{w_k(\mathbf{x}) w_j(\mathbf{y})} = 0, \quad \frac{\partial}{\partial x_k} \overline{w_k(\mathbf{x}) w_j(\mathbf{y}) w_l(\mathbf{z})} = 0, \quad \frac{\partial}{\partial y_k} \overline{w_i(\mathbf{x}) w_j(\mathbf{x}) w_k(\mathbf{y}) w_l(\mathbf{z})} = 0, \\
&\frac{\partial}{\partial y_k} \overline{q(\mathbf{x}) w_k(\mathbf{y})} = 0, \quad \frac{\partial}{\partial y_k} \overline{q(\mathbf{x}) w_k(\mathbf{y}) w_l(\mathbf{z})} = 0
\end{aligned} \tag{2.9}$$

$$\begin{aligned}
&\frac{\partial}{\partial t} \overline{w_i(\mathbf{x}) w_j(\mathbf{y})} + \left(x_2 \frac{\partial}{\partial x_1} + y_2 \frac{\partial}{\partial y_1} \right) \overline{w_i(\mathbf{x}) w_j(\mathbf{y})} + \delta_{i1} \overline{w_2(\mathbf{x}) w_j(\mathbf{y})} \\
&\quad + \delta_{j1} \overline{w_i(\mathbf{x}) w_2(\mathbf{y})} + \frac{\partial}{\partial x_k} \overline{w_i(\mathbf{x}) w_k(\mathbf{x}) w_j(\mathbf{y})} + \frac{\partial}{\partial y_k} \overline{w_i(\mathbf{x}) w_k(\mathbf{y}) w_j(\mathbf{y})} \\
&= -\frac{\partial}{\partial x_i} \overline{q(\mathbf{x}) w_j(\mathbf{y})} - \frac{\partial}{\partial y_j} \overline{w_i(\mathbf{x}) q(\mathbf{y})} + \left(\frac{\partial^2}{\partial x_k \partial x_k} + \frac{\partial^2}{\partial y_k \partial y_k} \right) \overline{w_i(\mathbf{x}) w_j(\mathbf{y})}
\end{aligned} \tag{2.10}$$

$$\begin{aligned}
&\frac{\partial}{\partial t} \overline{w_i(\mathbf{x}) w_j(\mathbf{y}) w_k(\mathbf{z})} + x_2 \frac{\partial}{\partial x_1} \overline{w_i(\mathbf{x}) w_j(\mathbf{y}) w_k(\mathbf{z})} + y_2 \frac{\partial}{\partial y_1} \overline{w_j(\mathbf{y}) w_i(\mathbf{x}) w_k(\mathbf{z})} \\
&+ z_2 \frac{\partial}{\partial z_1} \overline{w_i(\mathbf{x}) w_j(\mathbf{y}) w_k(\mathbf{z})} + \delta_{i1} \overline{w_2(\mathbf{x}) w_j(\mathbf{y}) w_k(\mathbf{z})} + \delta_{j1} \overline{w_2(\mathbf{y}) w_i(\mathbf{x}) w_k(\mathbf{z})} \\
&+ \delta_{k1} \overline{w_i(\mathbf{x}) w_j(\mathbf{y}) w_2(\mathbf{z})} + \frac{\partial}{\partial x_l} \overline{w_i(\mathbf{x}) w_l(\mathbf{x}) w_j(\mathbf{y}) w_k(\mathbf{z})} + \frac{\partial}{\partial y_l} \overline{w_j(\mathbf{y}) w_l(\mathbf{y}) w_i(\mathbf{x}) w_k(\mathbf{z})} \\
&+ \frac{\partial}{\partial z_l} \overline{w_k(\mathbf{z}) w_l(\mathbf{z}) w_i(\mathbf{x}) w_j(\mathbf{y})} = -\frac{\partial}{\partial x_i} \overline{q(\mathbf{x}) w_j(\mathbf{y}) w_k(\mathbf{z})} - \frac{\partial}{\partial y_j} \overline{q(\mathbf{y}) w_i(\mathbf{x}) w_k(\mathbf{z})} \\
&- \frac{\partial}{\partial z_k} \overline{q(\mathbf{z}) w_i(\mathbf{x}) w_j(\mathbf{y})} + \left(\frac{\partial^2}{\partial x_l \partial x_l} + \frac{\partial^2}{\partial y_l \partial y_l} + \frac{\partial^2}{\partial z_l \partial z_l} \right) \overline{w_i(\mathbf{x}) w_j(\mathbf{y}) w_k(\mathbf{z})}
\end{aligned} \tag{2.11}$$

$$\frac{\partial^2}{\partial x_k \partial x_k} \overline{q(\mathbf{x}) w_j(\mathbf{y})} = -2 \frac{\partial}{\partial x_1} \overline{w_2(\mathbf{x}) w_j(\mathbf{y})} - \frac{\partial^2}{\partial x_k \partial x_l} \overline{w_l(\mathbf{x}) w_k(\mathbf{x}) w_j(\mathbf{y})} \tag{2.12}$$

$$\frac{\partial^2}{\partial x_l \partial x_l}\overline{q(\mathbf{x})w_j(\mathbf{y})w_k(\mathbf{z})} = -2\,\frac{\partial}{\partial x_1}\overline{w_2(\mathbf{x})w_j(\mathbf{y})w_k(\mathbf{z})} - \frac{\partial^2}{\partial x_m \partial x_l}\overline{w_l(\mathbf{x})w_m(\mathbf{x})w_j(\mathbf{y})w_k(\mathbf{z})} \quad (2.13)$$

and

$$\frac{\partial^2}{\partial y_k \partial y_k}\overline{q(\mathbf{x})\,q(\mathbf{y})} = -2\,\frac{\partial}{\partial y_1}\overline{q(\mathbf{x})w_2(\mathbf{y})} - \frac{\partial^2}{\partial y_k \partial y_l}\overline{q(\mathbf{x})w_k(\mathbf{y})w_l(\mathbf{y})} \quad (2.14)$$

On the basis of the supposed homogeneity, we define

$$\begin{aligned}
&\overline{w_i(\mathbf{x})w_j(\mathbf{y})} = \overline{w_i(\mathbf{0})w_j(\mathbf{y}-\mathbf{x})} =: U_{ij}(\mathbf{r}), \quad \overline{w_i(\mathbf{x})w_j(\mathbf{x})w_k(\mathbf{y})} = \overline{w_i(\mathbf{0})w_j(\mathbf{0})w_k(\mathbf{r})} =: U_{(ij)k}(\mathbf{r}),\\
&\overline{w_i(\mathbf{x})w_j(\mathbf{y})w_k(\mathbf{z})} = \overline{w_i(\mathbf{0})w_j(\mathbf{r})w_k(\mathbf{s})} =: U_{ijk}(\mathbf{r},\mathbf{s}),\\
&\overline{w_i(\mathbf{x})w_j(\mathbf{x})w_k(\mathbf{y})w_l(\mathbf{z})} = \overline{w_i(\mathbf{0})w_j(\mathbf{0})w_k(\mathbf{r})w_l(\mathbf{s})} =: U_{(ij)kl}(\mathbf{r},\mathbf{s}), \quad \overline{q(\mathbf{x})\,q(\mathbf{y})} = \overline{q(\mathbf{0})\,q(\mathbf{r})} =: Q(\mathbf{r}),\\
&\overline{q(\mathbf{x})w_j(\mathbf{y})} = \overline{q(\mathbf{0})w_j(\mathbf{r})} =: Q_j(\mathbf{r}), \quad \overline{q(\mathbf{x})w_j(\mathbf{y})w_k(\mathbf{z})} = \overline{q(\mathbf{0})w_j(\mathbf{r})w_k(\mathbf{s})} =: Q_{jk}(\mathbf{r},\mathbf{s}) \qquad (2.15)
\end{aligned}$$

where $\mathbf{r} := \mathbf{y} - \mathbf{x}$ and $\mathbf{s} := \mathbf{z} - \mathbf{x}$. The dependence of the correlations on t is suppressed for the sake of brevity. For the third order correlation, we have adopted both the general and the spatially degenerated for the purpose to construct different models. Instead of the general fourth order correlation $\overline{w_i(\mathbf{x})w_j(\mathbf{y})w_k(\mathbf{z})w_l(\mathbf{z}')}$, the restriction to the spatially degenerated $\overline{w_i(\mathbf{x})w_j(\mathbf{x})w_k(\mathbf{y})w_l(\mathbf{z})}$ is motivated by the latter's involvement in (2.11) and (2.13), which results in less complexity in analysis and computation. Substitution of (2.15) into (2.9) through (2.14) results in

$$\begin{aligned}
&\frac{\partial}{\partial r_k}U_{kj}(\mathbf{r}) = \frac{\partial}{\partial r_j}U_{kj}(\mathbf{r}) = 0, \quad \frac{\partial}{\partial r_k}U_{(ij)k}(\mathbf{r}) = 0,\\
&\left(\frac{\partial}{\partial r_k} + \frac{\partial}{\partial s_k}\right)U_{kjl}(\mathbf{r},\mathbf{s}) = \frac{\partial}{\partial r_j}U_{kjl}(\mathbf{r},\mathbf{s}) = \frac{\partial}{\partial s_l}U_{kjl}(\mathbf{r},\mathbf{s}) = 0,\\
&\frac{\partial}{\partial r_k}U_{(ij)kl}(\mathbf{r},\mathbf{s}) = \frac{\partial}{\partial s_l}U_{(ij)kl}(\mathbf{r},\mathbf{s}) = 0, \quad \frac{\partial}{\partial r_k}Q_k(\mathbf{r}) = 0, \quad \frac{\partial}{\partial r_k}Q_{kl}(\mathbf{r},\mathbf{s}) = \frac{\partial}{\partial s_l}Q_{kl}(\mathbf{r},\mathbf{s}) = 0 \qquad (2.16)
\end{aligned}$$

$$\begin{aligned}
&\frac{\partial}{\partial t}U_{ij}(\mathbf{r}) + r_2\frac{\partial}{\partial r_1}U_{ij}(\mathbf{r}) + \delta_{i1}U_{2j}(\mathbf{r}) + \delta_{j1}U_{i2}(\mathbf{r}) - \frac{\partial}{\partial r_k}U_{(ik)j}(\mathbf{r}) + \frac{\partial}{\partial r_k}U_{(jk)i}(-\mathbf{r})\\
&= \frac{\partial}{\partial r_i}Q_j(\mathbf{r}) - \frac{\partial}{\partial r_j}Q_i(-\mathbf{r}) + 2\,\frac{\partial^2}{\partial r_k \partial r_k}U_{ij}(\mathbf{r}) \qquad (2.17)
\end{aligned}$$

$$\begin{aligned}
&\frac{\partial}{\partial t}U_{ij}(\mathbf{r}) + r_2\frac{\partial}{\partial r_1}U_{ij}(\mathbf{r}) + \delta_{i1}U_{2j}(\mathbf{r}) + \delta_{j1}U_{i2}(\mathbf{r}) - \frac{\partial}{\partial r_k}U_{ikj}(\mathbf{0},\mathbf{r}) + \frac{\partial}{\partial r_k}U_{jki}(\mathbf{0},-\mathbf{r})\\
&= \frac{\partial}{\partial r_i}Q_j(\mathbf{r}) - \frac{\partial}{\partial r_j}Q_i(-\mathbf{r}) + 2\frac{\partial^2}{\partial r_k \partial r_k}U_{ij}(\mathbf{r}) \qquad (2.18)
\end{aligned}$$

$$\frac{\partial}{\partial t}U_{ijk}(\mathbf{r},\mathbf{s}) + r_2\frac{\partial}{\partial r_1}U_{ijk}(\mathbf{r},\mathbf{s}) + s_2\frac{\partial}{\partial s_1}U_{ijk}(\mathbf{r},\mathbf{s}) + \delta_{i1}U_{2jk}(\mathbf{r},\mathbf{s}) + \delta_{j1}U_{i2k}(\mathbf{r},\mathbf{s}) + \delta_{k1}U_{ij2}(\mathbf{r},\mathbf{s})$$

$$
\begin{aligned}
&-\left(\frac{\partial}{\partial r_l}+\frac{\partial}{\partial s_l}\right)U_{(il)jk}(\mathbf{r},\mathbf{s})+\frac{\partial}{\partial r_l}U_{(jl)ik}(-\mathbf{r},\mathbf{s}-\mathbf{r})+\frac{\partial}{\partial s_l}U_{(kl)ij}(-\mathbf{s},\mathbf{r}-\mathbf{s})\\
&=\frac{\partial}{\partial r_i}Q_{jk}(\mathbf{r},\mathbf{s})+\frac{\partial}{\partial s_i}Q_{jk}(\mathbf{r},\mathbf{s})-\frac{\partial}{\partial r_j}Q_{ik}(-\mathbf{r},\mathbf{s}-\mathbf{r})-\frac{\partial}{\partial s_k}Q_{ij}(-\mathbf{s},\mathbf{r}-\mathbf{s})\\
&\quad+2\left(\frac{\partial^2}{\partial r_l\partial r_l}+\frac{\partial^2}{\partial s_l\partial s_l}+\frac{\partial^2}{\partial r_l\partial s_l}\right)U_{ijk}(\mathbf{r},\mathbf{s})
\end{aligned}
\tag{2.19}
$$

$$
\frac{\partial^2}{\partial r_k\partial r_k}Q_j(\mathbf{r})=2\,\frac{\partial}{\partial r_1}U_{2j}(\mathbf{r})-\frac{\partial^2}{\partial r_k\partial r_l}U_{(lk)j}(\mathbf{r})
\tag{2.20}
$$

$$
\frac{\partial^2}{\partial r_k\partial r_k}Q_j(\mathbf{r})=2\frac{\partial}{\partial r_1}U_{2j}(\mathbf{r})-\frac{\partial^2}{\partial r_k\partial r_l}U_{lkj}(\mathbf{0},\mathbf{r})
\tag{2.21}
$$

$$
\begin{aligned}
&\left(\frac{\partial}{\partial r_l}+\frac{\partial}{\partial s_l}\right)\left(\frac{\partial}{\partial r_l}+\frac{\partial}{\partial s_l}\right)Q_{jk}(\mathbf{r},\mathbf{s})\\
&=2\left(\frac{\partial}{\partial r_1}+\frac{\partial}{\partial s_1}\right)U_{2jk}(\mathbf{r},\mathbf{s})-\left(\frac{\partial}{\partial r_m}+\frac{\partial}{\partial s_m}\right)\left(\frac{\partial}{\partial r_l}+\frac{\partial}{\partial s_l}\right)U_{(lm)jk}(\mathbf{r},\mathbf{s})
\end{aligned}
\tag{2.22}
$$

and

$$
\frac{\partial^2}{\partial r_k\partial r_k}Q(\mathbf{r})=-2\frac{\partial}{\partial r_1}Q_2(\mathbf{r})-\frac{\partial^2}{\partial r_k\partial r_l}Q_{kl}(\mathbf{r},\mathbf{r})
\tag{2.23}
$$

To ensure the self-consistency, the definitions of (2.15) themselves require the following symmetric relations of

$$
\begin{aligned}
&U_{ij}(\mathbf{r})=U_{ji}(-\mathbf{r}),\quad U_{(ij)k}(\mathbf{r})=U_{(ji)k}(\mathbf{r}),\quad U_{(ij)k}(\mathbf{0})\ \text{ invariant under permutation of } \{i,j,k\},\\
&U_{ijk}(\mathbf{r},\mathbf{s})=U_{ikj}(\mathbf{s},\mathbf{r})=U_{jik}(-\mathbf{r},\mathbf{s}-\mathbf{r})=U_{kij}(-\mathbf{s},\mathbf{r}-\mathbf{s}),\\
&U_{(ij)kl}(\mathbf{r},\mathbf{s})=U_{(ji)kl}(\mathbf{r},\mathbf{s})=U_{(ij)lk}(\mathbf{s},\mathbf{r}),\quad U_{(ij)kl}(\mathbf{r},\mathbf{r})=U_{(kl)ij}(-\mathbf{r},-\mathbf{r}),\\
&U_{(ij)kl}(\mathbf{0},\mathbf{r})=U_{(ik)jl}(\mathbf{0},\mathbf{r}),\quad U_{(ij)kl}(\mathbf{0},\mathbf{0})\ \text{ invariant under permutation of } \{i,j,k,l\},\\
&Q(\mathbf{r})=Q(-\mathbf{r}),\quad Q_{jk}(\mathbf{r},\mathbf{s})=Q_{kj}(\mathbf{s},\mathbf{r})
\end{aligned}
\tag{2.24}
$$

Additionally, based on the geometric and kinematic symmetries of the mean flow field (2.1), we consider the fluctuation velocities and pressures at points $\mathbf{x}$, $\mathbf{y}$, $\mathbf{z}$ and their inversions $-\mathbf{x}$, $-\mathbf{y}$, $-\mathbf{z}$. It is sensible to assume that statistically the following equalities hold,

$$
\begin{aligned}
&\overline{w_i(\mathbf{x})w_j(\mathbf{y})}=\overline{(-w_i(-\mathbf{x}))\,(-w_j(-\mathbf{y}))},\quad \overline{w_i(\mathbf{x})w_j(\mathbf{y})w_k(\mathbf{z})}=\overline{(-w_i(-\mathbf{x}))\,(-w_j(-\mathbf{y}))\,(-w_k(-\mathbf{z}))},\\
&\overline{w_i(\mathbf{x})w_j(\mathbf{x})w_k(\mathbf{y})w_l(\mathbf{z})}=\overline{(-w_i(-\mathbf{x}))\,(-w_j(-\mathbf{x}))\,(-w_k(-\mathbf{y}))\,(-w_l(-\mathbf{z}))},\\
&\overline{q(\mathbf{x})q(\mathbf{y})}=\overline{q(-\mathbf{x})q(-\mathbf{y})},\quad \overline{q(\mathbf{x})w_j(\mathbf{y})}=\overline{q(-\mathbf{x})(-w_j(-\mathbf{y}))},\\
&\overline{q(\mathbf{x})w_j(\mathbf{y})w_k(\mathbf{z})}=\overline{q(-\mathbf{x})(-w_j(-\mathbf{y}))(-w_k(-\mathbf{z}))}
\end{aligned}
\tag{2.25}
$$

or

$$U_{ij}(\mathbf{r}) = U_{ij}(-\mathbf{r}), \quad U_{(ij)k}(\mathbf{r}) = -U_{(ij)k}(-\mathbf{r}), \quad U_{ijk}(\mathbf{r},\mathbf{s}) = -U_{ijk}(-\mathbf{r},-\mathbf{s}),$$
$$U_{(ij)kl}(\mathbf{r},\mathbf{s}) = U_{(ij)kl}(-\mathbf{r},-\mathbf{s}), \quad Q(\mathbf{r}) = Q(-\mathbf{r}), \quad Q_j(\mathbf{r}) = -Q_j(-\mathbf{r}), \quad Q_{jk}(\mathbf{r},\mathbf{s}) = Q_{jk}(-\mathbf{r},-\mathbf{s}) \tag{2.26}$$

These equalities reflect the statistical symmetry of inversion for the turbulent motion concerned. Further, the geometric and kinematic symmetries of the mean flow field suggest the statistical symmetry of mirror with respect to the plane of $x_3 = 0$,

$$\overline{w_i(\mathbf{x})\, w_j(\mathbf{y})} = (-1)^{\delta_{\underline{i}3}+\delta_{\underline{j}3}}\, \overline{w_{\underline{i}}(\mathbf{x}')\, w_{\underline{j}}(\mathbf{y}')},$$

$$\overline{w_i(\mathbf{x})\, w_j(\mathbf{y})\, w_k(\mathbf{z})} = (-1)^{\delta_{\underline{i}3}+\delta_{\underline{j}3}+\delta_{\underline{k}3}}\, \overline{w_{\underline{i}}(\mathbf{x}')\, w_{\underline{j}}(\mathbf{y}')\, w_{\underline{k}}(\mathbf{z}')},$$

$$\overline{w_i(\mathbf{x})\, w_j(\mathbf{x})\, w_k(\mathbf{y})\, w_l(\mathbf{z})} = (-1)^{\delta_{\underline{i}3}+\delta_{\underline{j}3}+\delta_{\underline{k}3}+\delta_{\underline{l}3}}\, \overline{w_{\underline{i}}(\mathbf{x}')\, w_{\underline{j}}(\mathbf{x}')\, w_{\underline{k}}(\mathbf{y}')\, w_{\underline{l}}(\mathbf{z}')},$$

$$\overline{q(\mathbf{x})\, q(\mathbf{y})} = \overline{q(\mathbf{x}')\, q(\mathbf{y}')}, \quad \overline{q(\mathbf{x})\, w_i(\mathbf{y})} = (-1)^{\delta_{\underline{i}3}}\, \overline{q(\mathbf{x}')\, w_{\underline{i}}(\mathbf{y}')},$$

$$\overline{q(\mathbf{x})\, w_i(\mathbf{y})\, w_j(\mathbf{z})} = (-1)^{\delta_{\underline{i}3}+\delta_{\underline{j}3}}\, \overline{q(\mathbf{x}')\, w_{\underline{i}}(\mathbf{y}')\, w_{\underline{j}}(\mathbf{z}')},$$

$$\mathbf{x}' := (x_1, x_2, -x_3), \quad \mathbf{y}' := (y_1, y_2, -y_3), \quad \mathbf{z}' := (z_1, z_2, -z_3) \tag{2.27}$$

Hereafter, the summation rule is suspended for the subscripts underlined, following the summation convention. Under the supposed homogeneity, the above mirror symmetry relations can be recast as

$$U_{ij}(\mathbf{r}) = (-1)^{\delta_{\underline{i}3}+\delta_{\underline{j}3}}\, U_{\underline{i}\,\underline{j}}(\mathbf{r}'), \quad U_{(ij)k}(\mathbf{r}) = (-1)^{\delta_{\underline{i}3}+\delta_{\underline{j}3}+\delta_{\underline{k}3}}\, U_{(\underline{i}\,\underline{j})\,\underline{k}}(\mathbf{r}'),$$

$$U_{ijk}(\mathbf{r},\mathbf{s}) = (-1)^{\delta_{\underline{i}3}+\delta_{\underline{j}3}+\delta_{\underline{k}3}}\, U_{\underline{i}\,\underline{j}\,\underline{k}}(\mathbf{r}',\mathbf{s}'), \quad U_{(ij)kl}(\mathbf{r},\mathbf{s}) = (-1)^{\delta_{\underline{i}3}+\delta_{\underline{j}3}+\delta_{\underline{k}3}+\delta_{\underline{l}3}}\, U_{(\underline{i}\,\underline{j})\,\underline{k}\,\underline{l}}(\mathbf{r}',\mathbf{s}'),$$

$$Q(\mathbf{r}) = Q(\mathbf{r}'), \quad Q_i(\mathbf{r}) = (-1)^{\delta_{\underline{i}3}}\, Q_{\underline{i}}(\mathbf{r}'), \quad Q_{ij}(\mathbf{r},\mathbf{s}) = (-1)^{\delta_{\underline{i}3}+\delta_{\underline{j}3}}\, Q_{\underline{i}\,\underline{j}}(\mathbf{r}',\mathbf{s}'),$$

$$\mathbf{r}' := (r_1, r_2, -r_3), \quad \mathbf{s}' := (s_1, s_2, -s_3) \tag{2.28}$$

The validity of such assumed symmetries may be checked partially by the comparison of their consequences with experimental data.

2.2 Fourier Transforms

It is convenient to formulate the mathematical problem with the help of Fourier transforms in $\mathbb{R}^n$, $n = 3,\ 6$,

$$U_{ij}(\mathbf{r}) = \int_{\mathbb{R}^3} d\mathbf{k}\, \tilde{U}_{ij}(\mathbf{k})\, \exp(\imath\, \mathbf{k}\cdot\mathbf{r}), \quad U_{(ij)k}(\mathbf{r}) = \int_{\mathbb{R}^3} d\mathbf{k}\, \tilde{U}_{(ij)k}(\mathbf{k})\, \exp(\imath\, \mathbf{k}\cdot\mathbf{r})\,,$$

$$U_{ijk}(\mathbf{r},\mathbf{s}) = \int_{\mathbb{R}^3\times\mathbb{R}^3} d\mathbf{k}\, d\mathbf{l}\, \tilde{U}_{ijk}(\mathbf{k},\mathbf{l})\, \exp[\imath\,(\mathbf{k}\cdot\mathbf{r}+\mathbf{l}\cdot\mathbf{s})]\,, \quad \tilde{U}_{(ij)k}(\mathbf{k}) = \int_{\mathbb{R}^3} d\mathbf{l}\, \tilde{U}_{ijk}(\mathbf{l},\mathbf{k}),$$

$$U_{(ij)kl}(\mathbf{r},\mathbf{s}) = \int_{\mathbb{R}^3\times\mathbb{R}^3} d\mathbf{k}\, d\mathbf{l}\, \tilde{U}_{(ij)kl}(\mathbf{k},\mathbf{l})\, \exp[\imath\,(\mathbf{k}\cdot\mathbf{r}+\mathbf{l}\cdot\mathbf{s})]\,, \quad Q(\mathbf{r}) = \int_{\mathbb{R}^3} d\mathbf{k}\, \tilde{Q}(\mathbf{k})\, \exp(\imath\,\mathbf{k}\cdot\mathbf{r}),$$

$$Q_j(\mathbf{r}) = \int_{\mathbb{R}^3} d\mathbf{k}\, \tilde{Q}_j(\mathbf{k})\, \exp(\imath\,\mathbf{k}\cdot\mathbf{r}), \quad Q_{jk}(\mathbf{r},\mathbf{s}) = \int_{\mathbb{R}^3\times\mathbb{R}^3} d\mathbf{k}\, d\mathbf{l}\, \tilde{Q}_{jk}(\mathbf{k},\mathbf{l})\, \exp[\imath\,(\mathbf{k}\cdot\mathbf{r}+\mathbf{l}\cdot\mathbf{s})] \tag{2.29}$$

That the multi-point correlations in the physical space are real requires that

$$\tilde{U}^*_{ij}(\mathbf{k}) = \tilde{U}_{ij}(-\mathbf{k}), \quad \tilde{U}^*_{(ij)k}(\mathbf{k}) = \tilde{U}_{(ij)k}(-\mathbf{k}), \quad \tilde{U}^*_{ijk}(\mathbf{k},\mathbf{l}) = \tilde{U}_{ijk}(-\mathbf{k},-\mathbf{l}),$$

$$\tilde{U}^*_{(ij)kl}(\mathbf{k},\mathbf{l}) = \tilde{U}_{(ij)kl}(-\mathbf{k},-\mathbf{l}), \quad \tilde{Q}^*(\mathbf{k}) = \tilde{Q}(-\mathbf{k}), \quad \tilde{Q}^*_j(\mathbf{k}) = \tilde{Q}_j(-\mathbf{k}), \quad \tilde{Q}^*_{jk}(\mathbf{k},\mathbf{l}) = \tilde{Q}_{jk}(-\mathbf{k},-\mathbf{l}) \tag{2.30}$$

where the superscript $*$ denotes the complex conjugate operation.

Combining (2.24), (2.26), (2.29) and (2.30), we obtain the symmetry properties of

$$\tilde{U}_{ij}(\mathbf{k}) = \tilde{U}_{ji}(\mathbf{k}) = \tilde{U}_{ij}(-\mathbf{k}) = \tilde{U}^*_{ij}(\mathbf{k}), \quad \tilde{U}_{(ij)k}(\mathbf{k}) = \tilde{U}_{(ji)k}(\mathbf{k}) = -\tilde{U}_{(ij)k}(-\mathbf{k}) = -\tilde{U}^*_{(ij)k}(\mathbf{k}),$$

$$\tilde{U}_{ijk}(\mathbf{k},\mathbf{l}) = \tilde{U}_{ikj}(\mathbf{l},\mathbf{k}) = \tilde{U}_{jik}(-\mathbf{k}-\mathbf{l},\mathbf{l}) = \tilde{U}_{kij}(-\mathbf{k}-\mathbf{l},\mathbf{k}) = -\tilde{U}_{ijk}(-\mathbf{k},-\mathbf{l}) = -\tilde{U}^*_{ijk}(\mathbf{k},\mathbf{l}),$$

$$\tilde{U}_{(ij)kl}(\mathbf{k},\mathbf{l}) = \tilde{U}_{(ji)kl}(\mathbf{k},\mathbf{l}) = \tilde{U}_{(ij)lk}(\mathbf{l},\mathbf{k}) = \tilde{U}_{(ij)kl}(-\mathbf{k},-\mathbf{l}) = \tilde{U}^*_{(ij)kl}(\mathbf{k},\mathbf{l}),$$

$$\int_{\mathbb{R}^3} d\mathbf{l}\, \Big[\tilde{U}_{(ij)kl}(\mathbf{k}+\mathbf{l},-\mathbf{l}) - \tilde{U}_{(kl)ij}(\mathbf{k}+\mathbf{l},-\mathbf{l})\Big] = 0, \quad \int_{\mathbb{R}^3} d\mathbf{k}\, \Big[\tilde{U}_{(ij)kl}(\mathbf{k},\mathbf{l}) - \tilde{U}_{(ik)jl}(\mathbf{k},\mathbf{l})\Big] = 0,$$

$$\tilde{Q}(\mathbf{k}) = \tilde{Q}(-\mathbf{k}) = \tilde{Q}^*(\mathbf{k}), \quad \tilde{Q}_j(\mathbf{k}) = -\tilde{Q}_j(-\mathbf{k}) = -\tilde{Q}^*_j(\mathbf{k}),$$

$$\tilde{Q}_{jk}(\mathbf{k},\mathbf{l}) = \tilde{Q}_{jk}(-\mathbf{k},-\mathbf{l}) = \tilde{Q}^*_{jk}(\mathbf{k},\mathbf{l}) = \tilde{Q}_{kj}(\mathbf{l},\mathbf{k}) \tag{2.31}$$

It immediately follows that $\tilde{U}_{ij}(\mathbf{k})$, $\tilde{U}_{(ij)kl}(\mathbf{k},\mathbf{l})$, $\tilde{Q}(\mathbf{k})$ and $\tilde{Q}_{ij}(\mathbf{k},\mathbf{l})$ are real and $\tilde{U}_{(ij)k}(\mathbf{k})$, $\tilde{U}_{ijk}(\mathbf{k},\mathbf{l})$ and $\tilde{Q}_j(\mathbf{k})$ are purely imaginary,

$$\tilde{U}_{(ij)k}(\mathbf{k}) = \imath\, \tilde{U}^{(I)}_{(ij)k}(\mathbf{k}), \quad \tilde{U}_{ijk}(\mathbf{k},\mathbf{l}) = \imath\, \tilde{U}^{(I)}_{ijk}(\mathbf{k},\mathbf{l}), \quad \tilde{Q}_j(\mathbf{k}) = \imath\, \tilde{Q}^{(I)}_j(\mathbf{k}) \tag{2.32}$$

Next, substitution of (2.29) into the statistical mirror symmetry of (2.28) results in

$$\tilde{U}_{ij}(\mathbf{k}) = (-1)^{\delta_{\underline{i}3}+\delta_{\underline{j}3}} \tilde{U}_{\underline{i}\,\underline{j}}(\mathbf{k}'), \quad \tilde{U}_{(ij)k}(\mathbf{k}) = (-1)^{\delta_{\underline{i}3}+\delta_{\underline{j}3}+\delta_{\underline{k}3}}\, \tilde{U}_{(\underline{i}\,\underline{j})\,\underline{k}}(\mathbf{k}'),$$

$$\tilde{U}_{ijk}(\mathbf{k},\mathbf{l}) = (-1)^{\delta_{\underline{i}3}+\delta_{\underline{j}3}+\delta_{\underline{k}3}}\, \tilde{U}_{\underline{i}\,\underline{j}\,\underline{k}}(\mathbf{k}',\mathbf{l}'), \quad \tilde{U}_{(ij)kl}(\mathbf{k},\mathbf{l}) = (-1)^{\delta_{\underline{i}3}+\delta_{\underline{j}3}+\delta_{\underline{k}3}+\delta_{\underline{l}3}}\, \tilde{U}_{(\underline{i}\,\underline{j})\,\underline{k}\,\underline{l}}(\mathbf{k}',\mathbf{l}'),$$

$$\tilde{Q}(\mathbf{k}) = \tilde{Q}(\mathbf{k}'), \quad \tilde{Q}_i(\mathbf{k}) = (-1)^{\delta_{\underline{i}3}}\, \tilde{Q}_{\underline{i}}(\mathbf{k}'), \quad \tilde{Q}_{ij}(\mathbf{k},\mathbf{l}) = (-1)^{\delta_{\underline{i}3}+\delta_{\underline{j}3}}\, \tilde{Q}_{\underline{i}\,\underline{j}}(\mathbf{k}',\mathbf{l}'),$$

$$\mathbf{k}' := (k_1,k_2,-k_3), \quad \mathbf{l}' := (l_1,l_2,-l_3) \tag{2.33}$$

We can now transform (2.16) through (2.23) of the physical space to their corresponding relations in the Fourier wave-number spaces,

$$k_k\,\tilde{U}_{kj}(\mathbf{k})=0,\quad k_k\,\tilde{U}^{(I)}_{(ij)k}(\mathbf{k})=0,\quad k_j\,\tilde{U}^{(I)}_{kjl}(\mathbf{k},\mathbf{l})=0,\quad k_k\,\tilde{U}_{(ij)kl}(\mathbf{k},\mathbf{l})=0 \tag{2.34}$$

$$\tilde{Q}(\mathbf{k})=-\frac{2\,k_1}{|\mathbf{k}|^2}\,\tilde{Q}^{(I)}_2(\mathbf{k})-\frac{k_k\,k_l}{|\mathbf{k}|^2}\int_{\mathbb{R}^3}d\mathbf{l}\,\tilde{Q}_{kl}(\mathbf{k}-\mathbf{l},\mathbf{l}) \tag{2.35}$$

$$\tilde{Q}^{(I)}_j(\mathbf{k})=-\frac{2\,k_1}{|\mathbf{k}|^2}\,\tilde{U}_{2j}(\mathbf{k})-\frac{k_k\,k_l}{|\mathbf{k}|^2}\,\tilde{U}^{(I)}_{(lk)j}(\mathbf{k}) \tag{2.36}$$

$$\tilde{Q}^{(I)}_j(\mathbf{k})=-\frac{2\,k_1}{|\mathbf{k}|^2}\,\tilde{U}_{2j}(\mathbf{k})-\frac{k_k\,k_l}{|\mathbf{k}|^2}\int_{\mathbb{R}^3}d\mathbf{l}\,\tilde{U}^{(I)}_{lkj}(\mathbf{l},\mathbf{k}) \tag{2.37}$$

$$\tilde{Q}_{jk}(\mathbf{k},\mathbf{l})=\frac{2\,(k_1+l_1)}{|\mathbf{k}+\mathbf{l}|^2}\,\tilde{U}^{(I)}_{2jk}(\mathbf{k},\mathbf{l})-\frac{(k_m+l_m)(k_l+l_l)}{|\mathbf{k}+\mathbf{l}|^2}\,\tilde{U}_{(lm)jk}(\mathbf{k},\mathbf{l}) \tag{2.38}$$

$$\begin{aligned}&\frac{\partial}{\partial t}\tilde{U}_{ij}(\mathbf{k})+2\,|\mathbf{k}|^2\,\tilde{U}_{ij}(\mathbf{k})-k_1\,\frac{\partial}{\partial k_2}\tilde{U}_{ij}(\mathbf{k})+\delta_{i1}\,\tilde{U}_{2j}(\mathbf{k})+\delta_{j1}\,\tilde{U}_{i2}(\mathbf{k})\\ &=-k_i\,\tilde{Q}^{(I)}_j(\mathbf{k})+k_j\,\tilde{Q}^{(I)}_i(-\mathbf{k})-k_k\left(\tilde{U}^{(I)}_{(ik)j}(\mathbf{k})-\tilde{U}^{(I)}_{(jk)i}(-\mathbf{k})\right)\end{aligned} \tag{2.39}$$

$$\begin{aligned}&\frac{\partial}{\partial t}\tilde{U}_{ij}(\mathbf{k})+2\,|\mathbf{k}|^2\,\tilde{U}_{ij}(\mathbf{k})-k_1\,\frac{\partial}{\partial k_2}\tilde{U}_{ij}(\mathbf{k})+\delta_{i1}\tilde{U}_{2j}(\mathbf{k})+\delta_{j1}\tilde{U}_{i2}(\mathbf{k})\\ &=-k_i\,\tilde{Q}^{(I)}_j(\mathbf{k})+k_j\,\tilde{Q}^{(I)}_i(-\mathbf{k})-k_k\int_{\mathbb{R}^3}\left(\tilde{U}^{(I)}_{ijk}(\mathbf{k},\mathbf{l})-\tilde{U}^{(I)}_{jik}(-\mathbf{k},\mathbf{l})\right)d\mathbf{l}\end{aligned} \tag{2.40}$$

and

$$\begin{aligned}&\frac{\partial}{\partial t}\tilde{U}^{(I)}_{ijk}(\mathbf{k},\mathbf{l})+2\,(|\mathbf{k}|^2+|\mathbf{l}|^2+\mathbf{k}\cdot\mathbf{l})\,\tilde{U}^{(I)}_{ijk}(\mathbf{k},\mathbf{l})-k_1\,\frac{\partial}{\partial k_2}\tilde{U}^{(I)}_{ijk}(\mathbf{k},\mathbf{l})-l_1\,\frac{\partial}{\partial l_2}\tilde{U}^{(I)}_{ijk}(\mathbf{k},\mathbf{l})\\ &\quad+\delta_{i1}\tilde{U}^{(I)}_{2jk}(\mathbf{k},\mathbf{l})+\delta_{j1}\tilde{U}^{(I)}_{i2k}(\mathbf{k},\mathbf{l})+\delta_{k1}\tilde{U}^{(I)}_{ij2}(\mathbf{k},\mathbf{l})\\ &=k_i\,\tilde{Q}_{jk}(\mathbf{k},\mathbf{l})+l_i\,\tilde{Q}_{jk}(\mathbf{k},\mathbf{l})-k_j\,\tilde{Q}_{ik}(-\mathbf{k}-\mathbf{l},\mathbf{l})-l_k\,\tilde{Q}_{ij}(-\mathbf{k}-\mathbf{l},\mathbf{k})\\ &\quad+(k_l+l_l)\,\tilde{U}_{(il)jk}(\mathbf{k},\mathbf{l})-k_l\,\tilde{U}_{(jl)ik}(-\mathbf{k}-\mathbf{l},\mathbf{l})-l_l\,\tilde{U}_{(kl)ij}(-\mathbf{k}-\mathbf{l},\mathbf{k})\end{aligned} \tag{2.41}$$

2.3 Primary Components

With the help of (2.31) and (2.32), we can solve (2.34) to obtain

$$\tilde{U}_{13}(\mathbf{k})=-\frac{k_1}{k_3}\,\tilde{U}_{11}(\mathbf{k})-\frac{k_2}{k_3}\,\tilde{U}_{12}(\mathbf{k}),\quad \tilde{U}_{23}(\mathbf{k})=-\frac{k_1}{k_3}\,\tilde{U}_{12}(\mathbf{k})-\frac{k_2}{k_3}\,\tilde{U}_{22}(\mathbf{k}),$$

$$\tilde{U}_{33}(\mathbf{k}) = \left(\frac{k_1}{k_3}\right)^2 \tilde{U}_{11}(\mathbf{k}) + \left(\frac{k_2}{k_3}\right)^2 \tilde{U}_{22}(\mathbf{k}) + \frac{2\,k_1\,k_2}{(k_3)^2}\,\tilde{U}_{12}(\mathbf{k}) \tag{2.42}$$

$$\tilde{U}^{(I)}_{(ij)3}(\mathbf{k}) = -\frac{k_1}{k_3}\,\tilde{U}^{(I)}_{(ij)1}(\mathbf{k}) - \frac{k_2}{k_3}\,\tilde{U}^{(I)}_{(ij)2}(\mathbf{k}), \quad ij = 11, 12, 13, 22, 23, 33 \tag{2.43}$$

$$\begin{aligned}
\tilde{U}^{(I)}_{113}(\mathbf{k},\mathbf{l}) &= -\frac{l_1}{l_3}\,\tilde{U}^{(I)}_{111}(\mathbf{k},\mathbf{l}) - \frac{l_2}{l_3}\,\tilde{U}^{(I)}_{112}(\mathbf{k},\mathbf{l}), \quad \tilde{U}^{(I)}_{123}(\mathbf{k},\mathbf{l}) = -\frac{l_1}{l_3}\,\tilde{U}^{(I)}_{112}(\mathbf{l},\mathbf{k}) - \frac{l_2}{l_3}\,\tilde{U}^{(I)}_{122}(\mathbf{k},\mathbf{l}),\\
\tilde{U}^{(I)}_{223}(\mathbf{k},\mathbf{l}) &= -\frac{l_1}{l_3}\,\tilde{U}^{(I)}_{122}(-\mathbf{l}-\mathbf{k},\mathbf{k}) - \frac{l_2}{l_3}\,\tilde{U}^{(I)}_{222}(\mathbf{k},\mathbf{l}),\\
\tilde{U}^{(I)}_{133}(\mathbf{k},\mathbf{l}) &= \frac{k_1}{k_3}\,\frac{l_1}{l_3}\,\tilde{U}^{(I)}_{111}(\mathbf{k},\mathbf{l}) + \frac{k_2}{k_3}\,\frac{l_1}{l_3}\,\tilde{U}^{(I)}_{112}(\mathbf{l},\mathbf{k}) + \frac{k_1}{k_3}\,\frac{l_2}{l_3}\,\tilde{U}^{(I)}_{112}(\mathbf{k},\mathbf{l}) + \frac{k_2}{k_3}\,\frac{l_2}{l_3}\,\tilde{U}^{(I)}_{122}(\mathbf{k},\mathbf{l}),\\
\tilde{U}^{(I)}_{233}(\mathbf{k},\mathbf{l}) &= \frac{k_1}{k_3}\,\frac{l_1}{l_3}\,\tilde{U}^{(I)}_{112}(\mathbf{k},-\mathbf{l}-\mathbf{k}) + \frac{k_2}{k_3}\,\frac{l_1}{l_3}\,\tilde{U}^{(I)}_{122}(-\mathbf{l}-\mathbf{k},\mathbf{k}) + \frac{k_1}{k_3}\,\frac{l_2}{l_3}\,\tilde{U}^{(I)}_{122}(-\mathbf{l}-\mathbf{k},\mathbf{l})\\
&\quad + \frac{k_2}{k_3}\,\frac{l_2}{l_3}\,\tilde{U}^{(I)}_{222}(\mathbf{k},\mathbf{l}),\\
\tilde{U}^{(I)}_{333}(\mathbf{k},\mathbf{l}) &= -\frac{l_1}{l_3}\,\frac{k_1}{k_3}\,\frac{l_1+k_1}{l_3+k_3}\,\tilde{U}^{(I)}_{111}(\mathbf{k},\mathbf{l}) - \frac{l_1}{l_3}\,\frac{k_2}{k_3}\,\frac{l_1+k_1}{l_3+k_3}\,\tilde{U}^{(I)}_{112}(\mathbf{l},\mathbf{k}) - \frac{l_1+k_1}{l_3+k_3}\,\frac{k_1}{k_3}\,\frac{l_2}{l_3}\,\tilde{U}^{(I)}_{112}(\mathbf{k},\mathbf{l})\\
&\quad - \frac{l_1}{l_3}\,\frac{k_1}{k_3}\,\frac{l_2+k_2}{l_3+k_3}\,\tilde{U}^{(I)}_{112}(\mathbf{k},-\mathbf{l}-\mathbf{k}) - \frac{l_1}{l_3}\,\frac{k_2}{k_3}\,\frac{l_2+k_2}{l_3+k_3}\,\tilde{U}^{(I)}_{122}(\mathbf{k},-\mathbf{l}-\mathbf{k})\\
&\quad - \frac{k_1}{k_3}\,\frac{l_2}{l_3}\,\frac{l_2+k_2}{l_3+k_3}\,\tilde{U}^{(I)}_{122}(\mathbf{l},-\mathbf{l}-\mathbf{k}) - \frac{l_1+k_1}{l_3+k_3}\,\frac{k_2}{k_3}\,\frac{l_2}{l_3}\,\tilde{U}^{(I)}_{122}(\mathbf{l},\mathbf{k}) - \frac{l_2}{l_3}\,\frac{k_2}{k_3}\,\frac{l_2+k_2}{l_3+k_3}\,\tilde{U}^{(I)}_{222}(\mathbf{k},\mathbf{l})
\end{aligned} \tag{2.44}$$

and

$$\tilde{U}_{(ij)3l}(\mathbf{k},\mathbf{l}) = -\frac{k_1}{k_3}\,\tilde{U}_{(ij)1l}(\mathbf{k},\mathbf{l}) - \frac{k_2}{k_3}\,\tilde{U}_{(ij)2l}(\mathbf{k},\mathbf{l}), \quad ij = 11, 12, 13, 22, 23, 33,\ l = 2, 3 \tag{2.45}$$

These expressions indicate that $\tilde{U}_{ij}(\mathbf{k})$, ij = 11, 12, 22, are the three primary components of $\tilde{U}_{ij}(\mathbf{k})$; $\tilde{U}^{(I)}_{(ij)k}(\mathbf{k})$, ijk = 111, 112, 121, 122, 131, 132, 221, 222, 231, 232, 331, 332, the twelve primary components of $\tilde{U}^{(I)}_{(ij)k}(\mathbf{k})$; $\tilde{U}^{(I)}_{ijk}(\mathbf{k},\mathbf{l})$, ijk = 111, 112, 122, 222, the four primary components of $\tilde{U}^{(I)}_{ijk}(\mathbf{k},\mathbf{l})$; and $\tilde{U}_{(ij)kl}(\mathbf{k},\mathbf{l})$, ij = 11, 12, 13, 22, 23, 33, kl = 11, 12, 13, 22, 23, the primary components of $\tilde{U}_{(ij)kl}(\mathbf{k},\mathbf{l})$. The components not presented explicitly above can be obtained with the help of (2.31). We should mention that the above selection of the primary components is not unique.

2.4 Primary Evolution Equations of $\tilde{U}_{ij}(\mathbf{k})$ under $\tilde{U}_{ijk}(\mathbf{k},\mathbf{l})$

Equation (2.40), along with (2.37) and (2.42), leads to

$$\left(\frac{\partial}{\partial t} - k_1\,\frac{\partial}{\partial k_2}\right)\Big\{|\mathbf{k}|^4\,\exp\big[2\,H(\mathbf{k})\big]\,\tilde{U}_{22}(\mathbf{k})\Big\} = 2\,|\mathbf{k}|^4\,\exp\big[2\,H(\mathbf{k})\big]\,\tilde{\gamma}_{22}(\mathbf{k}) \tag{2.46}$$

$$\left(\frac{\partial}{\partial t} - k_1 \frac{\partial}{\partial k_2}\right)\Big\{|\mathbf{k}|^2 \exp\big[2\,H(\mathbf{k})\big]\,\tilde{U}_{12}(\mathbf{k})\Big\}$$
$$= |\mathbf{k}|^2 \exp\big[2\,H(\mathbf{k})\big]\left[-\left(1 - \frac{2\,(k_1)^2}{|\mathbf{k}|^2}\right)\tilde{U}_{22}(\mathbf{k}) + \tilde{\gamma}_{12}(\mathbf{k})\right] \tag{2.47}$$

and

$$\left(\frac{\partial}{\partial t} - k_1 \frac{\partial}{\partial k_2}\right)\Big\{\exp\big[2\,H(\mathbf{k})\big]\,\tilde{U}_{11}(\mathbf{k})\Big\}$$
$$= 2\,\exp\big[2\,H(\mathbf{k})\big]\left[-\left(1 - \frac{2\,(k_1)^2}{|\mathbf{k}|^2}\right)\tilde{U}_{12}(\mathbf{k}) + \tilde{\gamma}_{11}(\mathbf{k})\right] \tag{2.48}$$

Here,

$$H(\mathbf{k}) := -\frac{k_2}{k_1}\left((k_1)^2 + \frac{1}{3}\,(k_2)^2 + (k_3)^2\right) \tag{2.49}$$

and

$$\tilde{\gamma}_{22}(\mathbf{k}) := \frac{k_k\,k_l}{|\mathbf{k}|^2}\int_{\mathbb{R}^3} d\mathbf{l}\,k_2\,\tilde{U}^{(I)}_{lk2}(\mathbf{l},\mathbf{k}) - k_k\int_{\mathbb{R}^3} d\mathbf{l}\,\tilde{U}^{(I)}_{22k}(\mathbf{k},\mathbf{l}),$$
$$\tilde{\gamma}_{12}(\mathbf{k}) := \frac{k_k\,k_l}{|\mathbf{k}|^2}\int_{\mathbb{R}^3} d\mathbf{l}\left(k_1\,\tilde{U}^{(I)}_{lk2}(\mathbf{l},\mathbf{k}) + k_2\,\tilde{U}^{(I)}_{lk1}(\mathbf{l},\mathbf{k})\right) - k_k\int_{\mathbb{R}^3} d\mathbf{l}\left(\tilde{U}^{(I)}_{12k}(\mathbf{k},\mathbf{l}) + \tilde{U}^{(I)}_{21k}(\mathbf{k},\mathbf{l})\right),$$
$$\tilde{\gamma}_{11}(\mathbf{k}) := \frac{k_k\,k_l}{|\mathbf{k}|^2}\int_{\mathbb{R}^3} d\mathbf{l}\,k_1\,\tilde{U}^{(I)}_{lk1}(\mathbf{l},\mathbf{k}) - k_k\int_{\mathbb{R}^3} d\mathbf{l}\,\tilde{U}^{(I)}_{11k}(\mathbf{k},\mathbf{l}) \tag{2.50}$$

with

$$\tilde{\gamma}_{ij}(-\mathbf{k}) = \tilde{\gamma}_{ij}(\mathbf{k}) = \tilde{\gamma}_{ij}(k_1, k_2, -k_3) \tag{2.51}$$

following from (2.31) through (2.33). $\tilde{\gamma}_{ij}(\mathbf{k})$, $ij = 11,\ 12,\ 22$, can be represented as the linear combinations of the degenerated third order correlation components too, on the basis of the relationship between the degenerated and the general third order correlations in (2.29). The three equations (2.46) through (2.48) are the evolution equations for the primary components of the second order correlation.

It can be verified directly from the definitions of $\tilde{\gamma}_{ij}(\mathbf{k})$ in (2.50) that

$$\left(1 + \left(\frac{k_1}{k_3}\right)^2\right)\tilde{\gamma}_{11}(\mathbf{k}) + \left(1 + \left(\frac{k_2}{k_3}\right)^2\right)\tilde{\gamma}_{22}(\mathbf{k}) + \frac{k_1\,k_2}{(k_3)^2}\,\tilde{\gamma}_{12}(\mathbf{k}) + k_k\int_{\mathbb{R}^3} d\mathbf{l}\,\tilde{U}^{(I)}_{jjk}(\mathbf{k},\mathbf{l}) = 0 \tag{2.52}$$

To obtain an equation involving only $\tilde{\gamma}_{ij}(\mathbf{k})$, we proceed as follows. Firstly, we have

$$\int_{\mathbb{R}^3}\int_{\mathbb{R}^3} d\mathbf{k}\,d\mathbf{l}\,k_k\,\tilde{U}^{(I)}_{\underline{jj}k}(\mathbf{k},\mathbf{l}) = 0 \tag{2.53}$$

which can be easily verified with the help of (2.31) and the procedure listed below,

$$\tilde{U}^{(I)}_{\underline{jj}k}(\mathbf{k},\mathbf{l}) = \tilde{U}^{(I)}_{\underline{jj}k}(-\mathbf{k}-\mathbf{l},\mathbf{l}), \quad \mathbf{k}\to -\mathbf{k}-\mathbf{l}, \quad l_k\,\tilde{U}^{(I)}_{\underline{jj}k}(\mathbf{k},\mathbf{l}) = 0$$

Secondly, we have

$$\int_{-\infty}^{0} dk_1 \int_{\mathbb{R}^2}\int_{\mathbb{R}^3} dk_2 dk_3\, d\mathbf{l}\, k_k\, \tilde{U}^{(I)}_{\underline{j}\,\underline{j}k}(\mathbf{k},\mathbf{l}) = \int_{0}^{+\infty} dk_1 \int_{\mathbb{R}^2}\int_{\mathbb{R}^3} dk_2 dk_3\, d\mathbf{l}\, k_k\, \tilde{U}^{(I)}_{\underline{j}\,\underline{j}k}(\mathbf{k},\mathbf{l}) = 0 \quad (2.54)$$

following from (2.53) and the procedure of

$$2\int_{-\infty}^{0} dk_1 = \int_{-\infty}^{0} dk_1 + \int_{-\infty}^{0} dk_1, \quad (\mathbf{k},\mathbf{l}) \to -(\mathbf{k},\mathbf{l}), \quad \tilde{U}^{(I)}_{\underline{jj}k}(-\mathbf{k},-\mathbf{l}) = -\tilde{U}^{(I)}_{\underline{jj}k}(\mathbf{k},\mathbf{l})$$

with the second and the third parts being applied to one of the $\int_{-\infty}^{0} dk_1$'s. Thirdly, we apply (2.54) to (2.52) to get

$$\int_{-\infty}^{0} dk_1 \int_{\mathbb{R}^2} dk_2\, dk_3 \left[\left(1+\left(\frac{k_1}{k_3}\right)^2\right)\tilde{\gamma}_{11}(\mathbf{k}) + \left(1+\left(\frac{k_2}{k_3}\right)^2\right)\tilde{\gamma}_{22}(\mathbf{k}) + \frac{k_1\, k_2}{(k_3)^2}\,\tilde{\gamma}_{12}(\mathbf{k})\right] = 0 \quad (2.55)$$

This equality should be imposed explicitly as a constraint on $\tilde{\gamma}_{ij}(\mathbf{k})$, if $\tilde{\gamma}_{ij}(\mathbf{k})$, $ij = 11,\ 12,\ 22$, are taken as the control variables.

Equations (2.46) through (2.48) are the primary differential equations of evolution for the second-order model composed of the correlations up to the (linearly combined) degenerated third order with $\tilde{\gamma}_{ij}(\mathbf{k})$, $ij = 11,\ 12,\ 22$, as the control variables. These differential equations can be formally solved with the aid of the method of characteristics.

The second-order model has a few intrinsic limitations delineated as follows. Within the model, the pointwise equality (2.52) merely plays the role of representing $k_k \int_{\mathbb{R}^3} d\mathbf{l}\, \tilde{U}^{(I)}_{jjk}(\mathbf{k},\mathbf{l})$ in terms of the control variables. Next, the model cannot satisfy the intrinsic equality of

$$\frac{\partial}{\partial y_k}\overline{q(\mathbf{x})w_k(\mathbf{y})} = 0,\ \forall \mathbf{y} \quad \text{or} \quad k_j\,\tilde{Q}^{(I)}_j(\mathbf{k}) = 0,\ \forall \mathbf{k} \quad (2.56)$$

which is the constraint for the lowest order correlation involving pressure fluctuations and is present in (2.39) and (2.40) under the contraction of $i = j$. Further, there is the issue regarding the two possible ways to determine $\tilde{U}_{33}$ (or equivalently $\tilde{U}_{kk}$): One is to use the expression of $(2.42)_3$, together with the primary component solutions of $\tilde{U}_{ij}$, $ij = 11,\ 12,\ 22$; The other is to solve directly

$$\begin{aligned}&\frac{\partial}{\partial t}\tilde{U}_{33}(\mathbf{k}) - k_1\,\frac{\partial}{\partial k_2}\tilde{U}_{33}(\mathbf{k}) + 2\,|\mathbf{k}|^2\,\tilde{U}_{33}(\mathbf{k})\\ &= 2\,k_3\,\frac{2\,k_1}{|\mathbf{k}|^2}\,\tilde{U}_{23}(\mathbf{k}) + 2\,k_3\,\frac{k_k\,k_l}{|\mathbf{k}|^2}\int_{\mathbb{R}^3} d\mathbf{l}\,\tilde{U}^{(I)}_{lk3}(\mathbf{l},\mathbf{k}) - 2\,k_k\int_{\mathbb{R}^3} d\mathbf{l}\,\tilde{U}^{(I)}_{33k}(\mathbf{k},\mathbf{l})\end{aligned} \quad (2.57)$$

derived from (2.40). This latter scheme, however, cannot be implemented within the model, since (2.57) contains the two integrals that cannot be represented completely in terms of $\tilde{\gamma}_{ij}$. Consequently, (2.57) cannot be used to solve for $\tilde{U}_{33}$ and it, together with $(2.42)_3$, merely provides an equation to find the sum of the two integral terms in terms of $\tilde{U}_{ij}$, $ij = 11,\ 12,\ 22$. All these limitations result from the integrated and summed relationship between $\tilde{\gamma}_{ij}(\mathbf{k})$ and $\tilde{U}_{klm}(\mathbf{k},\mathbf{l})$, the former inherit only very partially the properties of the latter.

Instead of $\tilde{\gamma}_{ij}(\mathbf{k})$, we may take $\tilde{U}^{(I)}_{(ij)k}(\mathbf{k})$ or its primary components as the control variables, as to be done in the third-order model where (2.56) can be satisfied; the pointwise equality,

(2.52), is satisfied automatically for the degenerated $\tilde{U}^{(I)}_{(ij)k}(\mathbf{k})$. These issues do not arise within the fourth-order model to be introduced in Subsection 2.6.

There is also the known relationship of

$$\frac{\partial U_{jj}(\mathbf{0})}{\partial t} + 2\,U_{12}(\mathbf{0}) - 2\,\frac{\partial^2 U_{jj}(\mathbf{r})}{\partial r_k \partial r_k}\bigg|_{\mathbf{r}=\mathbf{0}} = 0 \tag{2.58}$$

which is a consequence of $(2.42)_3$, (2.46) through (2.48) and (2.55). This relationship has the advantage of being expressed in the physical space, and will yield straight-forwardly some significant results as to be presented in Subsection 4.1.

2.5 Primary Evolution Equations of $\tilde{U}_{ij}(\mathbf{k})$ under $\tilde{U}_{(ij)k}(\mathbf{k})$

If the degenerated third order correlation $\tilde{U}^{(I)}_{(ij)k}$ are adopted as the control variables, equation (2.39), along with (2.36) and (2.43), provides the following primary evolution equations for $\tilde{U}_{ij}$,

$$\frac{\partial}{\partial t}\tilde{U}_{22}(\mathbf{k}) - k_1\,\frac{\partial}{\partial k_2}\tilde{U}_{22}(\mathbf{k}) + 2\left(|\mathbf{k}|^2 - \frac{2\,k_1\,k_2}{|\mathbf{k}|^2}\right)\tilde{U}_{22}(\mathbf{k}) = \frac{2\,k_2\,k_k\,k_l}{|\mathbf{k}|^2}\,\tilde{U}^{(I)}_{(kl)2}(\mathbf{k}) - 2\,k_k\,\tilde{U}^{(I)}_{(2k)2}(\mathbf{k}) \tag{2.59}$$

$$\begin{aligned}&\frac{\partial}{\partial t}\tilde{U}_{12}(\mathbf{k}) - k_1\,\frac{\partial}{\partial k_2}\tilde{U}_{12}(\mathbf{k}) + 2\left(|\mathbf{k}|^2 - \frac{k_1\,k_2}{|\mathbf{k}|^2}\right)\tilde{U}_{12}(\mathbf{k})\\ &= -\left(1 - \frac{2\,(k_1)^2}{|\mathbf{k}|^2}\right)\tilde{U}_{22}(\mathbf{k}) + \frac{k_k\,k_l}{|\mathbf{k}|^2}\left(k_1\,\tilde{U}^{(I)}_{(kl)2}(\mathbf{k}) + k_2\,\tilde{U}^{(I)}_{(kl)1}(\mathbf{k})\right) - k_k\left(\tilde{U}^{(I)}_{(1k)2}(\mathbf{k}) + \tilde{U}^{(I)}_{(2k)1}(\mathbf{k})\right)\end{aligned} \tag{2.60}$$

and

$$\begin{aligned}&\frac{\partial}{\partial t}\tilde{U}_{11}(\mathbf{k}) - k_1\,\frac{\partial}{\partial k_2}\tilde{U}_{11}(\mathbf{k}) + 2\,|\mathbf{k}|^2\,\tilde{U}_{11}(\mathbf{k})\\ &= -2\left(1 - \frac{2\,(k_1)^2}{|\mathbf{k}|^2}\right)\tilde{U}_{12}(\mathbf{k}) + \frac{2\,k_1\,k_k\,k_l}{|\mathbf{k}|^2}\,\tilde{U}^{(I)}_{(kl)1}(\mathbf{k}) - 2\,k_k\,\tilde{U}^{(I)}_{(1k)1}(\mathbf{k})\end{aligned} \tag{2.61}$$

where

$$\tilde{U}_{(ij)k}(\mathbf{k}) = \tilde{U}_{(ji)k}(\mathbf{k}) = -\tilde{U}_{(ij)k}(-\mathbf{k}) = (-1)^{\delta_{\underline{i}3}+\delta_{\underline{j}3}+\delta_{\underline{k}3}}\,\tilde{U}_{(\underline{i}\,\underline{j})\,\underline{k}}(k_1, k_2, -k_3) \tag{2.62}$$

following from (2.31) through (2.33).

The three equations (2.59) through (2.61) are the primary differential equations of evolution for the third-order model. This model intends to extend the second-order model by taking the primary components of $\tilde{U}^{(I)}_{(ij)k}$ as the control variables in order to account for the constraint of equality (2.56). This constraint redistributes the energy among the components of $\tilde{U}_{\underline{i}\,\underline{i}}(\mathbf{k})$ which can be seen from (2.39) under the contraction $j = i$, and thus, it redistributes the energy among the components of $U_{\underline{i}\,\underline{i}}(\mathbf{0})$ and it may tend to make the turbulent states more isotropic

[5]. In fact, we can test directly the supposed tendency by comparing the results of $U_{ij}(\mathbf{0})$ obtained from the second-order and the third-order models.

The restriction to the degenerated $\tilde{U}_{(ij)k}(\mathbf{k})$, instead of the general $\tilde{U}_{ijk}(\mathbf{k},\mathbf{l})$, takes into account the fact that the equations of motion, (2.10) and (2.12), involve only the degenerated third order correlation. This restriction reduces the computational size of the model tremendously. Due to the degenerated nature of $\tilde{U}^{(I)}_{(ij)k}(\mathbf{k})$, the intrinsic equalities like (2.54) need to be imposed explicitly,

$$\int_{-\infty}^{0} dk_1 \int_{\mathbb{R}^2} dk_2\, dk_3\, k_k\, \tilde{U}^{(I)}_{(k\underline{j})\,\underline{j}}(\mathbf{k}) = \int_{0}^{+\infty} dk_1 \int_{\mathbb{R}^2} dk_2\, dk_3\, k_k\, \tilde{U}^{(I)}_{(k\underline{j})\,\underline{j}}(\mathbf{k}) = 0 \tag{2.63}$$

which guarantees the holding of (2.58) within the third-order model.

The model has twelve control variables, compared with the three in the second-order model, which increases the computational complexity. It gains, however, the advantage to satisfy the intrinsic equality (2.56) for the lowest order correlation involving pressure fluctuations.

Both the second-order and the third-order models are not applicable to the transient states of $\tilde{U}_{ij}(\mathbf{k})$ which will be shown in Subsection 4.1. The limitations mentioned above can be fixed by the fourth-order model to be introduced below.

2.6 Primary Evolution Equations of $\tilde{U}_{ijk}(\mathbf{k},\mathbf{l})$

Equation (2.41), together with (2.31), (2.38) and (2.44), results in the following evolution equations for the primary components of $\tilde{U}_{ijk}(\mathbf{k},\mathbf{l})$,

$$\begin{aligned}
&\left(\frac{\partial}{\partial t} - k_1\frac{\partial}{\partial k_2} - l_1\frac{\partial}{\partial l_2}\right)\Big\{|\mathbf{k}|^2\,|\mathbf{l}|^2\,|\mathbf{k}+\mathbf{l}|^2\,\exp\big[H(\mathbf{k},\mathbf{l})\big]\,\tilde{U}^{(I)}_{222}(\mathbf{k},\mathbf{l})\Big\}\\
&= |\mathbf{k}|^2\,|\mathbf{l}|^2\,|\mathbf{k}+\mathbf{l}|^2\,\exp\big[H(\mathbf{k},\mathbf{l})\big]\\
&\quad\times\Bigg[(k_l+l_l)\,\tilde{U}_{(2l)22}(\mathbf{k},\mathbf{l}) - k_l\,\tilde{U}_{(2l)22}(-\mathbf{k}-\mathbf{l},\mathbf{l}) - l_l\,\tilde{U}_{(2l)22}(-\mathbf{k}-\mathbf{l},\mathbf{k})\\
&\qquad - (k_2+l_2)\,\frac{(k_m+l_m)(k_l+l_l)}{|\mathbf{k}+\mathbf{l}|^2}\,\tilde{U}_{(lm)22}(\mathbf{k},\mathbf{l}) + k_2\,\frac{k_m\,k_l}{|\mathbf{k}|^2}\,\tilde{U}_{(lm)22}(-\mathbf{k}-\mathbf{l},\mathbf{l})\\
&\qquad + l_2\,\frac{l_m\,l_l}{|\mathbf{l}|^2}\,\tilde{U}_{(lm)22}(-\mathbf{k}-\mathbf{l},\mathbf{k})\Bigg]
\end{aligned} \tag{2.64}$$

$$\begin{aligned}
&\left(\frac{\partial}{\partial t} - k_1\,\frac{\partial}{\partial k_2} - l_1\,\frac{\partial}{\partial l_2}\right)\Big\{|\mathbf{k}|^2\,|\mathbf{l}|^2\,\exp\big[H(\mathbf{k},\mathbf{l})\big]\,\tilde{U}^{(I)}_{122}(\mathbf{k},\mathbf{l})\Big\}\\
&+ |\mathbf{k}|^2\,|\mathbf{l}|^2\,\exp\big[H(\mathbf{k},\mathbf{l})\big]\left(1 - \frac{2\,(k_1+l_1)^2}{|\mathbf{k}+\mathbf{l}|^2}\right)\tilde{U}^{(I)}_{222}(\mathbf{k},\mathbf{l})\\
&= |\mathbf{k}|^2\,|\mathbf{l}|^2\,\exp\big[H(\mathbf{k},\mathbf{l})\big]\Bigg[(k_l+l_l)\,\tilde{U}_{(1l)22}(\mathbf{k},\mathbf{l}) - k_l\,\tilde{U}_{(2l)12}(-\mathbf{k}-\mathbf{l},\mathbf{l}) - l_l\,\tilde{U}_{(2l)12}(-\mathbf{k}-\mathbf{l},\mathbf{k})\\
&\qquad - (k_1+l_1)\,\frac{(k_m+l_m)(k_l+l_l)}{|\mathbf{k}+\mathbf{l}|^2}\,\tilde{U}_{(lm)22}(\mathbf{k},\mathbf{l}) + k_2\,\frac{k_m\,k_l}{|\mathbf{k}|^2}\,\tilde{U}_{(lm)12}(-\mathbf{k}-\mathbf{l},\mathbf{l})
\end{aligned}$$

$$+ l_2 \frac{l_m\, l_l}{|\mathbf{l}|^2}\, \tilde{U}_{(lm)12}(-\mathbf{k}-\mathbf{l},\mathbf{k})\Bigg] \tag{2.65}$$

$$\begin{aligned}
&\left(\frac{\partial}{\partial t} - k_1 \frac{\partial}{\partial k_2} - l_1 \frac{\partial}{\partial l_2}\right)\Big\{|\mathbf{l}|^2 \exp\big[H(\mathbf{k},\mathbf{l})\big]\, \tilde{U}^{(I)}_{112}(\mathbf{k},\mathbf{l})\Big\} \\
&\quad + |\mathbf{l}|^2 \exp\big[H(\mathbf{k},\mathbf{l})\big]\left[\left(1 - \frac{2\,(k_1+l_1)^2}{|\mathbf{k}+\mathbf{l}|^2}\right)\tilde{U}^{(I)}_{122}(-\mathbf{k}-\mathbf{l},\mathbf{l}) + \left(1 - \frac{2\,(k_1)^2}{|\mathbf{k}|^2}\right)\tilde{U}^{(I)}_{122}(\mathbf{k},\mathbf{l})\right] \\
&= |\mathbf{l}|^2 \exp\big[H(\mathbf{k},\mathbf{l})\big]\Bigg[(k_l+l_l)\,\tilde{U}_{(1l)12}(\mathbf{k},\mathbf{l}) - k_l\,\tilde{U}_{(1l)12}(-\mathbf{k}-\mathbf{l},\mathbf{l}) - l_l\,\tilde{U}_{(2l)11}(-\mathbf{k}-\mathbf{l},\mathbf{k}) \\
&\qquad - (k_1+l_1)\,\frac{(k_m+l_m)(k_l+l_l)}{|\mathbf{k}+\mathbf{l}|^2}\,\tilde{U}_{(lm)12}(\mathbf{k},\mathbf{l}) + k_1\,\frac{k_m\,k_l}{|\mathbf{k}|^2}\,\tilde{U}_{(lm)12}(-\mathbf{k}-\mathbf{l},\mathbf{l}) \\
&\qquad + l_2\,\frac{l_m\,l_l}{|\mathbf{l}|^2}\,\tilde{U}_{(lm)11}(-\mathbf{k}-\mathbf{l},\mathbf{k})\Bigg]
\end{aligned} \tag{2.66}$$

and

$$\begin{aligned}
&\left(\frac{\partial}{\partial t} - k_1 \frac{\partial}{\partial k_2} - l_1 \frac{\partial}{\partial l_2}\right)\Big\{\exp\big[H(\mathbf{k},\mathbf{l})\big]\, \tilde{U}^{(I)}_{111}(\mathbf{k},\mathbf{l})\Big\} \\
&\quad + \exp\big[H(\mathbf{k},\mathbf{l})\big]\Bigg[\tilde{U}^{(I)}_{112}(\mathbf{l},-\mathbf{k}-\mathbf{l}) + \tilde{U}^{(I)}_{112}(\mathbf{l},\mathbf{k}) + \tilde{U}^{(I)}_{112}(\mathbf{k},\mathbf{l}) \\
&\qquad - \frac{2\,(k_1+l_1)^2}{|\mathbf{k}+\mathbf{l}|^2}\,\tilde{U}^{(I)}_{112}(\mathbf{l},-\mathbf{k}-\mathbf{l}) - \frac{2\,(k_1)^2}{|\mathbf{k}|^2}\,\tilde{U}^{(I)}_{112}(\mathbf{l},\mathbf{k}) - \frac{2\,(l_1)^2}{|\mathbf{l}|^2}\,\tilde{U}^{(I)}_{112}(\mathbf{k},\mathbf{l})\Bigg] \\
&= \exp\big[H(\mathbf{k},\mathbf{l})\big]\Bigg[(k_l+l_l)\,\tilde{U}_{(1l)11}(\mathbf{k},\mathbf{l}) - k_l\,\tilde{U}_{(1l)11}(-\mathbf{k}-\mathbf{l},\mathbf{l}) - l_l\,\tilde{U}_{(1l)11}(-\mathbf{k}-\mathbf{l},\mathbf{k}) \\
&\qquad - (k_1+l_1)\,\frac{(k_m+l_m)(k_l+l_l)}{|\mathbf{k}+\mathbf{l}|^2}\,\tilde{U}_{(lm)11}(\mathbf{k},\mathbf{l}) + k_1\,\frac{k_m\,k_l}{|\mathbf{k}|^2}\,\tilde{U}_{(lm)11}(-\mathbf{k}-\mathbf{l},\mathbf{l}) \\
&\qquad + l_1\,\frac{l_m\,l_l}{|\mathbf{l}|^2}\,\tilde{U}_{(lm)11}(-\mathbf{k}-\mathbf{l},\mathbf{k})\Bigg]
\end{aligned} \tag{2.67}$$

where

$$H(\mathbf{k},\mathbf{l}) := H(\mathbf{k}) + H(\mathbf{l}) + H(\mathbf{k}+\mathbf{l}) \tag{2.68}$$

These partial differential equations can be solved formally with the method of characteristics. Equations (2.46) through (2.48) and (2.64) through (2.67) are the primary differential equations of evolution for the fourth-order model composed of the correlations up to the fourth order, which can determine the lower order correlations involving pressure fluctuations and can include certain variance constraints to be introduced in Subsection 2.9.

2.7 Consequence of Mirror Symmetry and Transformations

The statistical mirror symmetry of (2.33) implies that we need to consider only the distributions of the correlations over the sub-domain of $\mathbf{k} = (k_1, k_2, k_3)$ with $k_3 \geq 0$ within the

second-order model,

$$\tilde{U}_{ij}(k_1,k_2,-k_3)=(-1)^{\delta_{\underline{i}3}+\delta_{\underline{j}3}}\,\tilde{U}_{\underline{i}\,\underline{j}}(\mathbf{k}),\quad \tilde{\gamma}_{ij}(k_1,k_2,-k_3)=\tilde{\gamma}_{ij}(\mathbf{k}) \tag{2.69}$$

Here, the definition of (2.50) has been used. The first constraint of (2.69) implies that

$$U_{ij}(\mathbf{0})=0,\quad \overline{w_{i,k}(\mathbf{x})\,w_{j,k}(\mathbf{x})}=0,\quad ij=13,23 \tag{2.70}$$

which hold within the third-order and the fourth-order models too.

Similarly, within the fourth-order model, the statistical mirror symmetry of (2.33) or its corresponding representation in the physical space (2.28) implies that

$$\begin{aligned}
&U_{(ij)k}(\mathbf{r})=(-1)^{\delta_{\underline{i}3}+\delta_{\underline{j}3}+\delta_{\underline{k}3}}\,U_{(\underline{i}\,\underline{j})\,\underline{k}}(\mathbf{r}),\quad U_{ijk}(\mathbf{r},\mathbf{s})=(-1)^{\delta_{\underline{i}3}+\delta_{\underline{j}3}+\delta_{\underline{k}3}}\,U_{\underline{i}\,\underline{j}\,\underline{k}}(\mathbf{r},\mathbf{s}),\quad Q_3(\mathbf{r})=-Q_3(\mathbf{r}),\\
&U_{(ij)kl}(\mathbf{r},\mathbf{s})=(-1)^{\delta_{\underline{i}3}+\delta_{\underline{j}3}+\delta_{\underline{k}3}+\delta_{\underline{l}3}}\,U_{(\underline{i}\,\underline{j})\,\underline{k}\,\underline{l}}(\mathbf{r},\mathbf{s}),\quad Q_{ij}(\mathbf{r},\mathbf{s})=(-1)^{\delta_{\underline{i}3}+\delta_{\underline{j}3}}\,Q_{\underline{i}\,\underline{j}}(\mathbf{r},\mathbf{s}),\\
&\mathbf{r}:=(r_1,r_2,0),\quad \mathbf{s}:=(s_1,s_2,0)
\end{aligned} \tag{2.71}$$

Furthermore, in order to minimize computational complexity, we need to examine the symmetries of (2.31) and (2.33) for the third and fourth order correlations $\tilde{U}_{ijk}(\mathbf{k},\mathbf{l})$ and $\tilde{U}_{(ij)kl}(\mathbf{k},\mathbf{l})$ to see how the arguments $\mathbf{k}$ and $\mathbf{l}$ can be restricted to certain octants where the correlation distributions can be taken as the basic elements, the elements that can be employed to construct the distributions in the whole wave-number spaces of $\mathbf{k}$ and $\mathbf{l}$.

Motivated by the supposed boundedness of $\tilde{U}_{ij}(\mathbf{k})$, $\tilde{U}^{(I)}_{(ij)k}(\mathbf{k})$, $\tilde{U}^{(I)}_{ijk}(\mathbf{k},\mathbf{l})$ and $\tilde{U}_{(ij)kl}(\mathbf{k},\mathbf{l})$, the structures of (2.42) through (2.67), and the symmetries of (2.31) and (2.33), we adopt the following decompositions of

$$\tilde{U}_{ij}(\mathbf{k})=(k_3)^2\,\dot{U}_{ij}(\mathbf{k}),\quad ij=11,12,22 \tag{2.72}$$

$$\tilde{U}^{(I)}_{(ij)k}(\mathbf{k})=(k_3)^2\,\dot{U}^{(I)}_{(ij)k}(\mathbf{k}),\quad ij=11,12,13,22,23,33,\ k=1,2 \tag{2.73}$$

$$\tilde{U}^{(I)}_{ijk}(\mathbf{k},\mathbf{l})=(k_3)^2\,(l_3)^2\,(k_3+l_3)^2\,\dot{U}^{(I)}_{ijk}(\mathbf{k},\mathbf{l}),\quad ijk=111,112,122,222 \tag{2.74}$$

and

$$\tilde{U}_{(ij)kl}(\mathbf{k},\mathbf{l})=(k_3)^2\,(l_3)^2\,(k_3+l_3)^2\,\dot{U}_{(ij)kl}(\mathbf{k},\mathbf{l}),\ ij=11,12,13,22,23,33,\ kl=11,12,13,22,23 \tag{2.75}$$

These newly introduced quantities of $\dot{U}_{ij}(\mathbf{k})$, $\dot{U}^{(I)}_{(ij)k}(\mathbf{k})$, $\dot{U}^{(I)}_{ijk}(\mathbf{k},\mathbf{l})$ and $\dot{U}_{(ij)kl}(\mathbf{k},\mathbf{l})$ obey the same symmetries as those listed in (2.31) and (2.33). The above transformations cancel out the denominators contained in (2.42) through (2.45), and consequently, bounded distributions of the primary components of $\dot{U}_{ij}(\mathbf{k})$, $\dot{U}^{(I)}_{(ij)k}(\mathbf{k})$, $\dot{U}^{(I)}_{ijk}(\mathbf{k},\mathbf{l})$ and $\dot{U}_{(ij)kl}(\mathbf{k},\mathbf{l})$, together with finite supports for the correlations, automatically guarantee bounded distributions of $\tilde{U}_{ij}(\mathbf{k})$, $\tilde{U}^{(I)}_{(ij)k}(\mathbf{k})$, $\tilde{U}^{(I)}_{ijk}(\mathbf{k},\mathbf{l})$ and $\tilde{U}_{(ij)kl}(\mathbf{k},\mathbf{l})$.

Consistent with (2.73) and (2.74), we have

$$\tilde{\gamma}_{ij}(\mathbf{k})=(k_3)^2\,\dot{\gamma}_{ij}(\mathbf{k}),\quad \dot{\gamma}_{ij}(-\mathbf{k})=\dot{\gamma}_{ij}(\mathbf{k})=\dot{\gamma}_{ij}(k_1,k_2,-k_3),\quad ij=11,12,22 \tag{2.76}$$

2.8 Constraints of Inequality Involving Only $\tilde{U}_{ij}(\mathbf{k})$

We have the choice of adopting the second-order, the third-order or the fourth-order model. Accordingly, we may divide the constraints into two categories. The present category deals with the constraints involving only $\tilde{U}_{ij}(\mathbf{k})$, which can be enforced within any of the three models.

We can construct the constraints in the physical space and infer their counterparts in the Fourier wave-number space. More importantly, we can construct the constraints either directly based on $\overline{w_i(\mathbf{x})\, w_j(\mathbf{y})}$ as well as its spatial derivatives or based on the structure functions ([5], [15]).

2.8.1 Constraints Constructed Directly on $\overline{w_i(\mathbf{x})\, w_j(\mathbf{y})}$, $\overline{\omega_i(\mathbf{x})\, \omega_j(\mathbf{y})}$ or the Like

We discuss first the constraints for $\overline{w_i(\mathbf{x})\, w_j(\mathbf{x})}$, $\overline{w_i(\mathbf{x})\, w_j(\mathbf{y})}$, $\overline{w_{i,k}(\mathbf{x})\, w_{j,k}(\mathbf{x})}$, $\overline{\omega_i(\mathbf{x})\, \omega_j(\mathbf{y})}$, and $\overline{w_i(\mathbf{x})\, \omega_j(\mathbf{y})}$ that can be simply established. Here, $\omega_i(\mathbf{x})$ denotes the fluctuation vorticity field.

Physically, we need to impose the known realizability condition of

$$\overline{w_i(\mathbf{x})\, w_j(\mathbf{x})} \ \text{ being positive semi-definite} \tag{2.77}$$

With the help of (2.70), the requirement reduces to

$$U_{\underline{i}\,\underline{i}}(\mathbf{0}) \geq 0, \quad \big(U_{12}(\mathbf{0})\big)^2 \leq U_{11}(\mathbf{0})\, U_{22}(\mathbf{0}) \tag{2.78}$$

or

$$\int_{\mathbb{R}^3} d\mathbf{k}\, \tilde{U}_{\underline{i}\,\underline{i}}(\mathbf{k}) \geq 0, \quad \bigg(\int_{\mathbb{R}^3} d\mathbf{k}\, \tilde{U}_{12}(\mathbf{k})\bigg)^2 \leq \int_{\mathbb{R}^3} d\mathbf{k}\, \tilde{U}_{11}(\mathbf{k}) \int_{\mathbb{R}^3} d\mathbf{l}\, \tilde{U}_{22}(\mathbf{l}) \tag{2.79}$$

whose second part is a special case of the Cauchy-Schwarz inequality (2.81).

Next, we apply the Cauchy-Schwarz inequality $\big|\overline{ab}\big|^2 \leq \overline{aa}\,\overline{bb}$ to $\overline{w_i(\mathbf{x})\, w_j(\mathbf{y})}$ to get

$$\Big|\overline{w_i(\mathbf{x}) w_j(\mathbf{y})}\Big|^2 \leq \overline{w_{\underline{i}}(\mathbf{x}) w_{\underline{i}}(\mathbf{x})}\ \overline{w_{\underline{j}}(\mathbf{y}) w_{\underline{j}}(\mathbf{y})} \tag{2.80}$$

which can be recast equivalently as

$$\bigg|\int_{\mathbb{R}^3} d\mathbf{k}\, \tilde{U}_{ij}(\mathbf{k})\, \cos(\mathbf{k}\cdot\mathbf{r})\bigg|^2 \leq \int_{\mathbb{R}^3} d\mathbf{k}\, \tilde{U}_{\underline{i}\,\underline{i}}(\mathbf{k}) \int_{\mathbb{R}^3} d\mathbf{l}\, \tilde{U}_{\underline{j}\,\underline{j}}(\mathbf{l}), \quad ij = 12, 13, 23 \tag{2.81}$$

The case of $ij = 11$, 22 and 33 is trivial under both the supposed nonnegative spectra to be introduced and

$$\bigg|\int_{\mathbb{R}^3} d\mathbf{k}\, \tilde{U}_{\underline{i}\,\underline{i}}(\mathbf{k})\, \cos(\mathbf{k}\cdot\mathbf{r})\bigg| \leq \int_{\mathbb{R}^3} d\mathbf{k}\, \Big|\tilde{U}_{\underline{i}\,\underline{i}}(\mathbf{k})\, \cos(\mathbf{k}\cdot\mathbf{r})\Big| \leq \int_{\mathbb{R}^3} d\mathbf{k}\, \tilde{U}_{\underline{i}\,\underline{i}}(\mathbf{k})$$

To understand the necessity of (2.81), we examine the specific case of

$$\bigg|\int_{\mathbb{R}^3} d\mathbf{k}\, \tilde{U}_{12}(\mathbf{k})\, \cos(\mathbf{k}\cdot\mathbf{r})\bigg|^2 \leq \int_{\mathbb{R}^3} d\mathbf{k}\, \tilde{U}_{11}(\mathbf{k}) \int_{\mathbb{R}^3} d\mathbf{l}\, \tilde{U}_{22}(\mathbf{l})$$

Since $\tilde{U}_{11}(\mathbf{k})$, $\tilde{U}_{12}(\mathbf{k})$ and $\tilde{U}_{22}(\mathbf{k})$ are the three primary components of $\tilde{U}_{ij}(\mathbf{k})$, there is no automatic guarantee of the satisfaction of the above inequality, unlike the case of two-dimensional homogeneous shear turbulence discussed in PART II. Therefore, we need to impose (2.81) explicitly.

Considering its relevance to the viscous dissipation of turbulent fluctuation energy, we require that

$$\overline{w_{i,k}(\mathbf{x})\, w_{j,k}(\mathbf{x})} \ \text{ be positive semi-definite} \tag{2.82}$$

whose combination with (2.70) gives

$$\overline{w_{\underline{i},k}(\mathbf{x})\, w_{\underline{i},k}(\mathbf{x})} \geq 0, \quad \left(\overline{w_{1,k}(\mathbf{x})\, w_{2,k}(\mathbf{x})}\right)^2 \leq \overline{w_{1,k}(\mathbf{x})\, w_{1,k}(\mathbf{x})}\ \overline{w_{2,l}(\mathbf{x})\, w_{2,l}(\mathbf{x})} \tag{2.83}$$

or

$$\int_{\mathbb{R}^3} d\mathbf{k}\, |\mathbf{k}|^2\, \tilde{U}_{\underline{i}\,\underline{i}}(\mathbf{k}) \geq 0, \quad \left(\int_{\mathbb{R}^3} d\mathbf{k}\, |\mathbf{k}|^2\, \tilde{U}_{12}(\mathbf{k})\right)^2 \leq \int_{\mathbb{R}^3} d\mathbf{k}\, |\mathbf{k}|^2\, \tilde{U}_{11}(\mathbf{k}) \int_{\mathbb{R}^3} d\mathbf{l}\, |\mathbf{l}|^2\, \tilde{U}_{22}(\mathbf{l}) \tag{2.84}$$

The constraint should be imposed explicitly since $\tilde{U}_{11}(\mathbf{k})$, $\tilde{U}_{12}(\mathbf{k})$ and $\tilde{U}_{22}(\mathbf{k})$ are the primary components. There is still the question whether we should apply the Cauchy-Schwarz inequality to $\overline{w_{i,k}(\mathbf{x})\, w_{j,l}(\mathbf{y})}$ to obtain additional constraints about the correlation between the fluctuation velocity gradients.

The vorticity plays a significant role in turbulent flows ([3], [5]), and its effect on the turbulence modeling may be partially realized by the Cauchy-Schwarz inequality to $\overline{\omega_i(\mathbf{x})\, \omega_j(\mathbf{y})}$,

$$\overline{\omega_{\underline{i}}(\mathbf{x})\, \omega_{\underline{i}}(\mathbf{x})} \geq 0, \quad \left|\overline{\omega_i(\mathbf{x})\, \omega_j(\mathbf{y})}\right|^2 \leq \overline{\omega_{\underline{i}}(\mathbf{x})\, \omega_{\underline{i}}(\mathbf{x})}\ \overline{\omega_{\underline{j}}(\mathbf{y})\, \omega_{\underline{j}}(\mathbf{y})}, \quad i \leq j \tag{2.85}$$

with the vorticity field defined by

$$\omega_i(\mathbf{x}) := \epsilon_{imn}\, w_{m,n}(\mathbf{x})$$

Here, ϵ_{ijk} is the alternating tensor. In terms of the correlation in the wave-number space, we have the representations of

$$\overline{\omega_i(\mathbf{x})\, \omega_j(\mathbf{y})} = \overline{\omega_i\, \omega_j}(\mathbf{r}) = \int_{\mathbb{R}^3} d\mathbf{k}\, \overline{\tilde{\omega}_i\, \tilde{\omega}_j}(\mathbf{k})\, \cos(\mathbf{k}\cdot\mathbf{r}), \quad \overline{\tilde{\omega}_i\, \tilde{\omega}_j}(\mathbf{k}) = \epsilon_{imn}\, \epsilon_{jkl}\, k_n\, k_l\, \tilde{U}_{mk}(\mathbf{k}) \tag{2.86}$$

and

$$\int_{\mathbb{R}^3} d\mathbf{k}\, \overline{\tilde{\omega}_{\underline{i}}\, \tilde{\omega}_{\underline{i}}}(\mathbf{k}) \geq 0, \quad \left|\int_{\mathbb{R}^3} d\mathbf{k}\, \overline{\tilde{\omega}_i\, \tilde{\omega}_j}(\mathbf{k})\, \cos(\mathbf{k}\cdot\mathbf{r})\right|^2 \leq \int_{\mathbb{R}^3} d\mathbf{k}\, \overline{\tilde{\omega}_{\underline{i}}\, \tilde{\omega}_{\underline{i}}}(\mathbf{k}) \int_{\mathbb{R}^3} d\mathbf{l}\, \overline{\tilde{\omega}_{\underline{j}}\, \tilde{\omega}_{\underline{j}}}(\mathbf{l}), \quad i \leq j \tag{2.87}$$

As a natural company to $\overline{w_i(\mathbf{x})\, w_j(\mathbf{y})}$ of (2.80) and $\overline{\omega_i(\mathbf{x})\, \omega_j(\mathbf{y})}$ of (2.85), we consider $\overline{w_i(\mathbf{x})\, \omega_j(\mathbf{y})}$, a special case of $\overline{w_i(\mathbf{x})\, w_{j,k}(\mathbf{y})}$ and closely relevant to the notion of helicity and the concept of the Lamb vector [17]. The application of the Cauchy-Schwarz inequality to this correlation results in

$$\left|\overline{w_i(\mathbf{x})\, \omega_j(\mathbf{y})}\right|^2 \leq \overline{w_{\underline{i}}(\mathbf{x})\, w_{\underline{i}}(\mathbf{x})}\ \overline{\omega_{\underline{j}}(\mathbf{y})\, \omega_{\underline{j}}(\mathbf{y})}, \quad \forall i, j \tag{2.88}$$

where

$$\overline{w_i(\mathbf{x})\,\omega_j(\mathbf{y})} = \overline{w_i\,\omega_j}(\mathbf{r}) = \imath \int_{\mathbb{R}^3} d\mathbf{k}\,\overline{\tilde{w}_i\,\tilde{\omega}_j}(\mathbf{k})\,\sin(\mathbf{k}\cdot\mathbf{r}), \quad \overline{\tilde{w}_i\,\tilde{\omega}_j}(\mathbf{k}) = \imath\,\epsilon_{jpq}\,k_q\,\tilde{U}_{ip}(\mathbf{k}) \tag{2.89}$$

Therefore,

$$\left| \int_{\mathbb{R}^3} d\mathbf{k}\,\overline{\tilde{w}_i\,\tilde{\omega}_j}(\mathbf{k})\,\sin(\mathbf{k}\cdot\mathbf{r}) \right|^2 \leq \int_{\mathbb{R}^3} d\mathbf{k}\,\tilde{U}_{\underline{i}\,\underline{i}}(\mathbf{k}) \int_{\mathbb{R}^3} d\mathbf{l}\,\overline{\tilde{\omega}_{\underline{j}}\,\tilde{\omega}_{\underline{j}}}(\mathbf{l}), \quad \forall i,j \tag{2.90}$$

We have presented so far the constraints for the second order correlation based directly on the two-point correlations of fluctuation velocity and vorticity fields and the single-point correlation of fluctuation velocity gradient relevant to the viscous dissipation. Many other inequalities of correlations can be established related to the partial spatial derivatives of $\overline{w_i(\mathbf{x})\,w_j(\mathbf{y})}$ of various orders. More number of constraints may imply better optimal solutions, it can, however, add more complexity to the problem formulated and pose a greater challenge to the determination of these solutions.

The above constraints in the physical space are constructed with the straight-forward reasonings. There are, however, a few complications in the implementation of the constraints in numerical simulation. One is that all the constraints are global in nature from the integration over the Fourier wave-number space, these constraints are then not sparse in terms of the (discretized) control variables and pose greater challenges to the determination of the optimal solutions. Next is that an adequate set of spatial collocation points for $\mathbf{r}$ needs to be chosen in order to enforce the constraints. The third is that the constraints involve four-dimensional integrals or higher as to be seen; Coupled with the number of the integrals required at each and every collocation point, the computational time for the integrations is tremendous. For the constraints constructed above, there is a possible way to overcome the mentioned complications by converting these constraints to the ones in the Fourier wave-number space, which is pursued here.

Within the Fourier transforms of (2.29), we have

$$\overline{w_i(\mathbf{x})w_j(\mathbf{y})} = \int_{\mathbb{R}^3} d\mathbf{k}\,\tilde{U}_{ij}(\mathbf{k})\,\exp[\imath\,\mathbf{k}\cdot(\mathbf{y}-\mathbf{x})] = \int_{\mathbb{R}^3} d\mathbf{k}\,\tilde{U}_{ij}(\mathbf{k})\,\cos(\mathbf{k}\cdot(\mathbf{y}-\mathbf{x})) \tag{2.91}$$

Due to the restriction of the homogeneity, we have the combination of $\mathbf{y}-\mathbf{x}$ as the single spatial variable and the corresponding single wave-number variable $\mathbf{k}$ present in the integrands, which makes it impossible to apply straight-forwardly the Cauchy-Schwarz inequality to the correlation of $\tilde{U}_{ij}(\mathbf{k})$.

As a simple solution, let us look at the fact that the Cartesian coordinate system $\mathbf{x}$ underlying (2.91) can be arbitrarily oriented, and the corresponding Cartesian coordinate system $\mathbf{k}$ can be arbitrarily oriented too. In any of such coordinate system of $\mathbf{k}$, we impose the constraint of the turbulent energy spectra $\tilde{U}_{\underline{i}\,\underline{i}}(\mathbf{k}) \geq 0$, which implies that $\tilde{U}_{ij}(\mathbf{k})$ is positive semi-definite, i.e.,

$$\tilde{U}_{\underline{i}\,\underline{i}}(\mathbf{k}) \geq 0, \quad \left|\tilde{U}_{ij}(\mathbf{k})\right|^2 \leq \tilde{U}_{\underline{i}\underline{i}}(\mathbf{k})\;\tilde{U}_{\underline{j}\underline{j}}(\mathbf{k}), \quad i \leq j \tag{2.92}$$

which will be justified from another angle in Sub-subsection 2.8.2. Furthermore, with the help of the expressions like

$$\overline{\tilde{\omega}_1\,\tilde{\omega}_1}(\mathbf{k}) \geq \left(|k_3|\,\sqrt{\tilde{U}_{22}(\mathbf{k})} - |k_2|\,\sqrt{\tilde{U}_{33}(\mathbf{k})}\right)^2 + 2\,|k_2|\,|k_3|\,\left(\sqrt{\tilde{U}_{22}(\mathbf{k})}\,\sqrt{\tilde{U}_{33}(\mathbf{k})} - \left|\tilde{U}_{23}(\mathbf{k})\right|\right),$$

$$\begin{aligned}
&\overline{\tilde{\omega}_1\,\tilde{\omega}_1}(\mathbf{k})\,\overline{\tilde{\omega}_3\,\tilde{\omega}_3}(\mathbf{k}) - \left(\overline{\tilde{\omega}_1\,\tilde{\omega}_3}(\mathbf{k})\right)^2 \\
&= (k_2)^2\,\left[(k_3)^2 + 2\,(k_1)^2\right]\left(\tilde{U}_{11}(\mathbf{k})\,\tilde{U}_{22}(\mathbf{k}) - \left(\tilde{U}_{12}(\mathbf{k})\right)^2\right) + (k_1)^2\,(k_2)^2\,\left(\tilde{U}_{22}(\mathbf{k})\,\tilde{U}_{33}(\mathbf{k}) - \left(\tilde{U}_{23}(\mathbf{k})\right)^2\right) \\
&\quad + (k_2)^2\,\left[(k_2)^2 + 2\,(k_1)^2 + 2\,(k_3)^2\right]\left(\tilde{U}_{33}(\mathbf{k})\,\tilde{U}_{11}(\mathbf{k}) - \left(\tilde{U}_{13}(\mathbf{k})\right)^2\right)
\end{aligned} \tag{2.93}$$

and

$$\begin{aligned}
&\tilde{U}_{11}(\mathbf{k})\,\overline{\tilde{\omega}_1\,\tilde{\omega}_1}(\mathbf{k}) - \left|\overline{\tilde{w}_1\,\tilde{\omega}_1}(\mathbf{k})\right|^2 \\
&= \left[(k_3)^2 + 2\,(k_2)^2\right]\,\left(\tilde{U}_{11}(\mathbf{k})\,\tilde{U}_{22}(\mathbf{k}) - \left(\tilde{U}_{12}(\mathbf{k})\right)^2\right) + (k_2)^2\,\left(\tilde{U}_{11}(\mathbf{k})\,\tilde{U}_{33}(\mathbf{k}) - \left(\tilde{U}_{13}(\mathbf{k})\right)^2\right), \\
&\tilde{U}_{11}(\mathbf{k})\,\overline{\tilde{\omega}_2\,\tilde{\omega}_2}(\mathbf{k}) - \left|\overline{\tilde{w}_1\,\tilde{\omega}_2}(\mathbf{k})\right|^2 = (k_1)^2\,\left(\tilde{U}_{11}(\mathbf{k})\,\tilde{U}_{33}(\mathbf{k}) - \left(\tilde{U}_{13}(\mathbf{k})\right)^2\right)
\end{aligned} \tag{2.94}$$

we can verify that the inequality constraints of (2.92) guarantee that

$$\overline{\tilde{\omega}_{\underline{i}}\,\tilde{\omega}_{\underline{i}}}(\mathbf{k}) \geq 0, \quad \left|\overline{\tilde{\omega}_i\,\tilde{\omega}_j}(\mathbf{k})\right|^2 \leq \overline{\tilde{\omega}_{\underline{i}}\,\tilde{\omega}_{\underline{i}}}(\mathbf{k})\;\overline{\tilde{\omega}_{\underline{j}}\,\tilde{\omega}_{\underline{j}}}(\mathbf{k}), \tag{2.95}$$

and

$$\left|\overline{\tilde{w}_i\,\tilde{\omega}_j}(\mathbf{k})\right|^2 \leq \tilde{U}_{\underline{i}\,\underline{i}}(\mathbf{k})\;\overline{\tilde{\omega}_{\underline{j}}\,\tilde{\omega}_{\underline{j}}}(\mathbf{k}) \tag{2.96}$$

As expected, these inequalities in the wave-number space make the integral inequalities constructed above in the physical space satisfied automatically. To prove this claim, it is sufficient to consider the simpler form of

$$|\tilde{c}(\mathbf{k})|^2 \leq \tilde{a}(\mathbf{k})\,\tilde{b}(\mathbf{k}), \quad \tilde{a} \geq 0, \;\; \tilde{b} \geq 0 \tag{2.97}$$

This inequality can be linearized in the form of

$$|\tilde{c}| \leq \sqrt{\tilde{a}}\,\sqrt{\tilde{b}} \leq \frac{1}{2}\left(\lambda\,\tilde{a} + \frac{\tilde{b}}{\lambda}\right), \;\; \forall \lambda > 0 \tag{2.98}$$

with the help of $\left(\sqrt{\lambda}\,\sqrt{\tilde{a}} - \sqrt{\tilde{b}}/\sqrt{\lambda}\right)^2 \geq 0$. We now integrate (2.98) in the wave-number space and then set $\lambda = \left(\int d\mathbf{k}\,\tilde{b}/\int d\mathbf{k}\,\tilde{a}\right)^{1/2}$ to obtain

$$\left(\int_{\mathbb{R}^3} d\mathbf{k}\,|\tilde{c}|\right)^2 \leq \int_{\mathbb{R}^3} d\mathbf{k}\,\tilde{a}\,\int_{\mathbb{R}^3} d\mathbf{k}\,\tilde{b} \tag{2.99}$$

Furthermore, we have

$$\left|\int_{\mathbb{R}^3} d\mathbf{k}\,\tilde{c}\,f\right|^2 \leq \left(\int_{\mathbb{R}^3} d\mathbf{k}\,|\tilde{c}|\,|f|\right)^2 \leq \int_{\mathbb{R}^3} d\mathbf{k}\,\tilde{a}\,\int_{\mathbb{R}^3} d\mathbf{k}\,\tilde{b}, \quad \forall |f| \leq 1 \tag{2.100}$$

Consequently, it is sufficient to enforce only (2.92), to satisfy all the constraints listed in this sub-subsection.

2.8.2 Constraints Constructed on the Basis of Structure Functions

Besides the above inequalities, we can also generate the constraints of inequality involving only the second order correlation by applying the Cauchy-Schwarz inequality to the structure functions, such as [15]

$$\begin{aligned}
&\overline{[w_i(\mathbf{y}) - w_i(\mathbf{x}) + \alpha(w_i(\mathbf{z}') - w_i(\mathbf{z}))]\,[w_j(\mathbf{z}') - w_j(\mathbf{z}) - \beta(w_j(\mathbf{y}) - w_j(\mathbf{x}))]},\\
&\overline{[\omega_i(\mathbf{y}) - \omega_i(\mathbf{x}) + \alpha(\omega_i(\mathbf{z}') - \omega_i(\mathbf{z}))]\,[\omega_j(\mathbf{z}') - \omega_j(\mathbf{z}) - \beta(\omega_j(\mathbf{y}) - \omega_j(\mathbf{x}))]},\\
&\overline{[w_i(\mathbf{y}) - w_i(\mathbf{x}) + \alpha(w_i(\mathbf{z}') - w_i(\mathbf{z}))]\,[\omega_j(\mathbf{z}') - \omega_j(\mathbf{z}) - \beta(\omega_j(\mathbf{y}) - \omega_j(\mathbf{x}))]}
\end{aligned} \tag{2.101}$$

with α and β being any non-stochastic functions of time and spatial vectors. This specific set results in the following constraints of inequality,

$$\begin{aligned}
&\Big[2\,\alpha\Big(U_{ij}(\mathbf{0}) - U_{ij}(\mathbf{s}'-\mathbf{s})\Big) - 2\,\beta\Big(U_{ij}(\mathbf{0}) - U_{ij}(\mathbf{r})\Big)\\
&\quad + (1-\alpha\beta)\Big(U_{ij}(\mathbf{s}'-\mathbf{r}) - U_{ij}(\mathbf{s}-\mathbf{r}) - U_{ij}(\mathbf{s}') + U_{ij}(\mathbf{s})\Big)\Big]^2\\
&\le 4\,\Big[U_{\underline{i}\,\underline{i}}(\mathbf{0}) - U_{\underline{i}\,\underline{i}}(\mathbf{r}) + \alpha^2\Big(U_{\underline{i}\,\underline{i}}(\mathbf{0}) - U_{\underline{i}\,\underline{i}}(\mathbf{s}'-\mathbf{s})\Big)\\
&\qquad + \alpha\Big(U_{\underline{i}\,\underline{i}}(\mathbf{s}'-\mathbf{r}) - U_{\underline{i}\,\underline{i}}(\mathbf{s}-\mathbf{r}) - U_{\underline{i}\,\underline{i}}(\mathbf{s}') + U_{\underline{i}\,\underline{i}}(\mathbf{s})\Big)\Big]\\
&\quad \times \Big[U_{\underline{j}\,\underline{j}}(\mathbf{0}) - U_{\underline{j}\,\underline{j}}(\mathbf{s}'-\mathbf{s}) + \beta^2\Big(U_{\underline{j}\,\underline{j}}(\mathbf{0}) - U_{\underline{j}\,\underline{j}}(\mathbf{r})\Big)\\
&\qquad - \beta\Big(U_{\underline{j}\,\underline{j}}(\mathbf{s}'-\mathbf{r}) - U_{\underline{j}\,\underline{j}}(\mathbf{s}-\mathbf{r}) - U_{\underline{j}\,\underline{j}}(\mathbf{s}') + U_{\underline{j}\,\underline{j}}(\mathbf{s})\Big)\Big]
\end{aligned} \tag{2.102}$$

$$\begin{aligned}
&\Big[2\,\alpha\Big(\overline{\omega_i\omega_j}(\mathbf{0}) - \overline{\omega_i\omega_j}(\mathbf{s}'-\mathbf{s})\Big) - 2\,\beta\Big(\overline{\omega_i\omega_j}(\mathbf{0}) - \overline{\omega_i\omega_j}(\mathbf{r})\Big)\\
&\quad + (1-\alpha\beta)\Big(\overline{\omega_i\omega_j}(\mathbf{s}'-\mathbf{r}) - \overline{\omega_i\omega_j}(\mathbf{s}-\mathbf{r}) - \overline{\omega_i\omega_j}(\mathbf{s}') + \overline{\omega_i\omega_j}(\mathbf{s})\Big)\Big]^2\\
&\le 4\,\Big[\overline{\omega_{\underline{i}}\omega_{\underline{i}}}(\mathbf{0}) - \overline{\omega_{\underline{i}}\omega_{\underline{i}}}(\mathbf{r}) + \alpha^2\Big(\overline{\omega_{\underline{i}}\omega_{\underline{i}}}(\mathbf{0}) - \overline{\omega_{\underline{i}}\omega_{\underline{i}}}(\mathbf{s}'-\mathbf{s})\Big)\\
&\qquad + \alpha\Big(\overline{\omega_{\underline{i}}\omega_{\underline{i}}}(\mathbf{s}'-\mathbf{r}) - \overline{\omega_{\underline{i}}\omega_{\underline{i}}}(\mathbf{s}-\mathbf{r}) - \overline{\omega_{\underline{i}}\omega_{\underline{i}}}(\mathbf{s}') + \overline{\omega_{\underline{i}}\omega_{\underline{i}}}(\mathbf{s})\Big)\Big]\\
&\quad \times \Big[\overline{\omega_{\underline{j}}\omega_{\underline{j}}}(\mathbf{0}) - \overline{\omega_{\underline{j}}\omega_{\underline{j}}}(\mathbf{s}'-\mathbf{s}) + \beta^2\Big(\overline{\omega_{\underline{j}}\omega_{\underline{j}}}(\mathbf{0}) - \overline{\omega_{\underline{j}}\omega_{\underline{j}}}(\mathbf{r})\Big)\\
&\qquad - \beta\Big(\overline{\omega_{\underline{j}}\omega_{\underline{j}}}(\mathbf{s}'-\mathbf{r}) - \overline{\omega_{\underline{j}}\omega_{\underline{j}}}(\mathbf{s}-\mathbf{r}) - \overline{\omega_{\underline{j}}\omega_{\underline{j}}}(\mathbf{s}') + \overline{\omega_{\underline{j}}\omega_{\underline{j}}}(\mathbf{s})\Big)\Big]
\end{aligned} \tag{2.103}$$

and

$$\begin{aligned}
&\Big[(1+\alpha\beta)\Big(\overline{w_i\omega_j}(\mathbf{s}'-\mathbf{r}) - \overline{w_i\omega_j}(\mathbf{s}-\mathbf{r}) - \overline{w_i\omega_j}(\mathbf{s}') + \overline{w_i\omega_j}(\mathbf{s})\Big)\Big]^2\\
&\le 4\,\Big[U_{\underline{i}\,\underline{i}}(\mathbf{0}) - U_{\underline{i}\,\underline{i}}(\mathbf{r}) + \alpha^2\Big(U_{\underline{i}\,\underline{i}}(\mathbf{0}) - U_{\underline{i}\,\underline{i}}(\mathbf{s}'-\mathbf{s})\Big)
\end{aligned}$$

$$+\alpha\Big(U_{\underline{i}\,\underline{i}}(\mathbf{s}'-\mathbf{r})-U_{\underline{i}\,\underline{i}}(\mathbf{s}-\mathbf{r})-U_{\underline{i}\,\underline{i}}(\mathbf{s}')+U_{\underline{i}\,\underline{i}}(\mathbf{s})\Big)\Big]$$
$$\times\Big[\overline{\omega_{\underline{j}}\omega_{\underline{j}}}(\mathbf{0})-\overline{\omega_{\underline{j}}\omega_{\underline{j}}}(\mathbf{s}'-\mathbf{s})+\beta^2\Big(\overline{\omega_{\underline{j}}\omega_{\underline{j}}}(\mathbf{0})-\overline{\omega_{\underline{j}}\omega_{\underline{j}}}(\mathbf{r})\Big)$$
$$-\beta\Big(\overline{\omega_{\underline{j}}\omega_{\underline{j}}}(\mathbf{s}'-\mathbf{r})-\overline{\omega_{\underline{j}}\omega_{\underline{j}}}(\mathbf{s}-\mathbf{r})-\overline{\omega_{\underline{j}}\omega_{\underline{j}}}(\mathbf{s}')+\overline{\omega_{\underline{j}}\omega_{\underline{j}}}(\mathbf{s})\Big)\Big] \tag{2.104}$$

Here,

$$U_{ij}(\mathbf{r})=\int_{\mathbb{R}^3}d\mathbf{k}\,\tilde{U}_{ij}(\mathbf{k})\,\cos(\mathbf{k}\cdot\mathbf{r}),\quad \overline{\omega_i\omega_j}(\mathbf{r})=\int_{\mathbb{R}^3}d\mathbf{k}\,\overline{\tilde{\omega}_i\,\tilde{\omega}_j}(\mathbf{k})\,\cos(\mathbf{k}\cdot\mathbf{r}),$$
$$\overline{w_i\omega_j}(\mathbf{r})=\int_{\mathbb{R}^3}d\mathbf{k}\,\overline{\tilde{w}_i\,\tilde{\omega}_j}(\mathbf{k})\,\imath\,\sin(\mathbf{k}\cdot\mathbf{r}) \tag{2.105}$$

following from their respective properties of symmetry. Each inequality above involves essentially a scalar function defined in a high-dimensional space composed of the components of $\mathbf{r}$, $\mathbf{s}$, $\mathbf{s}'$ and t. Additional inequalities can be produced similarly based on other structure functions. We expect that these quadratic constraints play a significant role to constrain directly the structures of $\tilde{U}_{ij}(\mathbf{k})$, $ij=11,12,22$, and indirectly the structures of the control variables.

One concern is whether the constraints like (2.102) through (2.104) are redundant under (2.92). To answer this question, we substitute (2.105) into (2.102) through (2.104) to get

$$\Big|\int_{\mathbb{R}^3}d\mathbf{k}\,\tilde{U}_{ij}(\mathbf{k})\,f_c\Big|^2\le\Big(\int_{\mathbb{R}^3}d\mathbf{k}\,\tilde{U}_{\underline{i}\,\underline{i}}(\mathbf{k})\,f_a\Big)\Big(\int_{\mathbb{R}^3}d\mathbf{k}\,\tilde{U}_{\underline{j}\,\underline{j}}(\mathbf{k})\,f_b\Big),$$
$$\Big|\int_{\mathbb{R}^3}d\mathbf{k}\,\overline{\tilde{\omega}_i\,\tilde{\omega}_j}(\mathbf{k})\,f_c\Big|^2\le\Big(\int_{\mathbb{R}^3}d\mathbf{k}\,\overline{\tilde{\omega}_{\underline{i}}\tilde{\omega}_{\underline{i}}}(\mathbf{k})\,f_a\Big)\Big(\int_{\mathbb{R}^3}d\mathbf{k}\,\overline{\tilde{\omega}_{\underline{j}}\tilde{\omega}_{\underline{j}}}(\mathbf{k})\,f_b\Big) \tag{2.106}$$

with

$$f_a:=2\Big(1-\cos(\mathbf{k}\cdot\mathbf{r})+\alpha^2\big(1-\cos(\mathbf{k}\cdot(\mathbf{s}'-\mathbf{s}))\big)$$
$$+\alpha\big(\cos(\mathbf{k}\cdot(\mathbf{s}'-\mathbf{r}))-\cos(\mathbf{k}\cdot(\mathbf{s}-\mathbf{r}))-\cos(\mathbf{k}\cdot\mathbf{s}')+\cos(\mathbf{k}\cdot\mathbf{s})\big)\Big)$$
$$=4\bigg(\Big|\sin\frac{\mathbf{r}\cdot\mathbf{k}}{2}\Big|^2+\Big|\alpha\sin\frac{(\mathbf{s}'-\mathbf{s})\cdot\mathbf{k}}{2}\Big|^2+2\sin\frac{\mathbf{r}\cdot\mathbf{k}}{2}\,\alpha\sin\frac{(\mathbf{s}'-\mathbf{s})\cdot\mathbf{k}}{2}\,\cos\frac{(\mathbf{s}'+\mathbf{s}-\mathbf{r})\cdot\mathbf{k}}{2}\bigg)$$
$$\ge 4\bigg(\Big|\sin\frac{\mathbf{r}\cdot\mathbf{k}}{2}\Big|-\Big|\alpha\sin\frac{(\mathbf{s}'-\mathbf{s})\cdot\mathbf{k}}{2}\Big|\bigg)^2\ge 0,$$
$$f_b:=2\Big(1-\cos(\mathbf{k}\cdot(\mathbf{s}'-\mathbf{s}))+\beta^2\big(1-\cos(\mathbf{k}\cdot\mathbf{r})\big)$$
$$-\beta\big(\cos(\mathbf{k}\cdot(\mathbf{s}'-\mathbf{r}))-\cos(\mathbf{k}\cdot(\mathbf{s}-\mathbf{r}))-\cos(\mathbf{k}\cdot\mathbf{s}')+\cos(\mathbf{k}\cdot\mathbf{s})\big)\Big)$$
$$=4\bigg(\Big|\sin\frac{(\mathbf{s}'-\mathbf{s})\cdot\mathbf{k}}{2}\Big|^2+\Big|\beta\,\sin\frac{\mathbf{r}\cdot\mathbf{k}}{2}\Big|^2-2\beta\sin\frac{\mathbf{r}\cdot\mathbf{k}}{2}\,\sin\frac{(\mathbf{s}'-\mathbf{s})\cdot\mathbf{k}}{2}\,\cos\frac{(\mathbf{s}'+\mathbf{s}-\mathbf{r})\cdot\mathbf{k}}{2}\bigg)$$
$$\ge 4\bigg(\Big|\sin\frac{(\mathbf{s}'-\mathbf{s})\cdot\mathbf{k}}{2}\Big|-\Big|\beta\,\sin\frac{\mathbf{r}\cdot\mathbf{k}}{2}\Big|\bigg)^2\ge 0,$$

$$
\begin{aligned}
f_c :=\, & \cos(\mathbf{k}\cdot(\mathbf{s}'-\mathbf{r}))-\cos(\mathbf{k}\cdot(\mathbf{s}-\mathbf{r}))-\cos(\mathbf{k}\cdot\mathbf{s}')+\cos(\mathbf{k}\cdot\mathbf{s})\\
&+2\alpha\big(1-\cos(\mathbf{k}\cdot(\mathbf{s}'-\mathbf{s}))\big)-2\,\beta\big(1-\cos(\mathbf{k}\cdot\mathbf{r})\big)\\
&-\alpha\beta\big(\cos(\mathbf{k}\cdot(\mathbf{s}'-\mathbf{r}))-\cos(\mathbf{k}\cdot(\mathbf{s}-\mathbf{r}))-\cos(\mathbf{k}\cdot\mathbf{s}')+\cos(\mathbf{k}\cdot\mathbf{s})\big),\\
f_a\,f_b-|f_c|^2 =\, & 16(1+\alpha\beta)^2\Big|\sin\frac{\mathbf{r}\cdot\mathbf{k}}{2}\,\sin\frac{(\mathbf{s}'-\mathbf{s})\cdot\mathbf{k}}{2}\Big|^2\left(1-\Big|\cos\frac{(\mathbf{s}'+\mathbf{s}-\mathbf{r})\cdot\mathbf{k}}{2}\Big|^2\right)\geq 0
\end{aligned}
\tag{2.107}
$$

and

$$
\left|\int_{\mathbb{R}^3} d\mathbf{k}\,\overline{\tilde{w}_i\,\tilde{\omega}_j}(\mathbf{k})\,f_c\right|^2\leq\left(\int_{\mathbb{R}^3} d\mathbf{k}\,\overline{\tilde{w}_{\underline{i}}\tilde{w}_{\underline{i}}}(\mathbf{k})\,f_a\right)\left(\int_{\mathbb{R}^3} d\mathbf{k}\,\overline{\tilde{\omega}_{\underline{j}}\tilde{\omega}_{\underline{j}}}(\mathbf{k})\,f_b\right)
\tag{2.108}
$$

with

$$
\begin{aligned}
f_a :=\, & 2\Big(1-\cos(\mathbf{k}\cdot\mathbf{r})+\alpha^2\big(1-\cos(\mathbf{k}\cdot(\mathbf{s}'-\mathbf{s}))\big)\\
&+\alpha\big(\cos(\mathbf{k}\cdot(\mathbf{s}'-\mathbf{r}))-\cos(\mathbf{k}\cdot(\mathbf{s}-\mathbf{r}))-\cos(\mathbf{k}\cdot\mathbf{s}')+\cos(\mathbf{k}\cdot\mathbf{s})\big)\Big)\geq 0,\\
f_b :=\, & 2\Big(1-\cos(\mathbf{k}\cdot(\mathbf{s}'-\mathbf{s}))+\beta^2\big(1-\cos(\mathbf{k}\cdot\mathbf{r})\big)\\
&-\beta\big(\cos(\mathbf{k}\cdot(\mathbf{s}'-\mathbf{r}))-\cos(\mathbf{k}\cdot(\mathbf{s}-\mathbf{r}))-\cos(\mathbf{k}\cdot\mathbf{s}')+\cos(\mathbf{k}\cdot\mathbf{s})\big)\Big)\geq 0,\\
f_c :=\, & \imath\,(1+\alpha\beta)\Big(\sin(\mathbf{k}\cdot(\mathbf{s}'-\mathbf{r}))-\sin(\mathbf{k}\cdot(\mathbf{s}-\mathbf{r}))-\sin(\mathbf{k}\cdot\mathbf{s}')+\sin(\mathbf{k}\cdot\mathbf{s})\Big),\\
f_a\,f_b-|f_c|^2 =\, & 16\Bigg(\alpha\Big|\sin\frac{(\mathbf{s}'-\mathbf{s})\cdot\mathbf{k}}{2}\Big|^2-\beta\Big|\sin\frac{\mathbf{r}\cdot\mathbf{k}}{2}\Big|^2\\
&+(1-\alpha\beta)\sin\frac{\mathbf{r}\cdot\mathbf{k}}{2}\,\sin\frac{(\mathbf{s}'-\mathbf{s})\cdot\mathbf{k}}{2}\,\cos\frac{(\mathbf{s}'+\mathbf{s}-\mathbf{r})\cdot\mathbf{k}}{2}\Bigg)^2\geq 0
\end{aligned}
\tag{2.109}
$$

Motivated by the structures of (2.106) and (2.108) and taking into account the imposed constraints of (2.92), (2.95) and (2.96), we focus on the following type constraints

$$
|\tilde{c}(\mathbf{k})|^2\leq\tilde{a}(\mathbf{k})\,\tilde{b}(\mathbf{k}),\quad \tilde{a}(\mathbf{k})\geq 0,\ \tilde{b}(\mathbf{k})\geq 0
\tag{2.110}
$$

in the wave-number space. Associated with $\tilde{a}$, $\tilde{b}$ and $\tilde{c}$ are, respectively, the coefficients f'_a, f'_b and f'_c, functions of $\mathbf{k}$ and spatial vectors and time, satisfying the conditions of

$$
|f'_c|^2\leq f'_a\,f'_b,\quad f'_a\geq 0,\ f'_b\geq 0
\tag{2.111}
$$

Combining the above two sets of inequalities, we have

$$
\big|\tilde{c}(\mathbf{k})\,f'_c\big|\leq\sqrt{\tilde{a}(\mathbf{k})\,f'_a}\,\sqrt{\tilde{b}(\mathbf{k})\,f'_b}\leq\frac{1}{2}\left(\lambda\,\tilde{a}(\mathbf{k})\,f'_a+\frac{1}{\lambda}\,\tilde{b}(\mathbf{k})\,f'_b\right),\ \forall\lambda>0
$$

which can be integrated in the wave-number space to give

$$\int_{\mathbb{R}^3} d\mathbf{k}\,\left|\tilde{c}(\mathbf{k})\,f_c'\right| \le \frac{1}{2}\left(\lambda\int_{\mathbb{R}^3} d\mathbf{k}\,\tilde{a}(\mathbf{k})\,f_a' + \frac{1}{\lambda}\int_{\mathbb{R}^3} d\mathbf{k}\,\tilde{b}(\mathbf{k})\,f_b'\right),\ \forall\lambda>0$$

Next, by taking

$$\lambda = \left(\int_{\mathbb{R}^3} d\mathbf{k}\,\tilde{b}(\mathbf{k})\,f_b' \Big/ \int_{\mathbb{R}^3} d\mathbf{k}\,\tilde{a}(\mathbf{k})\,f_a'\right)^{1/2}$$

we get

$$\left|\int_{\mathbb{R}^3} d\mathbf{k}\,\tilde{c}(\mathbf{k})\,f_c'\right|^2 \le \left(\int_{\mathbb{R}^3} d\mathbf{k}\,\left|\tilde{c}(\mathbf{k})\,f_c'\right|\right)^2 \le \int_{\mathbb{R}^3} d\mathbf{k}\,\tilde{a}(\mathbf{k})\,f_a' \int_{\mathbb{R}^3} d\mathbf{k}\,\tilde{b}(\mathbf{k})\,f_b' \tag{2.112}$$

The above result demonstrates that (2.112) is redundant under (2.110) and (2.111).

We can easily see that the coefficients in (2.106) and (2.108) satisfy (2.111) and the above result implies that the constraints of (2.92) guarantee the automatic satisfaction of (2.102) through (2.104).

2.9 Constraints of Inequality Involving $\tilde{U}_{(ij)kl}(\mathbf{k},\mathbf{l})$

For the fourth-order model with the correlations up to the fourth order, we can include the constraints involving $\tilde{U}_{(ij)kl}(\mathbf{k},\mathbf{l})$. One way to construct the constraints is that we take a third or fourth order correlation among $w_i(\mathbf{x})$, $q(\mathbf{y})$, $\omega_j(\mathbf{z})$ as well as their associated spatial derivatives or a third or fourth order structure function analogous to (2.101), and then apply the Cauchy-Schwarz inequality with the decompositions involving only those correlations resolvable within the fourth-order model; Some examples as such can be found in [15]. We will not present these inequalities here since we focus on the second-order and the third-order models in the present study.

Within the fourth-order model, we can also construct constraints of inequality involving $\tilde{U}_{(ij)kl}(\mathbf{k},\mathbf{l})$ by evaluating the variance of products and demanding it to be non-negative.

$$\overline{\left(XY-\overline{XY}\right)^2} \ge 0, \quad \overline{XXYY} \ge \left(\overline{XY}\right)^2 \tag{2.113}$$

For example, in the case of $X = w_i(\mathbf{x})$, $Y = w_j(\mathbf{y})$,

$$U_{(\underline{i}\,\underline{i})\,\underline{j}\underline{j}}(\mathbf{r},\mathbf{r}) \ge \left(U_{ij}(\mathbf{r})\right)^2, \quad i \le j \tag{2.114}$$

A few more examples are given below,

$$\overline{w_{\underline{i}}(\mathbf{x})w_{\underline{i}}(\mathbf{x})w_{\underline{j},\underline{k}}(\mathbf{y})w_{\underline{j},\underline{k}}(\mathbf{y})} \ge \left(\overline{w_i(\mathbf{x})w_{j,k}(\mathbf{y})}\right)^2, \quad \overline{w_{\underline{i}}(\mathbf{x})w_{\underline{i}}(\mathbf{x})\omega_{\underline{j}}(\mathbf{y})\omega_{\underline{j}}(\mathbf{y})} \ge \left(\overline{w_i(\mathbf{x})\omega_j(\mathbf{y})}\right)^2,$$

$$\overline{w_{\underline{i},\underline{k}}(\mathbf{x})w_{\underline{i},\underline{k}}(\mathbf{x})w_{\underline{j},\underline{l}}(\mathbf{y})w_{\underline{j},\underline{l}}(\mathbf{y})} \ge \left(\overline{w_{i,k}(\mathbf{x})w_{j,l}(\mathbf{y})}\right)^2, \quad \overline{\omega_{\underline{i}}(\mathbf{x})\omega_{\underline{i}}(\mathbf{x})\omega_{\underline{j}}(\mathbf{y})\omega_{\underline{j}}(\mathbf{y})} \ge \left(\overline{\omega_i(\mathbf{x})\omega_j(\mathbf{y})}\right)^2 \tag{2.115}$$

Numerous such inequalities can be produced by including structure functions, like $X = w_i(\mathbf{y}) - w_i(\mathbf{x})$, $\omega_j(\mathbf{y}) - \omega_j(\mathbf{x}) + \alpha(\omega_j(\mathbf{z}') - \omega_j(\mathbf{z}))$, etc.

These constraints cannot be implemented within the second-order and the third-order models. Their significance can be seen from their mathematical structures in that they destroy the property of scaling invariance for the fourth-order model under the transformation of

$$\left\{\tilde{U}_{ij},\ \tilde{U}_{ijk},\ \tilde{U}_{(ij)kl}\right\} \to \left\{\lambda\,\tilde{U}_{ij},\ \lambda\,\tilde{U}_{ijk},\ \lambda\,\tilde{U}_{(ij)kl}\right\},\quad \forall\lambda > 0 \tag{2.116}$$

Such scaling invariance holds in the second-order and the third-order models due to the absence of the variance constraints there. These constraints play a crucial role in the determination of the upper bound for the exponential growth rate in the asymptotic state solutions which will be discussed in Section 3.

2.10 Objective Function

Following the same detailed reasoning as that presented in PART IV [15], we adopt tentatively the turbulent fluctuation energy per unit volume as the objective function to be maximized,

$$\begin{aligned} I_T^{\text{hom}} &= U_{kk}(\mathbf{0}) = \int_{\mathbb{R}^3} d\mathbf{k}\,\tilde{U}_{kk}(\mathbf{k}) \\ &= \int_{\mathbb{R}^3} d\mathbf{k}\left[\left(1+\left(\frac{k_1}{k_3}\right)^2\right)\tilde{U}_{11}(\mathbf{k}) + \left(1+\left(\frac{k_2}{k_3}\right)^2\right)\tilde{U}_{22}(\mathbf{k}) + \frac{2\,k_1\,k_2}{(k_3)^2}\,\tilde{U}_{12}(\mathbf{k})\right] \end{aligned} \tag{2.117}$$

There are three models of optimal control and optimization to employ the objective function. The second-order model takes the second order correlation as the state variables and $\tilde{\gamma}_{ij}(\mathbf{k})$ as the control variables. The third-order model treats the second order correlation as the state variables and the degenerated third order correlation as the control variables. The fourth-order model contains the correlations up to the degenerated fourth order with $\tilde{U}_{(ij)kl}(\mathbf{k},\mathbf{l})$ as the control variables. The fourth-order model can determine the lower order correlations involving pressure fluctuations and can account for the variance constraints of the lowest order like those listed in (2.114) and (2.115), but it has the complexity of containing much more control variables, state variables and constraints for analysis and simulation and it needs to deal with the integrals higher than 4-dimensions in the wave-number space.

3 Asymptotic State Solutions

To test the present formulation against the experimental and DNS data available, we apply it to the asymptotic states at large time.

The asymptotic states are characterized by the mathematical structure of

$$\psi = \psi^{(\infty)}\,\exp(\sigma\,t) \tag{3.1}$$

Here, ψ represents any of

$$\left\{\tilde{U}_{ij},\ \overline{\tilde{\omega}_i\tilde{\omega}_j},\ \overline{\tilde{w}_i\tilde{\omega}_j},\ \tilde{U}^{(I)}_{(ij)k},\ \tilde{U}^{(I)}_{ijk},\ \tilde{U}_{(ij)kl},\ \tilde{Q},\ \tilde{Q}^{(I)}_i,\ \tilde{Q}_{ij},\ \tilde{\gamma}_{ij},\ U_{ij},\ U_{ijk},\ U_{(ij)kl},\ Q,\ Q_i,\ Q_{ij},\ \cdots\right\}$$

$\psi^{(\infty)}$ is the time-independent part of ψ, and σ a constant representing the exponential growth rate. The structure is allowable by the mean shearing and all the equations of evolution and the constraints formulated and mentioned above.

We now derive the upper bound for σ within the fourth-order model with the help of the variance constraints (2.114) and (2.115). For example, (2.114) and (3.1) require that

$$U^{(\infty)}_{(\underline{i}\,\underline{i})\,\underline{j}\underline{j}}(\mathbf{r},\mathbf{r}) \geq \big(U^{(\infty)}_{ij}(\mathbf{r})\big)^2 \exp(\sigma t), \quad \forall t \text{ positively large}, \quad i \leq j \tag{3.2}$$

Due to the involvement of large t, the inequality demands that

$$\sigma \leq \max \sigma = 0 \tag{3.3}$$

Therefore, the turbulent energy per unit volume cannot grow indefinitely, and it will tend toward a constant state of $\sigma = 0$, if not decaying. This result is more restrictive than the growth rate values suggested by some of the experimental and DNS data ([11], [12]). This upper bound comes directly from the variance non-negativity requirement. We notice the roles played by the variance constraints in the asymptotic states: They forbid $\sigma > 0$ to occur, they are acting constraints at $\sigma = 0$ and are satisfied automatically if $\sigma < 0$.

Next, applying (3.1) to (2.46) through (2.48) and (2.64) through (2.67), we get

$$\frac{\partial}{\partial k_2}\Big\{|\mathbf{k}|^4 \exp\big[2H(\sigma,\mathbf{k})\big]\,\tilde{U}^{(\infty)}_{22}(\mathbf{k})\Big\} = -\frac{2\,|\mathbf{k}|^4}{k_1} \exp\big[2H(\sigma,\mathbf{k})\big]\tilde{\gamma}^{(\infty)}_{22}(\mathbf{k}) \tag{3.4}$$

$$\begin{aligned}&\frac{\partial}{\partial k_2}\Big\{|\mathbf{k}|^2 \exp\big[2H(\sigma,\mathbf{k})\big]\,\tilde{U}^{(\infty)}_{12}(\mathbf{k})\Big\}\\ &= -\frac{|\mathbf{k}|^2}{k_1} \exp\big[2H(\sigma,\mathbf{k})\big]\bigg[-\bigg(1-\frac{2\,(k_1)^2}{|\mathbf{k}|^2}\bigg)\tilde{U}^{(\infty)}_{22}(\mathbf{k}) + \tilde{\gamma}^{(\infty)}_{12}(\mathbf{k})\bigg]\end{aligned} \tag{3.5}$$

$$\frac{\partial}{\partial k_2}\Big\{\exp\big[2H(\sigma,\mathbf{k})\big]\,\tilde{U}^{(\infty)}_{11}(\mathbf{k})\Big\} = -\frac{2}{k_1}\exp\big[2H(\sigma,\mathbf{k})\big]\bigg[-\bigg(1-\frac{2\,(k_1)^2}{|\mathbf{k}|^2}\bigg)\tilde{U}^{(\infty)}_{12}(\mathbf{k}) + \tilde{\gamma}^{(\infty)}_{11}(\mathbf{k})\bigg] \tag{3.6}$$

$$\begin{aligned}&\bigg(k_1\frac{\partial}{\partial k_2} + l_1\frac{\partial}{\partial l_2}\bigg)\Big\{|\mathbf{k}|^2\,|\mathbf{l}|^2\,|\mathbf{k}+\mathbf{l}|^2 \exp\big[H(2\sigma/3,\mathbf{k},\mathbf{l})\big]\,\tilde{U}^{(I\infty)}_{222}(\mathbf{k},\mathbf{l})\Big\}\\ &= -|\mathbf{k}|^2\,|\mathbf{l}|^2\,|\mathbf{k}+\mathbf{l}|^2 \exp\big[H(2\sigma/3,\mathbf{k},\mathbf{l})\big]\\ &\quad\times\bigg[(k_l+l_l)\,\tilde{U}^{(\infty)}_{(2l)22}(\mathbf{k},\mathbf{l}) - k_l\,\tilde{U}^{(\infty)}_{(2l)22}(-\mathbf{k}-\mathbf{l},\mathbf{l}) - l_l\,\tilde{U}^{(\infty)}_{(2l)22}(-\mathbf{k}-\mathbf{l},\mathbf{k})\\ &\qquad-(k_2+l_2)\,\frac{(k_m+l_m)(k_l+l_l)}{|\mathbf{k}+\mathbf{l}|^2}\,\tilde{U}^{(\infty)}_{(lm)22}(\mathbf{k},\mathbf{l}) + k_2\,\frac{k_m\,k_l}{|\mathbf{k}|^2}\,\tilde{U}^{(\infty)}_{(lm)22}(-\mathbf{k}-\mathbf{l},\mathbf{l})\\ &\qquad+l_2\,\frac{l_m\,l_l}{|\mathbf{l}|^2}\,\tilde{U}^{(\infty)}_{(lm)22}(-\mathbf{k}-\mathbf{l},\mathbf{k})\bigg]\end{aligned} \tag{3.7}$$

$$
\begin{aligned}
&\left(k_1\,\frac{\partial}{\partial k_2}+l_1\,\frac{\partial}{\partial l_2}\right)\Big\{\,|\mathbf{k}|^2\,|\mathbf{l}|^2\,\exp\big[H(2\sigma/3,\mathbf{k},\mathbf{l})\big]\,\tilde U^{(I\infty)}_{122}(\mathbf{k},\mathbf{l})\Big\}\\
&=-\,|\mathbf{k}|^2\,|\mathbf{l}|^2\,\exp\big[H(2\sigma/3,\mathbf{k},\mathbf{l})\big]\\
&\quad\times\Bigg[-\left(1-\frac{2\,(k_1+l_1)^2}{|\mathbf{k}+\mathbf{l}|^2}\right)\tilde U^{(I\infty)}_{222}(\mathbf{k},\mathbf{l})+(k_l+l_l)\,\tilde U^{(\infty)}_{(1l)22}(\mathbf{k},\mathbf{l})-k_l\,\tilde U^{(\infty)}_{(2l)12}(-\mathbf{k}-\mathbf{l},\mathbf{l})\\
&\qquad-l_l\,\tilde U^{(\infty)}_{(2l)12}(-\mathbf{k}-\mathbf{l},\mathbf{k})-(k_1+l_1)\,\frac{(k_m+l_m)(k_l+l_l)}{|\mathbf{k}+\mathbf{l}|^2}\,\tilde U^{(\infty)}_{(lm)22}(\mathbf{k},\mathbf{l})\\
&\qquad+k_2\,\frac{k_m\,k_l}{|\mathbf{k}|^2}\,\tilde U^{(\infty)}_{(lm)12}(-\mathbf{k}-\mathbf{l},\mathbf{l})+l_2\,\frac{l_m\,l_l}{|\mathbf{l}|^2}\,\tilde U^{(\infty)}_{(lm)12}(-\mathbf{k}-\mathbf{l},\mathbf{k})\Bigg]
\end{aligned}
\tag{3.8}
$$

$$
\begin{aligned}
&\left(k_1\,\frac{\partial}{\partial k_2}+l_1\,\frac{\partial}{\partial l_2}\right)\Big\{\,|\mathbf{l}|^2\,\exp\big[H(2\sigma/3,\mathbf{k},\mathbf{l})\big]\,\tilde U^{(I\infty)}_{112}(\mathbf{k},\mathbf{l})\Big\}\\
&=-\,|\mathbf{l}|^2\,\exp\big[H(2\sigma/3,\mathbf{k},\mathbf{l})\big]\\
&\quad\times\Bigg[-\left(1-\frac{2\,(k_1+l_1)^2}{|\mathbf{k}+\mathbf{l}|^2}\right)\tilde U^{(I\infty)}_{122}(-\mathbf{k}-\mathbf{l},\mathbf{l})-\left(1-\frac{2\,(k_1)^2}{|\mathbf{k}|^2}\right)\tilde U^{(I\infty)}_{122}(\mathbf{k},\mathbf{l})\\
&\qquad+(k_l+l_l)\,\tilde U^{(\infty)}_{(1l)12}(\mathbf{k},\mathbf{l})-k_l\,\tilde U^{(\infty)}_{(1l)12}(-\mathbf{k}-\mathbf{l},\mathbf{l})-l_l\,\tilde U^{(\infty)}_{2l11}(-\mathbf{k}-\mathbf{l},\mathbf{k})\\
&\qquad-(k_1+l_1)\,\frac{(k_m+l_m)(k_l+l_l)}{|\mathbf{k}+\mathbf{l}|^2}\,\tilde U^{(\infty)}_{(lm)12}(\mathbf{k},\mathbf{l})+k_1\,\frac{k_m\,k_l}{|\mathbf{k}|^2}\,\tilde U^{(\infty)}_{(lm)12}(-\mathbf{k}-\mathbf{l},\mathbf{l})\\
&\qquad+l_2\,\frac{l_m\,l_l}{|\mathbf{l}|^2}\,\tilde U^{(\infty)}_{(lm)11}(-\mathbf{k}-\mathbf{l},\mathbf{k})\Bigg]
\end{aligned}
\tag{3.9}
$$

and

$$
\begin{aligned}
&\left(k_1\,\frac{\partial}{\partial k_2}+l_1\,\frac{\partial}{\partial l_2}\right)\Big\{\,\exp\big[H(2\sigma/3,\mathbf{k},\mathbf{l})\big]\,\tilde U^{(I\infty)}_{111}(\mathbf{k},\mathbf{l})\Big\}\\
&=-\exp\big[H(2\sigma/3,\mathbf{k},\mathbf{l})\big]\\
&\quad\times\Bigg[-\tilde U^{(I\infty)}_{112}(\mathbf{l},-\mathbf{k}-\mathbf{l})-\tilde U^{(I\infty)}_{112}(\mathbf{l},\mathbf{k})-\tilde U^{(I\infty)}_{112}(\mathbf{k},\mathbf{l})+\frac{2\,(k_1+l_1)^2}{|\mathbf{k}+\mathbf{l}|^2}\,\tilde U^{(I\infty)}_{112}(\mathbf{l},-\mathbf{k}-\mathbf{l})\\
&\qquad+\frac{2\,(k_1)^2}{|\mathbf{k}|^2}\,\tilde U^{(I\infty)}_{112}(\mathbf{l},\mathbf{k})+\frac{2\,(l_1)^2}{|\mathbf{l}|^2}\,\tilde U^{(I\infty)}_{112}(\mathbf{k},\mathbf{l})+(k_l+l_l)\,\tilde U^{(\infty)}_{(1l)11}(\mathbf{k},\mathbf{l})-k_l\,\tilde U^{(\infty)}_{(1l)11}(-\mathbf{k}-\mathbf{l},\mathbf{l})\\
&\qquad-l_l\,\tilde U^{(\infty)}_{(1l)11}(-\mathbf{k}-\mathbf{l},\mathbf{k})-(k_1+l_1)\,\frac{(k_m+l_m)(k_l+l_l)}{|\mathbf{k}+\mathbf{l}|^2}\,\tilde U^{(\infty)}_{(lm)11}(\mathbf{k},\mathbf{l})\\
&\qquad+k_1\,\frac{k_m\,k_l}{|\mathbf{k}|^2}\,\tilde U^{(\infty)}_{(lm)11}(-\mathbf{k}-\mathbf{l},\mathbf{l})+l_1\,\frac{l_m\,l_l}{|\mathbf{l}|^2}\,\tilde U^{(\infty)}_{(lm)11}(-\mathbf{k}-\mathbf{l},\mathbf{k})\Bigg]
\end{aligned}
\tag{3.10}
$$

where

$$
H(\sigma,\mathbf{k}):=-\frac{k_2}{k_1}\left(\frac{1}{2}\,\sigma+(k_1)^2+(k_3)^2+\frac{1}{3}\,(k_2)^2\right),
$$

$$H(2\sigma/3,\mathbf{k},\mathbf{l}) := H(2\sigma/3,\mathbf{k}) + H(2\sigma/3,\mathbf{l}) + H(2\sigma/3,\mathbf{k}+\mathbf{l}) \tag{3.11}$$

The differential equations corresponding to (2.59) through (2.61) of the third-order model have the same forms as those of (3.4) through (3.6), but with $\tilde{\gamma}_{ij}^{(\infty)}(\mathbf{k})$ represented explicitly in terms of $\tilde{U}_{(ij)k}^{(I\infty)}(\mathbf{k})$, following from (2.50) and the interrelationship between $\tilde{U}_{ijk}(\mathbf{k},\mathbf{l})$ and $\tilde{U}_{(ij)k}(\mathbf{k})$ presented in (2.29). In fact, $\tilde{\gamma}_{ij}^{(\infty)}(\mathbf{k})$ play the role of the control variables within the second-order model and the role of the intermediate variables within the third-order and the fourth-order models. All the relevant results in the rest of this section can be interpreted accordingly.

Under the boundary conditions of

$$\lim_{k_2\to\pm\infty} \tilde{U}_{ij}^{(\infty)}(\mathbf{k}) = 0 \tag{3.12}$$

we can integrate (3.4) through (3.6) to obtain

$$\tilde{U}_{22}^{(\infty)}(\mathbf{k}) = \frac{2}{|k_1|}\int_{-\infty}^{k_2} dk_2' \,\frac{|\mathbf{k}'|^4}{|\mathbf{k}|^4}\,\exp\big[2\left(H(\sigma,\mathbf{k}') - H(\sigma,\mathbf{k})\right)\big]\,\tilde{\gamma}_{22}^{(\infty)}(\mathbf{k}') \tag{3.13}$$

$$\begin{aligned}\tilde{U}_{12}^{(\infty)}(\mathbf{k}) = \frac{1}{|k_1|}\int_{-\infty}^{k_2} dk_2' \,\frac{|\mathbf{k}'|^2}{|\mathbf{k}|^2}\,\exp\big[2\left(H(\sigma,\mathbf{k}') - H(\sigma,\mathbf{k})\right)\big] \\ \times\left[-\left(1-\frac{2\,(k_1)^2}{|\mathbf{k}'|^2}\right)\tilde{U}_{22}^{(\infty)}(\mathbf{k}') + \tilde{\gamma}_{12}^{(\infty)}(\mathbf{k}')\right]\end{aligned} \tag{3.14}$$

and

$$\tilde{U}_{11}^{(\infty)}(\mathbf{k}) = \frac{2}{|k_1|}\int_{-\infty}^{k_2} dk_2' \,\exp\big[2\left(H(\sigma,\mathbf{k}') - H(\sigma,\mathbf{k})\right)\big]\left[-\left(1-\frac{2\,(k_1)^2}{|\mathbf{k}'|^2}\right)\tilde{U}_{12}^{(\infty)}(\mathbf{k}') + \tilde{\gamma}_{11}^{(\infty)}(\mathbf{k}')\right] \tag{3.15}$$

with

$$\mathbf{k}' := (k_1, k_2', k_3), \quad k_1 < 0;$$

$$H(\sigma,\mathbf{k}') - H(\sigma,\mathbf{k}) = -\frac{k_2 - k_2'}{|k_1|}\left[\frac{1}{2}\,\sigma + (k_1)^2 + (k_3)^2 + \frac{1}{3}\left((k_2)^2 + (k_2')^2 + k_2\,k_2'\right)\right] \tag{3.16}$$

Here, we have restricted the solutions to the subdomain of $k_1 < 0$. The solutions in the subdomain of $k_1 > 0$ have the same forms as the above or they can obtained through the symmetry property of (3.20) below.

Similarly, under the boundary conditions of

$$\lim_{k_2\to\pm\infty} \tilde{U}_{ijk}^{(I\infty)}(\mathbf{k},\mathbf{l}) = 0 \tag{3.17}$$

we can solve for $\tilde{U}_{ijk}^{(I\infty)}(\mathbf{k},\mathbf{l})$ using the method of characteristics, and as an example, we present

$\tilde{U}_{111}^{(I\infty)}(\mathbf{k},\mathbf{l})$

$$= -\frac{1}{k_1}\int_{-\infty}^{k_2} dk_2' \, \exp\big[H(2\sigma/3,\mathbf{k}',\mathbf{l}') - H(2\sigma/3,\mathbf{k},\mathbf{l})\big]$$
$$\times \Bigg[-\tilde{U}_{112}^{(I\infty)}(\mathbf{l}',-\mathbf{k}'-\mathbf{l}') - \tilde{U}_{112}^{(I\infty)}(\mathbf{l}',\mathbf{k}') - \tilde{U}_{112}^{(I\infty)}(\mathbf{k}',\mathbf{l}')$$
$$+ \frac{2\,(k_1+l_1)^2}{|\mathbf{k}'+\mathbf{l}'|^2}\,\tilde{U}_{112}^{(I\infty)}(\mathbf{l}',-\mathbf{k}'-\mathbf{l}') + \frac{2\,(k_1)^2}{|\mathbf{k}'|^2}\,\tilde{U}_{112}^{(I\infty)}(\mathbf{l}',\mathbf{k}') + \frac{2\,(l_1)^2}{|\mathbf{l}'|^2}\,\tilde{U}_{112}^{(I\infty)}(\mathbf{k}',\mathbf{l}')$$
$$+ (k_l'+l_l')\,\tilde{U}_{(1l)11}^{(\infty)}(\mathbf{k}',\mathbf{l}') - k_l'\,\tilde{U}_{(1l)11}^{(\infty)}(-\mathbf{k}'-\mathbf{l}',\mathbf{l}') - l_l'\,\tilde{U}_{(1l)11}^{(\infty)}(-\mathbf{k}'-\mathbf{l}',\mathbf{k}')$$
$$- (k_1+l_1)\,\frac{(k_m'+l_m')(k_l'+l_l')}{|\mathbf{k}'+\mathbf{l}'|^2}\,\tilde{U}_{(lm)11}^{(\infty)}(\mathbf{k}',\mathbf{l}') + k_1\,\frac{k_m'\,k_l'}{|\mathbf{k}'|^2}\,\tilde{U}_{(lm)11}^{(\infty)}(-\mathbf{k}'-\mathbf{l}',\mathbf{l}')$$
$$+ l_1\,\frac{l_m'\,l_l'}{|\mathbf{l}'|^2}\,\tilde{U}_{(lm)11}^{(\infty)}(-\mathbf{k}'-\mathbf{l}',\mathbf{k}')\Bigg] \tag{3.18}$$

with

$$\mathbf{k}' := (k_1,k_2',k_3), \quad k_1<0; \quad \mathbf{l}' := (l_1,l_2',l_3), \quad l_2' := l_2 + \frac{l_1}{k_1}\,(k_2'-k_2) \tag{3.19}$$

We record below certain relations and intrinsic equality constraints for $\tilde{U}_{ij}^{(\infty)}(\mathbf{k})$, $\tilde{\gamma}_{ij}^{(\infty)}(\mathbf{k})$, $\dot{U}_{ij}^{(\infty)}(\mathbf{k})$, $\dot{\gamma}_{ij}^{(\infty)}(\mathbf{k})$ and $\dot{U}_{(ij)k}^{(I\infty)}(\mathbf{k})$, due to their relevance to the numerical simulations to be conducted within the second-order and the third-order models.

Corresponding to (2.31), (2.51), (2.69) and (2.70), we have

$$\tilde{U}_{ij}^{(\infty)}(k_1,k_2,-k_3) = \tilde{U}_{ij}^{(\infty)}(\mathbf{k}) = \tilde{U}_{ij}^{(\infty)}(-\mathbf{k}), \quad \tilde{\gamma}_{ij}^{(\infty)}(k_1,k_2,-k_3) = \tilde{\gamma}_{ij}^{(\infty)}(\mathbf{k}) = \tilde{\gamma}_{ij}^{(\infty)}(-\mathbf{k}),$$
$$ij = 11,12,22;$$
$$U_{ij}^{(\infty)}(\mathbf{0}) = \overline{w_{i,k}(\mathbf{x})\,w_{j,k}(\mathbf{x})}^{(\infty)} = 0, \quad ij = 13,23 \tag{3.20}$$

part of which can be used to determine the solutions in the subdomain of $k_1>0$, along with (3.13) through (3.15). In the asymptotic states, the constraint of (2.55) becomes

$$\int_{-\infty}^{0} dk_1 \int_{\mathbb{R}^2} dk_2\,dk_3 \Bigg[\bigg(1+\Big(\frac{k_1}{k_3}\Big)^2\bigg)\,\tilde{\gamma}_{11}^{(\infty)}(\mathbf{k}) + \bigg(1+\Big(\frac{k_2}{k_3}\Big)^2\bigg)\,\tilde{\gamma}_{22}^{(\infty)}(\mathbf{k}) + \frac{k_1\,k_2}{(k_3)^2}\,\tilde{\gamma}_{12}^{(\infty)}(\mathbf{k})\Bigg] = 0 \tag{3.21}$$

and (2.58) reduces to

$$\sigma\,U_{jj}^{(\infty)}(\mathbf{0}) + 2\,U_{12}^{(\infty)}(\mathbf{0}) - 2\,\frac{\partial^2 U_{jj}^{(\infty)}(\mathbf{r})}{\partial r_k \partial r_k}\bigg|_{\mathbf{r}=\mathbf{0}} = 0 \tag{3.22}$$

which is a known relation ([11], [12]).

Corresponding to (2.62) and (2.63), we have

$$\tilde{U}_{(ij)k}^{(I\infty)}(\mathbf{k}) = \tilde{U}_{(ji)k}^{(I\infty)}(\mathbf{k}) = -\tilde{U}_{(ij)k}^{(I\infty)}(-\mathbf{k}) = (-1)^{\delta_{\underline{i}3}+\delta_{\underline{j}3}+\delta_{\underline{k}3}}\,\tilde{U}_{(\underline{i}\,\underline{j})\,\underline{k}}^{(I\infty)}(k_1,k_2,-k_3) \tag{3.23}$$

and

$$\int_{-\infty}^{0} dk_1 \int_{\mathbb{R}^2} dk_2\, dk_3\, k_k\, \tilde{U}^{(I\infty)}_{(k\underline{j})\,\underline{j}}(\mathbf{k}) = 0 \tag{3.24}$$

The transformations of (2.72) through (2.75) can be applied to the asymptotic states,

$$\begin{aligned}
&\tilde{U}^{(\infty)}_{ij}(\mathbf{k}) = (k_3)^2\, \dot{U}^{(\infty)}_{ij}(\mathbf{k}), \quad \tilde{\gamma}^{(\infty)}_{ij}(\mathbf{k}) = (k_3)^2\, \dot{\gamma}^{(\infty)}_{ij}(\mathbf{k}), \quad \tilde{U}^{(I\infty)}_{(ij)k}(\mathbf{k}) = (k_3)^2\, \dot{U}^{(I\infty)}_{(ij)k}(\mathbf{k}), \\
&\tilde{U}^{(I\infty)}_{ijk}(\mathbf{k},\mathbf{l}) = (k_3)^2\,(l_3)^2\,(k_3+l_3)^2\, \dot{U}^{(I\infty)}_{ijk}(\mathbf{k},\mathbf{l}), \quad \tilde{U}^{(\infty)}_{(ij)kl}(\mathbf{k},\mathbf{l}) = (k_3)^2\,(l_3)^2\,(k_3+l_3)^2\, \dot{U}^{(\infty)}_{(ij)kl}(\mathbf{k},\mathbf{l})
\end{aligned} \tag{3.25}$$

Then, equations (3.13) through (3.15) result in

$$\dot{U}^{(\infty)}_{22}(\mathbf{k}) = \frac{2}{|k_1|} \int_{-\infty}^{k_2} dk_2' \, \frac{|\mathbf{k}'|^4}{|\mathbf{k}|^4} \exp\big[2\left(H(\sigma,\mathbf{k}') - H(\sigma,\mathbf{k})\right)\big]\, \dot{\gamma}^{(\infty)}_{22}(\mathbf{k}') \tag{3.26}$$

$$\begin{aligned}
\dot{U}^{(\infty)}_{12}(\mathbf{k}) = \frac{1}{|k_1|} \int_{-\infty}^{k_2} dk_2' \, \frac{|\mathbf{k}'|^2}{|\mathbf{k}|^2} \exp\big[2\left(H(\sigma,\mathbf{k}') - H(\sigma,\mathbf{k})\right)\big] \\
\times \left[-\left(1 - \frac{2\,(k_1)^2}{|\mathbf{k}'|^2}\right) \dot{U}^{(\infty)}_{22}(\mathbf{k}') + \dot{\gamma}^{(\infty)}_{12}(\mathbf{k}') \right]
\end{aligned} \tag{3.27}$$

$$\dot{U}^{(\infty)}_{11}(\mathbf{k}) = \frac{2}{|k_1|} \int_{-\infty}^{k_2} dk_2' \, \exp\big[2\left(H(\sigma,\mathbf{k}') - H(\sigma,\mathbf{k})\right)\big] \left[-\left(1 - \frac{2\,(k_1)^2}{|\mathbf{k}'|^2}\right) \dot{U}^{(\infty)}_{12}(\mathbf{k}') + \dot{\gamma}^{(\infty)}_{11}(\mathbf{k}') \right] \tag{3.28}$$

where

$$\begin{aligned}
&\mathbf{k}' := (k_1, k_2', k_3), \quad k_1 < 0; \\
&H(\sigma,\mathbf{k}') - H(\sigma,\mathbf{k}) = -\frac{k_2 - k_2'}{|k_1|} \left[\frac{1}{2}\,\sigma + (k_1)^2 + (k_3)^2 + \frac{1}{3}\left((k_2)^2 + (k_2')^2 + k_2\, k_2' \right) \right]
\end{aligned} \tag{3.29}$$

The constraints of (3.20), (3.21), (3.23) and (3.24) take the corresponding forms of

$$\begin{aligned}
&\dot{U}^{(\infty)}_{ij}(k_1,k_2,-k_3) = \dot{U}^{(\infty)}_{ij}(\mathbf{k}) = \dot{U}^{(\infty)}_{ij}(-\mathbf{k}), \;\; \dot{\gamma}^{(\infty)}_{ij}(k_1,k_2,-k_3) = \dot{\gamma}^{(\infty)}_{ij}(\mathbf{k}) = \dot{\gamma}^{(\infty)}_{ij}(-\mathbf{k}), \\
&ij = 11, 12, 22
\end{aligned} \tag{3.30}$$

$$\int_{-\infty}^{0} dk_1 \int_{\mathbb{R}^2} dk_2\, dk_3 \left[\left((k_1)^2 + (k_3)^2 \right) \dot{\gamma}^{(\infty)}_{11}(\mathbf{k}) + \left((k_2)^2 + (k_3)^2 \right) \dot{\gamma}^{(\infty)}_{22}(\mathbf{k}) + k_1\, k_2\, \dot{\gamma}^{(\infty)}_{12}(\mathbf{k}) \right] = 0 \tag{3.31}$$

$$\dot{U}^{(I\infty)}_{(ij)k}(\mathbf{k}) = \dot{U}^{(I\infty)}_{(ji)k}(\mathbf{k}) = -\dot{U}^{(I\infty)}_{(ij)k}(-\mathbf{k}) = (-1)^{\delta_{\underline{i}3} + \delta_{\underline{j}3}}\, \dot{U}^{(I\infty)}_{(\underline{i}\,\underline{j})\,\underline{k}}(k_1,k_2,-k_3), \quad k = 1,2 \tag{3.32}$$

and

$$\int_{-\infty}^{0} dk_1 \int_{\mathbb{R}^2} dk_2\, dk_3\, (k_3)^2\, k_k\, \dot{U}^{(I\infty)}_{(k\underline{j})\,\underline{j}}(\mathbf{k}) = 0, \quad j = 1, 2;$$

$$\int_{-\infty}^{0} dk_1 \int_{\mathbb{R}^2} dk_2\, dk_3\, k_3\, k_k \Big(k_1\, \dot{U}^{(I\infty)}_{(k3)1}(\mathbf{k}) + k_2\, \dot{U}^{(I\infty)}_{(k3)2}(\mathbf{k}) \Big) = 0 \tag{3.33}$$

Here, (2.43) and (3.1) have been used to derive $(3.33)_2$.

Considering the peculiar nature of $k_1 \to 0^-$ involved in the primary solutions of (3.26) through (3.28), we need to discuss its impact, under the supposedly bounded $\dot{U}^{(\infty)}_{ij}(\mathbf{k})$ and $\dot{\gamma}^{(\infty)}_{ij}(\mathbf{k})$. We first deal with (3.28), which can be rewritten in the form of

$$\dot{U}^{(\infty)}_{11}(\mathbf{k}) = \int_{-\infty}^{k_2} dk_2'\; \rho^{(\infty)}_{11}(\mathbf{k}; k_2') \tag{3.34}$$

with

$$\rho^{(\infty)}_{11}(\mathbf{k}; k_2') := \frac{2}{|k_1|} \exp\big[2\big(H(\sigma, \mathbf{k}') - H(\sigma, \mathbf{k})\big)\big] \Big[- \left(1 - \frac{2\,(k_1)^2}{|\mathbf{k}'|^2} \right) \dot{U}^{(\infty)}_{12}(\mathbf{k}') + \dot{\gamma}^{(\infty)}_{11}(\mathbf{k}') \Big] \tag{3.35}$$

Supposing that $\dot{U}^{(\infty)}_{ij}(\mathbf{k})$ and $\dot{\gamma}^{(\infty)}_{11}(\mathbf{k})$ are bounded and continuous, we infer that the density $\rho^{(\infty)}_{11}(\mathbf{k}; k_2')$ possesses definite limits, respectively, along the following paths: (i) $\mathbf{k} = (k_1, k_2, k_3) \to (0^-, k_2, k_3)$, $k_2' \to k_2^-$; (ii) $\mathbf{k} = (k_1, 0, k_3) \to (0^-, 0, k_3)$, $k_2' \to 0^-$; (iii) $\mathbf{k} = (k_1, k_1, k_3) \to (0^-, 0^-, k_3)$, $k_2' \to 0^-$; and (iv) $\mathbf{k} = (k_1, k_1, k_1) \to (0^-, 0^-, 0^-)$, $k_2' \to 0^-$. Applying the existence of the limits, we get

$$\lim_{k_1 \to 0^-} \frac{\dot{\gamma}^{(\infty)}_{11}(k_1, 0, 0)}{k_1} = \lim_{k_1 \to 0^-} \frac{\dot{U}^{(\infty)}_{12}(k_1, 0, 0)}{k_1} = \lim_{k_1 \to 0^-} \frac{3\,\dot{\gamma}^{(\infty)}_{11}(k_1, k_1, k_1) - \dot{U}^{(\infty)}_{12}(k_1, k_1, k_1)}{k_1}$$

$$= \lim_{k_1 \to 0^-} \frac{\dot{\gamma}^{(\infty)}_{11}(k_1, k_2, k_3) - \dot{U}^{(\infty)}_{12}(k_1, k_2, k_3)}{k_1} = 0 \tag{3.36}$$

Other paths of $\mathbf{k}$ approaching $\mathbf{0}$ can be similarly explored.

The above relations indicate the existence of $\dot{U}^{(\infty)}_{12}(\mathbf{k})/k_1$, which motivates us to analyze (3.27) in the form of

$$\frac{\dot{U}^{(\infty)}_{12}(\mathbf{k})}{k_1} = \int_{-\infty}^{k_2} dk_2'\; \rho^{(\infty)}_{12}(\mathbf{k}; k_2') \tag{3.37}$$

where

$$\rho^{(\infty)}_{12}(\mathbf{k}; k_2') := -\frac{|\mathbf{k}'|^2}{|k_1|^2\, |\mathbf{k}|^2} \exp\big[2\big(H(\sigma, \mathbf{k}') - H(\sigma, \mathbf{k})\big)\big] \Big[- \left(1 - \frac{2\,(k_1)^2}{|\mathbf{k}'|^2} \right) \dot{U}^{(\infty)}_{22}(\mathbf{k}') + \dot{\gamma}^{(\infty)}_{12}(\mathbf{k}') \Big] \tag{3.38}$$

The supposed existence of the limits of $\rho^{(\infty)}_{12}(\mathbf{k}; k_2')$ along the paths listed above results in

$$\lim_{k_1 \to 0^-} \frac{\dot{\gamma}^{(\infty)}_{12}(k_1, 0, 0)}{(k_1)^2} = \lim_{k_1 \to 0^-} \frac{\dot{U}^{(\infty)}_{22}(k_1, 0, 0)}{(k_1)^2} = \lim_{k_1 \to 0^-} \frac{3\,\dot{\gamma}^{(\infty)}_{12}(k_1, k_1, k_1) - \dot{U}^{(\infty)}_{22}(k_1, k_1, k_1)}{(k_1)^2}$$

$$= \lim_{k_1 \to 0^-} \frac{\dot{\gamma}_{12}^{(\infty)}(k_1, k_2, k_3) - \dot{U}_{22}^{(\infty)}(k_1, k_2, k_3)}{(k_1)^2} = 0 \tag{3.39}$$

In the above derivation, $\lim_{k_1 \to 0^-} \dot{U}_{22}^{(\infty)}(\mathbf{k}) = 0$ has been employed, justified by the existence of $\lim_{k_1 \to 0^-} \dot{U}_{22}^{(\infty)}(\mathbf{k})/(k_1)^2$ which is consistent with (3.39) itself.

We now consider $\dot{U}_{22}^{(\infty)}(\mathbf{k})/(k_1)^2$ and rewrite (3.26) as

$$\frac{\dot{U}_{22}^{(\infty)}(\mathbf{k})}{(k_1)^2} = \int_{-\infty}^{k_2} dk_2' \; \rho_{22}^{(\infty)}(\mathbf{k}; k_2') \tag{3.40}$$

where

$$\rho_{22}^{(\infty)}(\mathbf{k}; k_2') := \frac{2\,|\mathbf{k}'|^4}{|k_1|^3\,|\mathbf{k}|^4} \exp\big[2\big(H(\sigma, \mathbf{k}') - H(\sigma, \mathbf{k})\big)\big]\, \dot{\gamma}_{22}^{(\infty)}(\mathbf{k}') \tag{3.41}$$

With the arguments similar to the above, we infer that

$$\lim_{k_1 \to 0^-} \frac{\dot{\gamma}_{22}^{(\infty)}(k_1, k_2, k_3)}{(k_1)^3} = \lim_{k_1 \to 0^-} \frac{\dot{\gamma}_{22}^{(\infty)}(k_1, k_1, k_3)}{(k_1)^3} = \lim_{k_1 \to 0^-} \frac{\dot{\gamma}_{22}^{(\infty)}(k_1, k_1, k_1)}{(k_1)^3} = 0 \tag{3.42}$$

The above limits for $\dot{\gamma}_{ij}^{(\infty)}(\mathbf{k})$ can be easily recast in terms of $\tilde{U}_{ijk}^{(I\infty)}(\mathbf{k}, \mathbf{l})$ and $\tilde{U}_{(ij)k}^{(I\infty)}(\mathbf{k})$.

We should mention that we have derived (3.36), (3.39) and (3.42) under the restriction of $\sigma \geq 0$. In the case of $\sigma < 0$, more stringent limits are expected along the paths of $\mathbf{k} \to \mathbf{0}$, due to the singularity to be discussed in Subsection 4.3.

4 Asymptotic State Solutions of Second-order Model

Considering the computing resources available and to guide our exploration of the three-dimensional homogeneous shear turbulence modeling, we now restrict our discussion to the second-order model and its asymptotic state solutions in the form of (3.1). This restriction to the asymptotic states will also be demonstrated as a necessity for the second-order model. We have $\dot{\gamma}_{11}^{(\infty)}(\mathbf{k})$, $\dot{\gamma}_{12}^{(\infty)}(\mathbf{k})$ and $\dot{\gamma}_{22}^{(\infty)}(\mathbf{k})$ as the control variables, and $\dot{U}_{11}^{(\infty)}(\mathbf{k})$, $\dot{U}_{12}^{(\infty)}(\mathbf{k})$ and $\dot{U}_{22}^{(\infty)}(\mathbf{k})$ as the primary state variables. Because of the symmetry properties of (3.30), we will restrict the control and state variables to $k_1 < 0$ and $k_3 \geq 0$. We present the analytical results first.

For the sake of convenience, we summarize here the mathematical relations involved in the optimal control and optimization problem.

1. Equations (2.42), (3.25) and (3.30) result in

$$\begin{aligned}
&\tilde{U}_{13}^{(\infty)}(\mathbf{k}) = -k_1\, k_3\, \dot{U}_{11}^{(\infty)}(\mathbf{k}) - k_2\, k_3\, \dot{U}_{12}^{(\infty)}(\mathbf{k}), \quad \tilde{U}_{23}^{(\infty)}(\mathbf{k}) = -k_1\, k_3\, \dot{U}_{12}^{(\infty)}(\mathbf{k}) - k_2\, k_3\, \dot{U}_{22}^{(\infty)}(\mathbf{k}), \\
&\tilde{U}_{33}^{(\infty)}(\mathbf{k}) = (k_1)^2\, \dot{U}_{11}^{(\infty)}(\mathbf{k}) + (k_2)^2\, \dot{U}_{22}^{(\infty)}(\mathbf{k}) + 2\, k_1\, k_2\, \dot{U}_{12}^{(\infty)}(\mathbf{k}), \quad \tilde{U}_{ij}^{(\infty)}(\mathbf{k}) = (k_3)^2\, \dot{U}_{ij}^{(\infty)}(\mathbf{k}), \\
&\tilde{U}_{ij}^{(\infty)}(\mathbf{k}) = \tilde{U}_{ji}^{(\infty)}(\mathbf{k})
\end{aligned} \tag{4.1}$$

and

$$\dot{U}_{ij}^{(\infty)}(k_1, k_2, -k_3) = \dot{U}_{ij}^{(\infty)}(\mathbf{k}) = \dot{U}_{ij}^{(\infty)}(-\mathbf{k}), \quad ij = 11, 12, 22 \tag{4.2}$$

Equation (2.105), (3.20) and the symmetric properties of the second order correlation give that

$$U_{ij}^{(\infty)}(\mathbf{0}) = \overline{w_{i,k}(\mathbf{x})\, w_{j,k}(\mathbf{x})}^{(\infty)} = \overline{\omega_i \omega_j}^{(\infty)}(\mathbf{0}) = 0,\ ij = 13, 23; \quad \overline{w_i \omega_j}^{(\infty)}(\mathbf{0}) = 0,\ \forall i, j \tag{4.3}$$

whose first is consistent with the experimental and DNS data (see [11] and [12]).

2. The fluctuation vorticity-vorticity and velocity-vorticity correlations are related to $\tilde{U}_{ij}^{(\infty)}(\mathbf{k})$ through

$$\overline{\tilde{\omega}_i\, \tilde{\omega}_j}^{(\infty)}(\mathbf{k}) = \epsilon_{imn}\, \epsilon_{jkl}\, k_n\, k_l\, \tilde{U}_{mk}^{(\infty)}(\mathbf{k}), \quad \overline{\tilde{w}_i\, \tilde{\omega}_j}^{(\infty)}(\mathbf{k}) = \imath\, \epsilon_{jpq}\, k_q\, \tilde{U}_{ip}^{(\infty)}(\mathbf{k}) \tag{4.4}$$

following from (2.86), (2.89) and (3.1).

3. We can simplify (3.27) and (3.28) by integration. Introduce first

$$E(\mathbf{k}; k_2'; \sigma) := \exp\left[-\frac{2\,(k_2 - k_2')}{|k_1|} \left(\frac{1}{2}\,\sigma + (k_1)^2 + (k_3)^2 + \frac{1}{3}\left((k_2)^2 + (k_2')^2 + k_2\, k_2' \right) \right) \right] \tag{4.5}$$

and

$$F(\mathbf{k}) := \frac{(k_3)^2}{\left[|k_1|^2 + (k_3)^2\right]^{1/2}} \arctan \frac{k_2}{\left[|k_1|^2 + (k_3)^2\right]^{1/2}} - \frac{|k_1|^2\, k_2}{|\mathbf{k}|^2},$$
$$\left| \arctan \frac{k_2}{\left[|k_1|^2 + (k_3)^2\right]^{1/2}} \right| < \frac{\pi}{2} \tag{4.6}$$

We have from (3.26)

$$\dot{U}_{22}^{(\infty)}(\mathbf{k}) = \frac{2}{|k_1|\, |\mathbf{k}|^4} \int_{-\infty}^{k_2} dk_2'\, E(\mathbf{k}; k_2'; \sigma)\, |\mathbf{k}'|^4\, \dot{\gamma}_{22}^{(\infty)}(\mathbf{k}') \tag{4.7}$$

Substituting (4.7) into (3.27), changing the order of the double integration and then integrating once, we get

$$\begin{aligned} \dot{U}_{12}^{(\infty)}(\mathbf{k}) = &- \frac{2}{|k_1|^2\, [|k_1|^2 + (k_3)^2]\, |\mathbf{k}|^2} \int_{-\infty}^{k_2} dk_2'\, E(\mathbf{k}; k_2'; \sigma) \left(F(\mathbf{k}) - F(\mathbf{k}') \right) |\mathbf{k}'|^4\, \dot{\gamma}_{22}^{(\infty)}(\mathbf{k}') \\ &+ \frac{1}{|k_1|\, |\mathbf{k}|^2} \int_{-\infty}^{k_2} dk_2'\, E(\mathbf{k}; k_2'; \sigma)\, |\mathbf{k}'|^2\, \dot{\gamma}_{12}^{(\infty)}(\mathbf{k}') \end{aligned} \tag{4.8}$$

Similarly, (3.28) can be integrated once to yield

$$\begin{aligned} \dot{U}_{11}^{(\infty)}(\mathbf{k}) = &\frac{2}{|k_1|^3\, [|k_1|^2 + (k_3)^2]^2} \int_{-\infty}^{k_2} dk_2'\, E(\mathbf{k}; k_2'; \sigma) \left(F(\mathbf{k}) - F(\mathbf{k}') \right)^2 |\mathbf{k}'|^4\, \dot{\gamma}_{22}^{(\infty)}(\mathbf{k}') \\ &- \frac{2}{|k_1|^2\, [|k_1|^2 + (k_3)^2]} \int_{-\infty}^{k_2} dk_2'\, E(\mathbf{k}; k_2'; \sigma) \left(F(\mathbf{k}) - F(\mathbf{k}') \right) |\mathbf{k}'|^2\, \dot{\gamma}_{12}^{(\infty)}(\mathbf{k}') \end{aligned}$$

$$+\frac{2}{|k_1|}\int_{-\infty}^{k_2} dk_2'\, E(\mathbf{k};k_2';\sigma)\,\dot\gamma_{11}^{(\infty)}(\mathbf{k}') \tag{4.9}$$

The above operation of integration reduces the dimensions of integrals involved in the objective function below, and thus, it reduces the complexity of numerical computations to be implemented.

Another useful relation for the later use is that, under $k_1<0$,

$$\tilde U_{kk}^{(\infty)}(\mathbf{k})=\left[(k_1)^2+(k_3)^2\right]\dot U_{11}^{(\infty)}(\mathbf{k})+\left[(k_2)^2+(k_3)^2\right]\dot U_{22}^{(\infty)}(\mathbf{k})+2\,|k_1|\,k_2\left(-\dot U_{12}^{(\infty)}(\mathbf{k})\right) \tag{4.10}$$

following from (4.1).

4. As discussed in Subsection 2.8, we enforce the constraints of inequality (2.92)

$$\tilde U_{\underline{i}\underline{i}}^{(\infty)}(\mathbf{k})\ge 0,\quad \left|\tilde U_{ij}^{(\infty)}(\mathbf{k})\right|^2\le \tilde U_{\underline{i}\underline{i}}^{(\infty)}(\mathbf{k})\;\tilde U_{\underline{j}\underline{j}}^{(\infty)}(\mathbf{k}),\quad i<j \tag{4.11}$$

5. The intrinsic equalities of (3.30) and (3.31) result in

$$\frac{\partial}{\partial k_3}\dot\gamma_{ij}^{(\infty)}(k_1,k_2,k_3)\bigg|_{k_3=0}=0,\quad ij=11,12,22 \tag{4.12}$$

and

$$\int_{-\infty}^{0}dk_1\int_{\mathbb{R}}dk_2\int_0^{+\infty}dk_3\Big[\left((k_1)^2+(k_3)^2\right)\dot\gamma_{11}^{(\infty)}(\mathbf{k})+\left((k_2)^2+(k_3)^2\right)\dot\gamma_{22}^{(\infty)}(\mathbf{k}) + k_1\,k_2\,\dot\gamma_{12}^{(\infty)}(\mathbf{k})\Big]=0 \tag{4.13}$$

We have the constraints of limits, (3.36), (3.39) and (3.42),

$$\lim_{k_1\to0^-}\frac{\dot\gamma_{11}^{(\infty)}(k_1,0,0)}{k_1}=\lim_{k_1\to0^-}\frac{\dot U_{12}^{(\infty)}(k_1,0,0)}{k_1}=\lim_{k_1\to0^-}\frac{3\,\dot\gamma_{11}^{(\infty)}(k_1,k_1,k_1)-\dot U_{12}^{(\infty)}(k_1,k_1,k_1)}{k_1}$$

$$=\lim_{k_1\to0^-}\frac{\dot\gamma_{11}^{(\infty)}(k_1,k_2,k_3)-\dot U_{12}^{(\infty)}(k_1,k_2,k_3)}{k_1}=0,$$

$$\lim_{k_1\to0^-}\frac{\dot\gamma_{12}^{(\infty)}(k_1,0,0)}{(k_1)^2}=\lim_{k_1\to0^-}\frac{\dot U_{22}^{(\infty)}(k_1,0,0)}{(k_1)^2}=\lim_{k_1\to0^-}\frac{3\,\dot\gamma_{12}^{(\infty)}(k_1,k_1,k_1)-\dot U_{22}^{(\infty)}(k_1,k_1,k_1)}{(k_1)^2}$$

$$=\lim_{k_1\to0^-}\frac{\dot\gamma_{12}^{(\infty)}(k_1,k_2,k_3)-\dot U_{22}^{(\infty)}(k_1,k_2,k_3)}{(k_1)^2}=0,$$

$$\lim_{k_1\to0^-}\frac{\dot\gamma_{22}^{(\infty)}(k_1,k_2,k_3)}{(k_1)^3}=\lim_{k_1\to0^-}\frac{\dot\gamma_{22}^{(\infty)}(k_1,k_1,k_3)}{(k_1)^3}=\lim_{k_1\to0^-}\frac{\dot\gamma_{22}^{(\infty)}(k_1,k_1,k_1)}{(k_1)^3}=0 \tag{4.14}$$

These constraints are automatically satisfied in the numerical simulations if the supports of $\dot\gamma_{ij}^{(\infty)}(\mathbf{k})$ and $\dot U_{ij}^{(\infty)}(\mathbf{k})$ are restricted to $\mathbf{k}$ with $k_1\le\max k_1<0$, which will be adopted.

6. We need to set the bound to the control variables such as

$$\left|\dot{\gamma}_{ij}^{(\infty)}(\mathbf{k})\right| \le C = 1, \quad ij = 11, 12, 22 \tag{4.15}$$

Though the optimal control of the asymptotic state solutions does not yield absolute values for $\tilde{U}_{ij}^{(\infty)}(\mathbf{k})$, it provides us the normalized distributions as represented by the dimensionless anisotropy tensor of

$$b_{ij}^{(\infty)} := \frac{U_{ij}^{(\infty)}(\mathbf{0})}{U_{kk}^{(\infty)}(\mathbf{0})} - \frac{1}{3}\,\delta_{ij} = \frac{U_{ij}(\mathbf{0})}{U_{kk}(\mathbf{0})} - \frac{1}{3}\,\delta_{ij} \tag{4.16}$$

The value of the tensor is not affected by the special bound selected in (4.15) within the second-order model, because of the property of scaling invariance under

$$\left\{\tilde{U}_{ij}^{(\infty)}, \dot{\gamma}_{ij}^{(\infty)}(\mathbf{k})\right\} \to \lambda \left\{\tilde{U}_{ij}^{(\infty)}, \dot{\gamma}_{ij}^{(\infty)}(\mathbf{k})\right\}, \quad \forall \lambda > 0 \tag{4.17}$$

In contrast, certain complication might arise regarding the effect of the bound in the fourth-order model due to the variance inequalities being acting under $\sigma = 0$.

7. The objective function of (2.117) reduces to

$$\begin{aligned} I_T^{\hom}(\sigma) &= U_{kk}^{(\infty)}(\mathbf{0}) \\ &= 4\int_{-\infty}^{0} dk_1 \int_{\mathbb{R}} dk_2 \int_{0}^{+\infty} dk_3 \Big[\left((k_1)^2 + (k_3)^2\right) \dot{U}_{11}^{(\infty)}(\mathbf{k}) + \left((k_2)^2 + (k_3)^2\right) \dot{U}_{22}^{(\infty)}(\mathbf{k}) \\ &\qquad + 2\,k_1\,k_2\,\dot{U}_{12}^{(\infty)}(\mathbf{k})\Big] \end{aligned} \tag{4.18}$$

We have a second-order cone programming problem as to be argued in Subsection 4.2. To help solve the problem numerically, we need to know the range for the values of σ and the finite support estimates for $\dot{\gamma}_{ij}^{(\infty)}(\mathbf{k})$ and $\dot{U}_{ij}^{(\infty)}(\mathbf{k})$.

4.1 Other Upper Bound for σ and Its Implication

We have obtained the upper bound for the exponential growth rate σ, $\max \sigma = 0$ in (3.3), within the fourth-order model. This bound is provided by the variance constraints that are beyond the scope of the second-order and the third-order models. As to be demonstrated here, the second-order model itself has an upper bound on σ greater than that of $\max \sigma = 0$, and thus, we need to enforce it explicitly by setting $\sigma \le 0$ within the model.

We have from (3.22)

$$\frac{\sigma}{2}\,U_{kk}^{(\infty)}(\mathbf{0}) = -U_{12}^{(\infty)}(\mathbf{0}) - \overline{\frac{\partial w_k(\mathbf{x})}{\partial x_j}\,\frac{\partial w_k(\mathbf{x})}{\partial x_j}}^{(\infty)} \tag{4.19}$$

The constraint of inequality (4.11) or its integral form (2.78) results in

$$\mp U_{12}^{(\infty)}(\mathbf{0}) \le \left(U_{11}^{(\infty)}(\mathbf{0})\right)^{1/2} \left(U_{22}^{(\infty)}(\mathbf{0})\right)^{1/2} \le \frac{1}{2}\left(U_{11}^{(\infty)}(\mathbf{0}) + U_{22}^{(\infty)}(\mathbf{0})\right) < \frac{1}{2}\,U_{kk}^{(\infty)}(\mathbf{0}) \tag{4.20}$$

Combining the above two equations and accounting for the imposition of the positive turbulent fluctuation energy and viscous dissipation, we get

$$\sigma < 1 - \frac{2}{U_{kk}^{(\infty)}(\mathbf{0})} \overline{\frac{\partial w_k(\mathbf{x})}{\partial x_j} \frac{\partial w_k(\mathbf{x})}{\partial x_j}}^{(\infty)} < 1 \tag{4.21}$$

The inequality implies that the second-order model prohibits $\sigma \geq 1$ from occurrence, but it may allow the asymptotic state solutions of $\sigma \in (0, 1)$ to emerge. To obtain an affirmative answer to this possibility, we resort to the fact that the model depends on σ only through (4.5),

$$E(\mathbf{k}; k_2'; \sigma) = \exp\Bigg[- \frac{2\,(k_2 - k_2')}{|k_1|} \left(\frac{1}{2}\,\sigma + (k_1)^2 + (k_3)^2 + \frac{1}{3} \left((k_2)^2 + (k_2')^2 + k_2\, k_2' \right) \right) \Bigg]$$

whose mathematical structure indicates that, only in certain region of the wave-number space, σ can significantly affect $\tilde{U}_{ij}^{(\infty)}(\mathbf{k})$ (and indirectly $\dot{\gamma}_{ij}^{(\infty)}(\mathbf{k})$ through the satisfaction of the constraints of inequality). Suppose that in the case of $\sigma = 0$ there exists a feasible solution $\left\{\tilde{U}_{ij}^{(\infty)}(\mathbf{k}),\, \dot{\gamma}_{ij}^{(\infty)}(\mathbf{k})\right\}_{\sigma\,=\,0}$ which has the trivial value in the region of

$$\mathcal{R}_0 := \left\{ \mathbf{k} :\ k_1 \in \left[-\sqrt{K_0}, 0 \right] \right\} \tag{4.22}$$

where K_0 is a positive constant. It then follows that under the condition of

$$|\sigma| < \frac{K_0}{50}, \quad \text{say,} \tag{4.23}$$

we have

$$\forall k_1 \leq -\sqrt{K_0}, \quad (k_1)^2 + (k_3)^2 + \frac{1}{3} \left((k_2)^2 + (k_2')^2 + k_2\, k_2' \right) \geq K_0 >> \frac{|\sigma|}{2} \tag{4.24}$$

That is, within the bound of (4.23), σ has a negligible effect on $E(\mathbf{k}; k_2'; \sigma)$ and $\tilde{U}_{ij}^{(\infty)}(\mathbf{k})$ outside $\mathcal{R}_0$. Inside $\mathcal{R}_0$, σ has no effect on $\tilde{U}_{ij}^{(\infty)}(\mathbf{k})$, due to the supposed trivial value of the feasible solution underlying the definition of $\mathcal{R}_0$. Therefore, this feasible solution $\left\{\tilde{U}_{ij}^{(\infty)}(\mathbf{k}),\, \dot{\gamma}_{ij}^{(\infty)}(\mathbf{k})\right\}_{\sigma\,=\,0}$ is also a feasible solution to the values of σ satisfying (4.23), whether σ is positive or negative. Such feasible solutions can be obtained as to be presented in Subsection 4.5, and thus, the second-order model allows $\sigma > 0$, violating (3.3).

The above result holds for the third-order model too. The result demonstrates a key role played by the variance constraints like (2.114) and (2.115) in homogeneous shear turbulence. One crucial difference between the second-order and the third-order models and the fourth-order model lies in that the former two cannot but the latter can accommodate such constraints. This type of constraints makes the fourth-order model non-invariant under the transformation of (2.116), and consequently, within the fourth-order model the absolute values of the initial distributions of the correlations may have a significant impact on the evolution of the turbulence concerned, in contrast to the second-order and the third-order. The second-order and the third-order models may be adequate to the description of the asymptotic states where the value of σ (≤ 0) can be set explicitly, they are inadequate to describe the transient state evolutions.

The above limitation of the two lowest order models indicates the necessity of the fourth-order model or the higher to solve the transient homogeneous shear turbulence. The tremendous challenge of such a solution lies in that the much greater numbers of (discretized) state variables, control variables and constraints and integrals of higher dimensions are involved in the numerical computations.

It is interesting to notice that homogeneous turbulence is a rather peculiar motion. In this motion, the two-way coupling between the mean flow field of $\{\mathbf{V}, P\}$ and the correlation $\overline{w_i(\mathbf{x})w_j(\mathbf{y})}$ degenerates to one-way due to the dropping of the feedback from the correlation to the mean flow field, and as a consequence, the evolution equations for $\overline{w_i(\mathbf{x})w_j(\mathbf{y})}$ are linearized. This one-way decoupling gives rise to the emergence of $\sigma > 0$ in the second-order and the third-order models for homogeneous shear turbulence. For inhomogeneous turbulent flows, the two-way nonlinear coupling remains intact even within the two lowest order models, and an asymptotic state solution of $\Psi(\mathbf{x}, \mathbf{y}, t) = \Psi^{(\infty)}(\mathbf{x}, \mathbf{y}) \exp(\sigma t)$, $\sigma > 0$, will be excluded by the differential equations of evolution for both $\{\mathbf{V}, P\}$ and $\overline{w_i(\mathbf{x})w_j(\mathbf{y})}$. Consequently, if generalized appropriately, the two models may still produce bounded flow fields for inhomogeneous turbulence, and within the models, the absolute values of the initial distributions of the correlation may have a significant impact on their evolutions.

Under $\sigma = 0$, we can recast (3.22) in the form of

$$-U_{12}^{(\infty)}(\mathbf{0}) - \overline{\frac{\partial w_k(\mathbf{x})}{\partial x_j}\,\frac{\partial w_k(\mathbf{x})}{\partial x_j}}^{(\infty)} = \frac{\sigma}{2}\,U_{kk}^{(\infty)}(\mathbf{0}) = 0$$

which requires that

$$-U_{12}^{(\infty)}(\mathbf{0}) = \overline{\frac{\partial w_k(\mathbf{x})}{\partial x_j}\,\frac{\partial w_k(\mathbf{x})}{\partial x_j}}^{(\infty)} > 0, \quad b_{12}^{(\infty)} = \frac{U_{12}^{(\infty)}(\mathbf{0})}{U_{kk}^{(\infty)}(\mathbf{0})} < 0 \tag{4.25}$$

indicating that $-\tilde{U}_{12}^{(\infty)}(\mathbf{k})$ balances the turbulent energy dissipation directly. The negativity of $b_{12}^{(\infty)}$ is consistent with those experimental data listed in Table 2.1 of [11], but incompatible with the RDT prediction listed in Table 6.1 of [12]. We may also understand the role of a non-trivial $U_{12}^{(\infty)}(\mathbf{0})$ in the asymptotic states by setting $U_{12}^{(\infty)}(\mathbf{0}) = 0$ in (3.22) to get

$$\sigma\,U_{jj}^{(\infty)}(\mathbf{0}) = -2\,\overline{\frac{\partial w_k(\mathbf{x})}{\partial x_j}\,\frac{\partial w_k(\mathbf{x})}{\partial x_j}}^{(\infty)} < 0 \tag{4.26}$$

which results in $\sigma < 0$ and does not allow $\max \sigma = 0$ to occur.

4.2 Second-Order Cone Programming

Within the context of numerical simulation, the quadratic constraints in (4.11) are of the form

$$c^2 \le a\,b, \quad a = a_j\,\gamma_j \ge 0, \quad b = b_j\,\gamma_j \ge 0, \quad c = c_j\,\gamma_j \tag{4.27}$$

Here, it is supposed to adopt certain scheme to discretize the distributions of $\dot{\gamma}_{ij}^{(\infty)}(\mathbf{k})$, $ij = 22$, 12, 11, with (γ_i) as their representative discrete variables, say at a finite collection of nodes.

The coefficients of (a_i), (b_i) and (c_i) depend on $\mathbf{k}$ for each inequality. Next, (4.27) can be rewritten as

$$0 \le a_i\,\gamma_i, \quad 0 \le b_i\,\gamma_i, \quad \left|\left|\left[\begin{array}{c} 2\,c_i\,\gamma_i \\ (a_i - b_i)\,\gamma_i \end{array}\right]\right|\right|_2 \le (a_i + b_i)\,\gamma_i \tag{4.28}$$

It then follows that the discretized second-order model is a second-order cone programming problem with the constraints adopted [10]. We may check later whether the optimal solution of the SOCP problem produces a non-negative determinant of $\tilde{U}_{ij}^{(\infty)}(\mathbf{k})$. Similarly, the discretized third-order model can be shown to be a SOCP problem.

Within the fourth-order model, all the quadratic constraints for the third and fourth order correlations constructed on the basis of the Cauchy-Schwarz inequality in the physical space can be discretized and cast in the form like that of (4.28) too, except that the discretized primary component variables of the fourth order correlation, (δ_i), need to be used, instead of (γ_i). Also, the variance constraints such as (2.114) and (2.115) are present. For the asymptotic state solutions of $\sigma < 0$, these constraints are satisfied automatically. In the case of $\sigma = 0$, the constraints take the form like

$$\left(U_{ij}^{(\infty)}(\mathbf{r})\right)^2 \le U_{\underline{ij}\underline{ij}}^{(\infty)}(\mathbf{0}, \mathbf{r}, \mathbf{r}), \ \cdots \tag{4.29}$$

which can be represented in numerical computations in the form of [10]

$$\delta_i\,P_{ij}\,\delta_j - b_i'\,\delta_i \le 0, \quad P_{ij} := a_i'\,a_j' \tag{4.30}$$

or

$$\left|\left|\left[\begin{array}{c} \frac{1}{2}\,(1 - b_k'\,\delta_k) \\ a_k'\,\delta_k \end{array}\right]\right|\right|_2 \le \frac{1}{2}\,(1 + b_k'\,\delta_k) \tag{4.31}$$

Consequently, the asymptotic states of the fourth-order model under discretization is also a SOCP problem.

The above conclusion of SOCP holds also for the second-order, the third-order and the fourth-order models in the discretized solutions of transient states, with the possibility of the supports of the correlations evolving in time.

4.3 Boundedness of $\tilde{U}_{ij}^{(\infty)}(\mathbf{k})$ and Its Effects on $\dot{\gamma}_{ij}^{(\infty)}(\mathbf{k}')$ under $\sigma < 0$

We deal with the asymptotic states of $\sigma < 0$ here, considering the peculiar structure of $E(\mathbf{k}; k_2'; \sigma)$ in (4.7) through (4.9), whose value can be extremely great for certain values of $\mathbf{k}$ and k_2' under $\sigma < 0$.

To have an estimate on the lower bound for σ, we combine (4.19) and (4.20) to get

$$\sigma > -1 - \frac{2}{U_{kk}^{(\infty)}(\mathbf{0})}\,\overline{\frac{\partial w_k(\mathbf{x})}{\partial x_j}\,\frac{\partial w_k(\mathbf{x})}{\partial x_j}}^{(\infty)} \tag{4.32}$$

We then have a rough estimate of $\sigma > -3$, if we assume $\overline{\partial_j w_k(\mathbf{x})\,\partial_j w_k(\mathbf{x})}^{(\infty)} \le U_{kk}^{(\infty)}(\mathbf{0})$. More analysis is needed to resolve the issue.

Let us discuss first the impact of $\sigma < 0$ on $\dot{U}_{22}^{(\infty)}(\mathbf{k})$ and $\dot{\gamma}_{22}^{(\infty)}(\mathbf{k}')$. Recast (4.7) in the form of

$$\dot{U}_{22}^{(\infty)}(\mathbf{k}) = \frac{2}{|k_1|}\int_{-\infty}^{k_2} dk_2' \, \frac{|\mathbf{k}'|^4}{|\mathbf{k}|^4} \exp\Bigg[-\frac{2\,(k_2-k_2')}{|k_1|}\left(\frac{1}{2}\,\sigma + (k_1)^2 + (k_3)^2 + \frac{1}{3}\left((k_2)^2 + (k_2')^2 + k_2\,k_2'\right)\right)\Bigg] \dot{\gamma}_{22}^{(\infty)}(\mathbf{k}') \tag{4.33}$$

It follows that the supposedly bounded $\dot{U}_{22}^{(\infty)}(\mathbf{k})$ can be achieved if $\dot{\gamma}_{22}^{(\infty)}(\mathbf{k}')$ balances the possibly extremely great value of $E(\mathbf{k}; k_2'; \sigma)$ under $\sigma < 0$. To quantify this extremity, we introduce

$$-\frac{2\,(k_2-k_2')}{|k_1|}\left(\frac{1}{2}\,\sigma + (k_1)^2 + (k_3)^2 + \frac{1}{3}\left((k_2)^2 + (k_2')^2 + k_2\,k_2'\right)\right) \geq K_2' > 0, \quad k_2' < k_2 \tag{4.34}$$

such as $K_2' = 5$ or 10. Inside the region of $\mathbf{k}'$ defined by (4.34), we will assume $\dot{\gamma}_{22}^{(\infty)}(\mathbf{k}') = 0$ to guarantee a bounded $\dot{U}_{22}^{(\infty)}(\mathbf{k})$. The above equation is a cubic inequality for k_2'; For it to have a solution under $k_2' < k_2$, it is necessary to have

$$0.5\,\sigma + (k_1)^2 + (k_3)^2 < 0 \tag{4.35}$$

$$-1 < \frac{k_2}{\left|0.5\,\sigma + (k_1)^2 + (k_3)^2\right|^{1/2}} < 2 \tag{4.36}$$

and

$$-2 < \frac{k_2'}{\left|0.5\,\sigma + (k_1)^2 + (k_3)^2\right|^{1/2}} < 1 \tag{4.37}$$

For any $\sigma < 0$, (4.34) has solutions under some small $|\mathbf{k}'|$, which may be demonstrated by the special case of $k_2 = k_3 = 0$ and $|k_1| \to 0^+$,

$$k_2'\left((k_2')^2 + 1.5\,\sigma\right) \geq 0, \quad k_2' \in \left[-(1.5\,|\sigma|)^{1/2},\ 0\right) \tag{4.38}$$

We can solve (4.34) under the condition of

$$D = \left[0.75\,K_2'\,|k_1| + 1.5\,k_2\left(0.5\,\sigma + |k_1|^2 + (k_3)^2 + \frac{1}{3}\,(k_2)^2\right)\right]^2 - \left|0.5\,\sigma + |k_1|^2 + (k_3)^2\right|^3 \leq 0 \tag{4.39}$$

to obtain

$$-\cos\frac{\pi/2-\theta}{3} - \sqrt{3}\,\sin\frac{\pi/2-\theta}{3} \leq \frac{k_2'}{\left|0.5\,\sigma + |k_1|^2 + (k_3)^2\right|^{1/2}} \leq -\cos\frac{\pi/2-\theta}{3} + \sqrt{3}\,\sin\frac{\pi/2-\theta}{3} \tag{4.40}$$

where

$$\theta = \tan^{-1}\frac{0.75\,K_2'\,|k_1| + 1.5\,k_2\left(0.5\,\sigma + |k_1|^2 + (k_3)^2 + \frac{1}{3}\,(k_2)^2\right)}{|D|^{1/2}} \tag{4.41}$$

To obtain the specific information regarding where to set $\dot{\gamma}_{22}^{(\infty)}(\mathbf{k}') = 0$, we fix k_1 and k_3 first according to (4.35) and then follow the procedure below.

1. Pick k_2 which satisfies the necessary condition of (4.36) and guarantees the existence of solution of (4.40). Then, (4.40) gives the interval of k_2' where $E(\mathbf{k}; k_2'; \sigma)$ is great. The structure of (4.33) requires that

$$\dot{\gamma}_{22}^{(\infty)}(\mathbf{k}') = 0, \quad k_2' \text{ in the interval} \tag{4.42}$$

   in order to make $\dot{U}_{22}^{(\infty)}(\mathbf{k})$ bounded under $\sigma < 0$.

2. That $\dot{\gamma}_{22}^{(\infty)}(\mathbf{k}')$ is independent of k_2 (except the condition of $k_2' \le k_2$) and the integration structure of (4.33) imply that we need to take

$$\dot{\gamma}_{22}^{(\infty)}(\mathbf{k}') = 0, \quad k_2' \in \big[\min k_2',\ \max k_2'\big] \tag{4.43}$$

   Here, $[\min k_2',\ \max k_2']$ is the maximum interval of k_2' inferred from (4.40),

$$\frac{\min k_2'}{\big|0.5\,\sigma + (k_1)^2 + (k_3)^2\big|^{1/2}} = \min_{k_2}\left\{ -\cos\frac{\pi/2-\theta}{3} - \sqrt{3}\,\sin\frac{\pi/2-\theta}{3}\right\}, \tag{4.44}$$

   and

$$\frac{\max k_2'}{\big|0.5\,\sigma + (k_1)^2 + (k_3)^2\big|^{1/2}} = \max_{k_2}\left\{ -\cos\frac{\pi/2-\theta}{3} + \sqrt{3}\,\sin\frac{\pi/2-\theta}{3}\right\}, \tag{4.45}$$

   The two search domains of k_2 in (4.44) and (4.45) are determined, respectively, by the necessary condition of (4.36) and the existence of solution for k_2' in (4.40).

One specific example will be displayed in Fig. 4.2.

Next, we discuss the effects on $\dot{\gamma}_{12}^{(\infty)}(\mathbf{k}')$ and $\dot{\gamma}_{11}^{(\infty)}(\mathbf{k}')$. Recall (4.8),

$$\begin{aligned}\dot{U}_{12}^{(\infty)}(\mathbf{k}) = &-\frac{2}{|k_1|^2\,[|k_1|^2 + (k_3)^2]\,|\mathbf{k}|^2}\int_{-\infty}^{k_2} dk_2'\,E(\mathbf{k}; k_2'; \sigma)\,\big(F(\mathbf{k}) - F(\mathbf{k}')\big)\,|\mathbf{k}'|^4\,\dot{\gamma}_{22}^{(\infty)}(\mathbf{k}') \\ &+\frac{1}{|k_1|\,|\mathbf{k}|^2}\int_{-\infty}^{k_2} dk_2'\,E(\mathbf{k}; k_2'; \sigma)\,|\mathbf{k}'|^2\,\dot{\gamma}_{12}^{(\infty)}(\mathbf{k}')\end{aligned}$$

Applying (4.43) and ensuring the boundedness of $\dot{U}_{12}^{(\infty)}(\mathbf{k})$, we infer

$$\dot{\gamma}_{12}^{(\infty)}(\mathbf{k}') = 0, \quad k_2' \in \big[\min k_2',\ \max k_2'\big]$$

Similarly, we consider (4.9) to get

$$\dot{\gamma}_{11}^{(\infty)}(\mathbf{k}') = 0, \quad k_2' \in \big[\min k_2',\ \max k_2'\big]$$

Consequently, we have

$$\dot{\gamma}_{ij}^{(\infty)}(\mathbf{k}') = 0, \quad k_2' \in \big[\min k_2',\ \max k_2'\big] \tag{4.46}$$

in order to guarantee that $\dot{U}_{ij}^{(\infty)}(\mathbf{k})$ are bounded under $\sigma < 0$.

4.4 Finite Support Estimates of $\dot{\gamma}_{ij}^{(\infty)}(\mathbf{k})$ and $\tilde{U}_{ij}^{(\infty)}(\mathbf{k})$

We provide a finite estimate of the support of $\dot{\gamma}_{ij}^{(\infty)}(\mathbf{k})$ as follows.

1. Inequality (4.21) can be recast in the form of

$$\int_{-\infty}^{0} dk_1 \int_{\mathbb{R}} dk_2 \int_{0}^{+\infty} dk_3 \left(1-\sigma-2\left|\mathbf{k}\right|^2\right) \tilde{U}_{kk}^{(\infty)}(\mathbf{k}) > 0 \tag{4.47}$$

which, along with $\tilde{U}_{kk}^{(\infty)}(\mathbf{k}) \geq 0$ and $U_{kk}^{(\infty)}(\mathbf{0})$ being maximized, suggests that

$$\tilde{U}_{kk}^{(\infty)}(\mathbf{k}) \text{ should be predominant under } |\mathbf{k}|^2 < \frac{1-\sigma}{2} \tag{4.48}$$

Next, motivated by (4.10), (4.11) and (4.48) and that $\dot{U}_{ij}^{(\infty)}(\mathbf{k})$ have the same support, we adopt the following approximate condition for the three primary components of $\dot{U}_{ij}^{(\infty)}(\mathbf{k})$,

$$\dot{U}_{11}^{(\infty)}(\mathbf{k}),\ \dot{U}_{22}^{(\infty)}(\mathbf{k}),\ \dot{U}_{12}^{(\infty)}(\mathbf{k}) \text{ should be predominant under } |\mathbf{k}|^2 < \frac{1-\sigma}{2} \tag{4.49}$$

2. The mathematical structures of (4.7) through (4.9) and the requirement of (4.49) suggest a preliminary estimate of $|\mathbf{k}| \leq [(1-\sigma)/2]^{1/2}$ for the support of $\dot{\gamma}_{ij}^{(\infty)}(\mathbf{k})$. Taking into account the rough nature of this estimate and the desired robustness for numerical simulation, we enlarge it λ times to

$$|\mathbf{k}| \leq \lambda \left[(1-\sigma)/2\right]^{1/2}, \quad \lambda \in [1,5] \tag{4.50}$$

Considering that a rather regular support offers more flexibility to have its size fixed and is convenient for structured meshing and coding in numerical computations, we will replace (4.50) with a cuboid of

$$|k_i| \leq \lambda_i \left[(1-\sigma)/2\right]^{1/2}, \quad \lambda_i \in [1,5], \quad i=1,2,3 \tag{4.51}$$

It then follows from (4.46) and (4.51) that

$$\begin{aligned} \mathcal{D}_{\gamma}(\sigma) = \Big\{ \mathbf{k} :\ & k_1 \in \big[-\lambda_1 \left[(1-\sigma)/2\right]^{1/2}, 0\big),\ |k_2| \leq \lambda_2 \left[(1-\sigma)/2\right]^{1/2}, \\ & k_3 \in \left[0, \lambda_3 \left[(1-\sigma)/2\right]^{1/2}\right] \Big\} \\ \Big/ \Big\{ \mathbf{k} :\ & k_1 < 0,\ k_3 \geq 0,\ k_2 \in \big(\min k_2',\ \max k_2'\big) \Big\} \end{aligned} \tag{4.52}$$

is taken as the support estimate for $\dot{\gamma}_{ij}^{(\infty)}(\mathbf{k})$. The specific values of λ_i are to be fixed, especially from the aspect of computational complexity. For the convenience of simulation, we may approximate $\min k_2'$ and $\max k_2'$ with constants.

3. The structure of (4.7) and the requirement $\tilde{U}_{22}^{(\infty)}(\mathbf{k}) \geq 0$ of (4.11) provide us some rough estimate on the distribution of $\dot{\gamma}_{22}^{(\infty)}(\mathbf{k}')$. Considering that $E(\mathbf{k}; k_2'; \sigma)$ is a positive, monotonically increasing function of k_2' at fixed $\mathbf{k}$ and σ, say, under $0.5\,\sigma + (k_1)^2 + (k_3)^2 \geq 0$ for the sake of simplicity, we may infer that

$$\int_{-\infty}^{k_2} dk_2' \, |\mathbf{k}'|^4 \, \dot{\gamma}_{22}^{(\infty)}(\mathbf{k}') \geq 0, \quad \forall k_2 \tag{4.53}$$

which can be demonstrated with an argument similar to the one used in PART II.

The above necessary condition to satisfy $\dot{U}_{22}^{(\infty)}(\mathbf{k}) \geq 0$ implies that, if $\dot{\gamma}_{22}^{(\infty)}(\mathbf{k}')$ takes negative values, these values should distribute in the region of small $|\mathbf{k}'|$ and $|k_2'|$. For instance, we may add that

$$\begin{aligned} &\dot{\gamma}_{22}^{(\infty)}(\mathbf{k}') \text{ has its positive located mainly in the local peak region and its negative} \\ &\qquad \text{mainly in the local valley region of } |\mathbf{k}'|^4 \, E(\mathbf{k}; k_2'; \sigma) \end{aligned} \tag{4.54}$$

The local peak and valley regions of $|\mathbf{k}'|^4 \, E(\mathbf{k}; k_2'; \sigma)$ can be determined through

$$\begin{aligned} &\frac{\partial}{\partial k_2'}\big(|\mathbf{k}'|^4 \, E(\mathbf{k}; k_2'; \sigma)\big) = 0, \\ &2\,|k_1|\,k_2' + \big((k_1)^2 + (k_2')^2 + (k_3)^2\big)\left(\frac{1}{2}\,\sigma + (k_1)^2 + (k_2')^2 + (k_3)^2\right) = 0 \end{aligned} \tag{4.55}$$

similar to that discussed in PART II. The region of $\partial\big(|\mathbf{k}'|^4 \, E(\mathbf{k}; k_2'; \sigma)\big)/\partial k_2' \leq 0$ is bounded by

$$k_1 < 0, \;\; k_3 \geq 0, \;\; k_2' < 0, \;\; |\mathbf{k}'| \leq 1 + \frac{1}{2}\,|\sigma| \tag{4.56}$$

Further, (4.7) results in

$$\begin{aligned} \dot{U}_{22}^{(\infty)}(\mathbf{k}) = &\frac{\big|(k_1, \lambda_2\,[(1-\sigma)/2]^{1/2}, k_3)\big|^4}{|\mathbf{k}|^4} \, E\Big(\mathbf{k}; \lambda_2\,[(1-\sigma)/2]^{1/2}; \sigma\Big) \\ &\times \dot{U}_{22}^{(\infty)}\Big(k_1, \lambda_2\,[(1-\sigma)/2]^{1/2}, k_3\Big), \quad \forall k_2 \geq \lambda_2\,[(1-\sigma)/2]^{1/2} \end{aligned} \tag{4.57}$$

It then follows that the implementation of $\tilde{U}_{22}^{(\infty)}(\mathbf{k}) \geq 0$ can be restricted to the above $\mathcal{D}_\gamma$, which reduces the number of constraints in simulation.

We now seek a finite support estimate of $\dot{U}_{ij}^{(\infty)}(\mathbf{k})$, denoted as $\mathcal{D}_U(\sigma)$. To this end, we introduce, under $k_1 \in \big[-\lambda_1\,[(1-\sigma)/2]^{1/2}, 0\big)$ and $k_3 \in \big[0, \lambda_3\,[(1-\sigma)/2]^{1/2}\big]$,

$$K_{2L}^{\gamma}(k_1, k_3; \sigma) := -\lambda_2\,[(1-\sigma)/2]^{1/2}, \quad K_{2U}^{\gamma}(k_1, k_3; \sigma) := \lambda_2\,[(1-\sigma)/2]^{1/2} \tag{4.58}$$

These are, respectively, the bottom and top bounding surfaces for k_2 of the support $\mathcal{D}_\gamma(\sigma)$ in (4.52). Considering the relationship between $\dot{U}_{ij}^{(\infty)}$ and $\dot{\gamma}_{ij}^{(\infty)}$ in (4.7) through (4.9), we take $k_2 =$

$K^{\gamma}_{2L}(k_1,k_3;\sigma)$ as the lower bound for $\mathcal{D}_U(\sigma)$ too. For the upper bound of $k_2 = K^{U}_{2U}(k_1,k_3;\sigma)$ for $\mathcal{D}_U(\sigma)$, we need to take into account the integral nature of the expressions for $\dot{U}^{(\infty)}_{ij}(\mathbf{k})$ as follows.

Under $k_2 \geq K^{\gamma}_{2U}(k_1,k_3;\sigma)$, (4.7) through (4.9) can be cast in the forms of

$$\begin{aligned}
&\dot{U}^{(\infty)}_{22}(\mathbf{k}) \\
&= \frac{2\,E(\mathbf{k};K^{\gamma}_{2U}(k_1,k_3;\sigma);\sigma)}{|k_1|\,|\mathbf{k}|^4}\int_{K^{\gamma}_{2L}(k_1,k_3;\sigma)}^{K^{\gamma}_{2U}(k_1,k_3;\sigma)} dk'_2\,E((k_1,K^{\gamma}_{2U}(k_1,k_3;\sigma),k_3);k'_2;\sigma)\,|\mathbf{k}'|^4\,\dot{\gamma}^{(\infty)}_{22}(\mathbf{k}')
\end{aligned} \tag{4.59}$$

$$\begin{aligned}
&\dot{U}^{(\infty)}_{12}(\mathbf{k}) \\
&= \frac{E(\mathbf{k};K^{\gamma}_{2U}(k_1,k_3;\sigma);\sigma)}{|k_1|\,|\mathbf{k}|^2} \\
&\quad\times\Bigg[-\int_{K^{\gamma}_{2L}(k_1,k_3;\sigma)}^{K^{\gamma}_{2U}(k_1,k_3;\sigma)} dk'_2\,\frac{2\,E((k_1,K^{\gamma}_{2U}(k_1,k_3;\sigma),k_3);k'_2;\sigma)\left(F(\mathbf{k})-F(\mathbf{k}')\right)|\mathbf{k}'|^4}{|k_1|\,[|k_1|^2+(k_3)^2]}\,\dot{\gamma}^{(\infty)}_{22}(\mathbf{k}') \\
&\qquad+\int_{K^{\gamma}_{2L}(k_1,k_3;\sigma)}^{K^{\gamma}_{2U}(k_1,k_3;\sigma)} dk'_2\,E((k_1,K^{\gamma}_{2U}(k_1,k_3;\sigma),k_3);k'_2;\sigma)|\mathbf{k}'|^2\,\dot{\gamma}^{(\infty)}_{12}(\mathbf{k}')\Bigg]
\end{aligned} \tag{4.60}$$

and

$$\begin{aligned}
&\dot{U}^{(\infty)}_{11}(\mathbf{k}) \\
&= \frac{2\,E(\mathbf{k};K^{\gamma}_{2U}(k_1,k_3;\sigma);\sigma)}{|k_1|} \\
&\quad\times\Bigg[\int_{K^{\gamma}_{2L}(k_1,k_3;\sigma)}^{K^{\gamma}_{2U}(k_1,k_3;\sigma)} dk'_2\,\frac{E((k_1,K^{\gamma}_{2U}(k_1,k_3;\sigma),k_3);k'_2;\sigma)\left(F(\mathbf{k})-F(\mathbf{k}')\right)^2|\mathbf{k}'|^4}{|k_1|^2\,[|k_1|^2+(k_3)^2]^2}\,\dot{\gamma}^{(\infty)}_{22}(\mathbf{k}') \\
&\qquad-\int_{K^{\gamma}_{2L}(k_1,k_3;\sigma)}^{K^{\gamma}_{2U}(k_1,k_3;\sigma)} dk'_2\,\frac{E((k_1,K^{\gamma}_{2U}(k_1,k_3;\sigma),k_3);k'_2;\sigma)\left(F(\mathbf{k})-F(\mathbf{k}')\right)|\mathbf{k}'|^2}{|k_1|\,[|k_1|^2+(k_3)^2]}\,\dot{\gamma}^{(\infty)}_{12}(\mathbf{k}') \\
&\qquad+\int_{K^{\gamma}_{2L}(k_1,k_3;\sigma)}^{K^{\gamma}_{2U}(k_1,k_3;\sigma)} dk'_2\,E((k_1,K^{\gamma}_{2U}(k_1,k_3;\sigma),k_3);k'_2;\sigma)\,\dot{\gamma}^{(\infty)}_{11}(\mathbf{k}')\Bigg]
\end{aligned} \tag{4.61}$$

The structures in the above three expressions indicate that $\left|\tilde{U}^{(\infty)}_{ij}(\mathbf{k})\right|$ at $k_2 = K^{U}_{2U}$ are controlled by $E\big(\big(k_1,K^{U}_{2U},k_3\big);K^{\gamma}_{2U};\sigma\big)$ and its three coefficients that are $\mathcal{D}_{\gamma}(\sigma)$-dependent. Theoretically, there are several possible ways to achieve negligibly small $\left|\tilde{U}^{(\infty)}_{ij}(\mathbf{k})\right|$ at $k_2 = K^{U}_{2U}$ (and beyond). The simplest is to have negligible $E\big(\big(k_1,K^{U}_{2U},k_3\big);K^{\gamma}_{2U};\sigma\big)$ by taking a great value of K^{U}_{2U}, as indicated by (4.5), which can be computationally costly, resulting from the great size of $\mathcal{D}_U(\sigma)$ for the computation of the objective (4.18) and the imposition of constraints (4.11). Also, the resultant small values of the state variables in the subregion close to $k_2 = K^{U}_{2U}$ make the satisfaction of the quadratic constraints computationally difficult. The second is to have the

three coefficients themselves small by employing adequate $\mathcal{D}_\gamma(\sigma)$. In this case, K_{2U}^U may be set close to K_{2U}^γ. We need to test this scheme numerically, considering the complexity of the equations involved.

As a rough and illustrative treatment, we estimate K_{2U}^U through, say,

$$
\begin{aligned}
&E\big((k_1, K_{2U}^U, k_3); K_{2U}^\gamma(k_1, k_3; \sigma); \sigma\big) = \exp(-K_2),\\
&\big(K_{2U}^U\big)^3 + 3\left(\frac{1}{2}\,\sigma + (k_1)^2 + (k_3)^2\right) K_{2U}^U\\
&- 3\,K_{2U}^\gamma\left(\frac{1}{2}\,\sigma + (k_1)^2 + (k_3)^2 + \frac{1}{3}\,\big(K_{2U}^\gamma\big)^2\right) - \frac{3\,K_2\,|k_1|}{2} = 0
\end{aligned}
\tag{4.62}
$$

where K_2 is a positive constant. Relation $(4.62)_2$ is a cubic equation for K_{2U}^U with the solution

$$
K_{2U}^U = \left(d - \frac{b}{2}\right)^{1/3} - \left(d + \frac{b}{2}\right)^{1/3} \tag{4.63}
$$

where

$$
\begin{aligned}
&d := \left[\left(\frac{a}{3}\right)^3 + \left(\frac{b}{2}\right)^2\right]^{1/2}, \quad a := 3\left(\frac{1}{2}\,\sigma + (k_1)^2 + (k_3)^2\right),\\
&b := -3\,K_{2U}^\gamma\left(\frac{1}{2}\,\sigma + (k_1)^2 + (k_3)^2 + \frac{1}{3}\,\big(K_{2U}^\gamma\big)^2\right) - \frac{3\,K_2\,|k_1|}{2}
\end{aligned}
$$

We now have the support estimate of $\dot{U}_{ij}^{(\infty)}(\mathbf{k})$,

$$
\begin{aligned}
\mathcal{D}_U(\sigma) = \Big\{\mathbf{k}:\ & k_1 \in \big[-\lambda_1\,[(1-\sigma)/2]^{1/2},\ 0\big),\ k_3 \in \big[0,\ \lambda_3\,[(1-\sigma)/2]^{1/2}\big],\\
& k_2 \in \big[K_{2L}^\gamma(k_1, k_3; \sigma),\ K_{2U}^U(k_1, k_3; \sigma)\big]\Big\}
\end{aligned}
\tag{4.64}
$$

Here, due to the integral nature of (4.7) through (4.9), (4.46) does not affect the support.

To have some idea about the size of the supports, two specific estimates of $\sigma = 0$ and $\sigma = -0.5$ are plotted in Fig. 4.1 and Fig. 4.2, respectively, in the case of $\lambda_1 = \lambda_2 = \lambda_3 = 3$ and $K_2 = 20$.

Clearly, the size of the support increases as σ decreases, which may be understood as follows. A greater support leads possibly to a greater integral of $|\mathbf{k}'|^2\,\tilde{U}_{kk}^{(\infty)}(\mathbf{k}')$ which indicates a greater viscous dissipation rate of turbulent energy into heat, and thus, the turbulence is decaying faster. According to this interpretation, the dominant values of $\tilde{U}_{kk}^{(\infty)}(\mathbf{k}')$ expectedly distribute in a region rather away from the origin of $\mathbf{k}' = \mathbf{0}$ in order to produce a substantial amount of viscous dissipation quantified by $|\mathbf{k}'|^2\,\tilde{U}_{kk}^{(\infty)}(\mathbf{k}')$, and consequently, not much turbulent energy is carried by the very small wave-numbers in the asymptotic states of decaying. This result is consistent with the proposed constraint of (4.46) associated with the subregion of great $E(\mathbf{k}; k_2', \sigma)$ under $\sigma < 0$, whose boundary is indicated by the broken curve close to the origin in Fig. 4.2. In the case of small $|\sigma|$, we may take a small threshold value of $\max k_1 < 0$ satisfying $0.5\,\sigma + |\max k_1|^2 \geq 0$, and construct $\mathcal{D}_\gamma(\sigma)$ such that $k_1 \leq \max k_1$ for all $\mathbf{k} \in \mathcal{D}_\gamma(\sigma)$. This

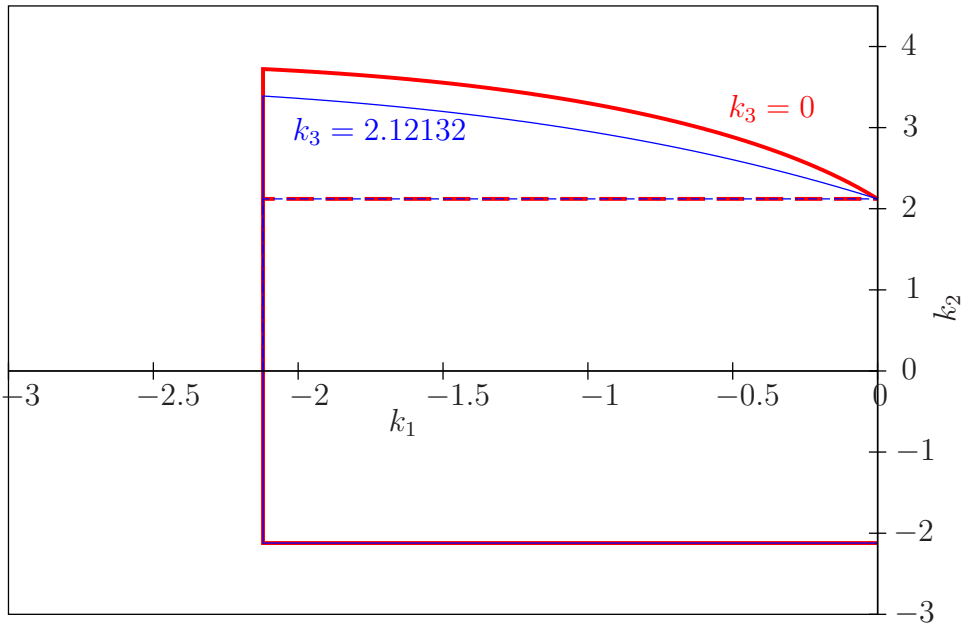

Figure 4.1: The support estimate of $\mathcal{D}_U(0)$ is represented by the sections of $k_3 = 0$ (thick curves) and $k_3 = 2.12132$ (thin curves), under $\lambda_1 = \lambda_2 = \lambda_3 = 3$ and $K_2 = 20$. The support estimate $\mathcal{D}_\gamma(0)$ of (4.52) is indicated by the broken lines.

restriction bypasses the region of the extremity (4.34) and the apparent singularity at $k_1 = 0$, and makes (4.14) satisfied automatically.

Both figures show that, under $\lambda_1 = \lambda_2 = \lambda_3 = 3$, $\mathcal{D}_U(\sigma)$ differs rather significantly from the corresponding $\mathcal{D}_\gamma(\sigma)$. The difference is expected to decrease under greater values of λ_i on the basis of (4.62). However, larger values of λ_i lead to the support estimates of greater size and the resultant computational problems of greater size for simulation. We should mention that the value of $K_2 = 20$ is used to plot the figures, such a large value is sufficient but maybe unnecessary to obtain an adequate K_{2U}^U, considering that the three coefficients of $E(\mathbf{k}; K_{2U}^\gamma; \sigma)$'s in (4.59) through (4.61) affect K_{2U}^U too. This issue will be examined further through numerical testing.

4.5 Numerical Simulation

We carry out numerical simulations under $\sigma = 0$ for both feasible and optimal solutions. For brevity, we intend to use $\mathcal{D}_\gamma(0)$ and $\mathcal{D}_U(0)$ to denote the supports for feasible solutions too. For the simplicity of coding, we take the hexahedra for $\mathcal{D}_\gamma(0)$ and $\mathcal{D}_U(0)$ as follows,

$$\mathcal{D}_\gamma(0) = [\min k_1, \max k_1] \times [\min k_2, \max k_2] \times [0, \max k_3]\,, \quad \max k_1 < 0 \tag{4.65}$$

and

$$\mathcal{D}_U(0) = [\min k_1, \max k_1] \times \left[\min k_2, \max k_2^U\right] \times [0, \max k_3] \tag{4.66}$$

Here, the value of $\max k_2^U$ is determined by $\left|\tilde{U}_{ij}^{(\infty)}(k_1, k_2, \max k_2^U)\right|$ being negligible, like that discussed in Subsection 4.4. The adoption of $\max k_1 < 0$ and the trivial boundary condition

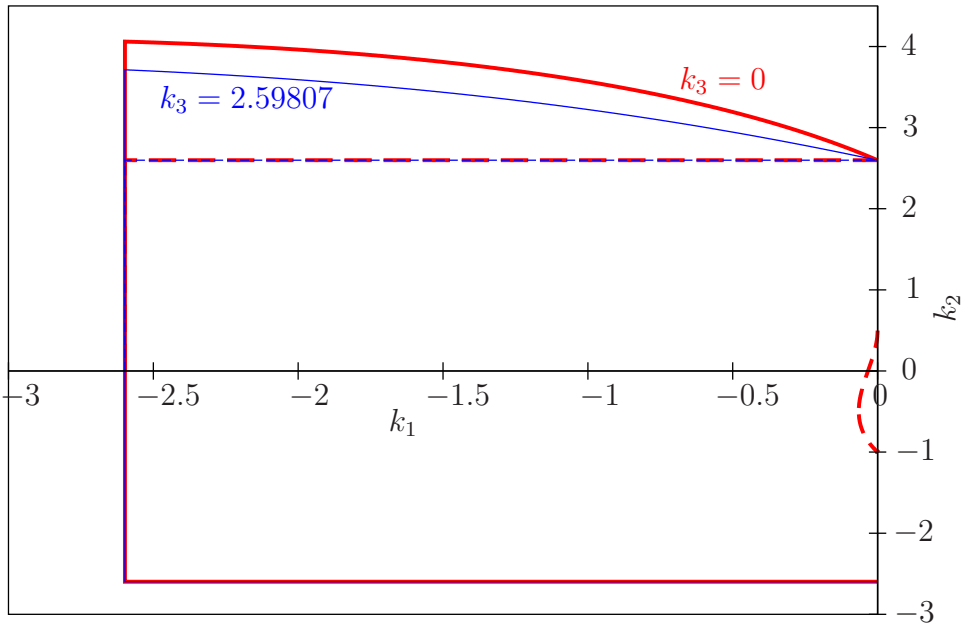

Figure 4.2: The support estimate of $\mathcal{D}_U(-0.5)$ in the sections of $k_3 = 0$ (thick curves) and $k_3 = 2.59807$ (thin curves), under $\lambda_1 = \lambda_2 = \lambda_3 = 3$, $K_2' = 5$ and $K_2 = 20$. The support estimate $\mathcal{D}_\gamma(-0.5)$ of (4.52) in the section of $k_3 = 0$ is indicated by the broken lines. The adoption of $K_2' = 5$ is to make the effect of $\sigma < 0$ on $\mathcal{D}_\gamma(-0.5)$ displayed prominently. The value of $\sigma = -0,5$ is taken for the purpose of illustration and whether such a rate of decaying can be achieved is yet to be examined.

for the control variables at $k_1 = \max k_1$ make the limits in (4.14) satisfied automatically. Next, $\mathcal{D}_\gamma(0)$ and $\mathcal{D}_U(0)$ are discretized with the structured hexahedral meshes,

$$\mathcal{D}_\gamma(0) = \bigcup_{n_1=1}^{N_1-1} \bigcup_{n_2=1}^{N_2-1} \bigcup_{n_3=1}^{N_3-1} \mathcal{H}(n_1, n_2, n_3), \quad \mathcal{D}_U(0) = \bigcup_{n_1=1}^{N_1-1} \bigcup_{n_2=1}^{M_2-1} \bigcup_{n_3=1}^{N_3-1} \mathcal{H}(n_1, n_2, n_3),$$

$$\mathcal{H}(n_1, n_2, n_3) = [k_{1,n_1}, k_{1,n_1+1}] \times [k_{2,n_2}, k_{2,n_2+1}] \times [k_{3,n_3}, k_{3,n_3+1}] \tag{4.67}$$

The distributions of $\dot\gamma_{ij}^{(\infty)}(\mathbf{k}')$, $ij = 22, 12, 11$, in each hexahedral cell $\mathcal{H}(n_1, n_2, n_3)$ of $\mathcal{D}_\gamma(0)$ is approximated by the tri-linear distribution,

$$\dot\gamma_{ij}^{(\infty)}(\mathbf{k}') = \chi_{[k_{1,n_1}, k_{1,n_1+1}]}(k_1)\, \chi_{[k_{2,n_2}, k_{2,n_2+1}]}(k_2')\, \chi_{[k_{3,n_3}, k_{3,n_3+1}]}(k_3)\, \dot\gamma_{ij}^{(\infty)\prime}(\mathbf{k}', n_1, n_2, n_3) \tag{4.68}$$

Here, $\chi_{[k_{1,n_1}, k_{1,n_1+1}]}$ and the like are the characteristic functions and

$$\begin{aligned} &\dot\gamma_{ij}^{(\infty)\prime}(\mathbf{k}', n_1, n_2, n_3) \\ &:= \left(\dot\gamma_{ij}^{(0)}(n_1, n_2, n_3) \frac{k_{2,n_2+1} - k_2'}{k_{2,n_2+1} - k_{2,n_2}} + \dot\gamma_{ij}^{(0)}(n_1, n_2+1, n_3) \frac{k_2' - k_{2,n_2}}{k_{2,n_2+1} - k_{2,n_2}} \right) \\ &\qquad \times \frac{k_{1,n_1+1} - k_1}{k_{1,n_1+1} - k_{1,n_1}} \frac{k_{3,n_3+1} - k_3}{k_{3,n_3+1} - k_{3,n_3}} \end{aligned}$$

$$
\begin{aligned}
&+\left(\dot\gamma_{ij}^{(0)}(n_1+1,n_2,n_3)\,\frac{k_{2,n_2+1}-k_2'}{k_{2,n_2+1}-k_{2,n_2}}+\dot\gamma_{ij}^{(0)}(n_1+1,n_2+1,n_3)\,\frac{k_2'-k_{2,n_2}}{k_{2,n_2+1}-k_{2,n_2}}\right)\\
&\qquad\times\frac{k_1-k_{1,n_1}}{k_{1,n_1+1}-k_{1,n_1}}\,\frac{k_{3,n_3+1}-k_3}{k_{3,n_3+1}-k_{3,n_3}}\\
&+\left(\dot\gamma_{ij}^{(0)}(n_1,n_2,n_3+1)\,\frac{k_{2,n_2+1}-k_2'}{k_{2,n_2+1}-k_{2,n_2}}+\dot\gamma_{ij}^{(0)}(n_1,n_2+1,n_3+1)\,\frac{k_2'-k_{2,n_2}}{k_{2,n_2+1}-k_{2,n_2}}\right)\\
&\qquad\times\frac{k_{1,n_1+1}-k_1}{k_{1,n_1+1}-k_{1,n_1}}\,\frac{k_3-k_{3,n_3}}{k_{3,n_3+1}-k_{3,n_3}}\\
&+\left(\dot\gamma_{ij}^{(0)}(n_1+1,n_2,n_3+1)\,\frac{k_{2,n_2+1}-k_2'}{k_{2,n_2+1}-k_{2,n_2}}+\dot\gamma_{ij}^{(0)}(n_1+1,n_2+1,n_3+1)\,\frac{k_2'-k_{2,n_2}}{k_{2,n_2+1}-k_{2,n_2}}\right)\\
&\qquad\times\frac{k_1-k_{1,n_1}}{k_{1,n_1+1}-k_{1,n_1}}\,\frac{k_3-k_{3,n_3}}{k_{3,n_3+1}-k_{3,n_3}}
\end{aligned}
\tag{4.69}
$$

The above piecewise trilinear approximation may be adequate at small cell sizes since only the integration operations are involved for the control variables. The discrete control variables at the vertices are directly constrained by (4.15), the definition of support and the symmetry of (4.12),

$$
\begin{aligned}
&\left|\dot\gamma_{ij}^{(0)}(n_1,n_2,n_3)\right|\le 1,\quad 1\le n_1\le N_1,\ 1\le n_2\le N_2,\ 1\le n_3\le N_3;\\
&\dot\gamma_{ij}^{(0)}(n_1,n_2,n_3)=0,\quad n_1\in\{1,N_1\}\text{ or }n_2\in\{1,N_2\}\text{ or }n_3=N_3;\\
&\dot\gamma_{ij}^{(0)}(n_1,n_2,2)=\dot\gamma_{ij}^{(0)}(n_1,n_2,1)
\end{aligned}
\tag{4.70}
$$

Substitution of (4.68) into (4.7) through (4.9) gives

$$
\begin{aligned}
\dot U_{22}^{(\infty)}(\mathbf{k}) =&\frac{2}{|k_1|\,|\mathbf{k}|^4}\,\chi_{[k_{1,n_1},k_{1,n_1+1}]}(k_1)\,\chi_{[k_{3,n_3},k_{3,n_3+1}]}(k_3)\\
&\times\sum_{n_2=1}^{N_2-1}\int_{k_{2,1}}^{k_2}dk_2'\,E(\mathbf{k};k_2';0)\,|\mathbf{k}'|^4\,\chi_{[k_{2,n_2},\,k_{2,n_2+1}]}(k_2')\,\dot\gamma_{22}^{(\infty)\prime}(\mathbf{k}',n_1,n_2,n_3)
\end{aligned}
\tag{4.71}
$$

$$
\begin{aligned}
&\dot U_{12}^{(\infty)}(\mathbf{k})\\
=&-\frac{2}{|k_1|^2\,[|k_1|^2+(k_3)^2]\,|\mathbf{k}|^2}\,\chi_{[k_{1,n_1},k_{1,n_1+1}]}(k_1)\,\chi_{[k_{3,n_3},k_{3,n_3+1}]}(k_3)\\
&\quad\times\sum_{n_2=1}^{N_2-1}\int_{k_{2,1}}^{k_2}dk_2'\,E(\mathbf{k};k_2';0)\,\big(F(\mathbf{k})-F(\mathbf{k}')\big)\,|\mathbf{k}'|^4\,\chi_{[k_{2,n_2},\,k_{2,n_2+1}]}(k_2')\,\dot\gamma_{22}^{(\infty)\prime}(\mathbf{k}',n_1,n_2,n_3)\\
&+\frac{1}{|k_1|\,|\mathbf{k}|^2}\,\chi_{[k_{1,n_1},k_{1,n_1+1}]}(k_1)\,\chi_{[k_{3,n_3},k_{3,n_3+1}]}(k_3)\\
&\quad\times\sum_{n_2=1}^{N_2-1}\int_{k_{2,1}}^{k_2}dk_2'\,E(\mathbf{k};k_2';0)\,|\mathbf{k}'|^2\,\chi_{[k_{2,n_2},\,k_{2,n_2+1}]}(k_2')\,\dot\gamma_{12}^{(\infty)\prime}(\mathbf{k}',n_1,n_2,n_3)
\end{aligned}
\tag{4.72}
$$

and

$$
\begin{aligned}
&\dot{U}_{11}^{(\infty)}(\mathbf{k}) \\
&= \frac{2}{|k_1|^3\,[|k_1|^2+(k_3)^2]^2}\,\chi_{[k_{1,n_1},k_{1,n_1+1}]}(k_1)\,\chi_{[k_{3,n_3},k_{3,n_3+1}]}(k_3) \\
&\quad\times\sum_{n_2=1}^{N_2-1}\int_{k_{2,1}}^{k_2} dk_2'\,E(\mathbf{k};k_2';0)\,\big(F(\mathbf{k})-F(\mathbf{k}')\big)^2\,|\mathbf{k}'|^4\,\chi_{(k_{2,n_2},k_{2,n_2+1}]}(k_2')\,\dot{\gamma}_{22}^{(\infty)\prime}(\mathbf{k}',n_1,n_2,n_3) \\
&\quad-\frac{2}{|k_1|^2\,[|k_1|^2+(k_3)^2]}\,\chi_{[k_{1,n_1},k_{1,n_1+1}]}(k_1)\,\chi_{[k_{3,n_3},k_{3,n_3+1}]}(k_3) \\
&\quad\times\sum_{n_2=1}^{N_2-1}\int_{k_{2,1}}^{k_2} dk_2'\,E(\mathbf{k};k_2';0)\,\big(F(\mathbf{k})-F(\mathbf{k}')\big)\,|\mathbf{k}'|^2\,\chi_{(k_{2,n_2},k_{2,n_2+1}]}(k_2')\,\dot{\gamma}_{12}^{(\infty)\prime}(\mathbf{k}',n_1,n_2,n_3) \\
&\quad+\frac{2}{|k_1|}\,\chi_{[k_{1,n_1},k_{1,n_1+1}]}(k_1)\,\chi_{[k_{3,n_3},k_{3,n_3+1}]}(k_3) \\
&\quad\times\sum_{n_2=1}^{N_2-1}\int_{k_{2,1}}^{k_2} dk_2'\,E(\mathbf{k};k_2';0)\;\chi_{(k_{2,n_2},k_{2,n_2+1}]}(k_2')\,\dot{\gamma}_{11}^{(\infty)\prime}(\mathbf{k}',n_1,n_2,n_3)
\end{aligned}
\tag{4.73}
$$

To apply the constraints of (4.11), we select three types of collocation points in $\mathcal{D}_U(0)$ as follows. (i) The points located in the middle of the cell edges parallel to the k_2-axis,

$$
k_1 = k_{1,n1},\;\; k_3 = k_{3,n_3},\;\; k_2 = 0.5\,(k_{2,n_2}+k_{2,n_2+1}) \tag{4.74}
$$

It is easy to verify from (4.71) through (4.73) that the $\tilde{U}_{ij}^{(\infty)}(\mathbf{k})$ at such points involve only the discrete control variables $\dot{\gamma}_{ij}^{(0)}(n_1,n_2',n_3)$, $n_2'\in\{1,\cdots,n_2+1\}$, like 1-dimensional, to be denoted as 1D. (ii) The points located in the center of the cell facets parallel to the k_2-axis,

$$
\begin{aligned}
&k_1 = k_{1,n1},\;\; k_3 = 0.5\,(k_{3,n_3}+k_{3,n_3+1}),\;\; k_2 = 0.5\,(k_{2,n_2}+k_{2,n_2+1}); \\
&k_1 = 0.5\,(k_{1,n_1}+k_{1,n_1+1}),\;\; k_3 = k_{3,n3},\;\; k_2 = 0.5\,(k_{2,n_2}+k_{2,n_2+1})
\end{aligned}
\tag{4.75}
$$

The $\tilde{U}_{ij}^{(\infty)}(\mathbf{k})$ at such points involve only the discrete control variables either $\dot{\gamma}_{ij}^{(0)}(n_1,n_2',n_3')$, $n_3'\in\{n_3,n_3+1\}$, $n_2'\in\{1,\cdots,n_2+1\}$ or $\dot{\gamma}_{ij}^{(0)}(n_1',n_2',n_3)$, $n_1'\in\{n_1,n_1+1\}$, $n_2'\in\{1,\cdots,n_2+1\}$, like 2-dimensional, to be denoted as 2D. (iii) The points located in the center of the cells,

$$
k_1 = 0.5\,(k_{1,n_1}+k_{1,n_1+1}),\;\; k_3 = 0.5\,(k_{3,n_3}+k_{3,n_3+1}),\;\; k_2 = 0.5\,(k_{2,n_2}+k_{2,n_2+1}); \tag{4.76}
$$

The $\tilde{U}_{ij}^{(\infty)}(\mathbf{k})$ at such points involve the discrete control variables $\dot{\gamma}_{ij}^{(0)}(n_1',n_2',n_3')$, $n_1'\in\{n_1,n_1+1\}$, $n_3'\in\{n_3,n_3+1\}$, $n_2'\in\{1,\cdots,n_2+1\}$, like 3-dimensional, to be referred to as 3D.

Substituting (4.68) into (4.13) and integrating analytically the integrals over the cells in $\mathcal{D}_\gamma(0)$ give us the global equality constraint for $\dot{\gamma}_{ij}^{(0)}(n_1,n_2,n_3)$, $n_1\in\{1,\cdots,N_1\}$, $n_2\in\{1,\cdots,N_2\}$, $n_3\in\{1,\cdots,N_3\}$. This global constraint and (4.70) will always be imposed in the following simulations of feasible and optimal solutions; For the inequality constraints (4.11), we apply them either with 1D or with the combination of 1D, 2D and 3D denoted as 1D & 2D & 3D.

In the evaluation of the objective function (4.18) and the second order correlations in the physical space, we need to deal with three types of global integrals, resulting from that there are three primary components of $\tilde{U}_{ij}^{(\infty)}(\mathbf{k})$, $ij = 22,\, 12,\, 11$. These three types are

$$\begin{aligned}
&\int_{-\infty}^{0} dk_1 \int_{0}^{+\infty} dk_3 \int_{\mathbb{R}} dk_2\, \Psi_{22}(\mathbf{k},\mathbf{r})\, \dot{U}_{22}^{(\infty)}(\mathbf{k}) \\
&= \sum_{n_1=1}^{N_1-1} \sum_{n_3=1}^{N_3-1} \sum_{n_2=1}^{N_2-1} \int_{k_{1,n_1}}^{k_{1,n_1+1}} dk_1 \int_{k_{3,n_3}}^{k_{3,n_3+1}} dk_3 \left[\int_{k_{2,n_2}}^{k_{2,n_2+1}} dk_2 \int_{k_{2,n_2}}^{k_2} dk_2' + \int_{k_{2,n_2}}^{k_{2,n_2+1}} dk_2' \int_{k_{2,n_2+1}}^{k_{2,M_2}} dk_2 \right] \\
&\qquad\qquad \times \frac{2\,\Psi_{22}(\mathbf{k},\mathbf{r})\, E(\mathbf{k}; k_2'; 0)\, |\mathbf{k}'|^4}{|k_1|\, |\mathbf{k}|^4}\, \dot{\gamma}_{22}^{(\infty)\prime}(\mathbf{k}', n_1, n_2, n_3) \qquad (4.77)
\end{aligned}$$

$$\begin{aligned}
&\int_{-\infty}^{0} dk_1 \int_{0}^{+\infty} dk_3 \int_{\mathbb{R}} dk_2\, \Psi_{12}(\mathbf{k},\mathbf{r})\, \dot{U}_{12}^{(\infty)}(\mathbf{k}) \\
&= \sum_{n_1=1}^{N_1-1} \sum_{n_3=1}^{N_3-1} \sum_{n_2=1}^{N_2-1} \int_{k_{1,n_1}}^{k_{1,n_1+1}} dk_1 \int_{k_{3,n_3}}^{k_{3,n_3+1}} dk_3 \left[\int_{k_{2,n_2}}^{k_{2,n_2+1}} dk_2 \int_{k_{2,n_2}}^{k_2} dk_2' + \int_{k_{2,n_2}}^{k_{2,n_2+1}} dk_2' \int_{k_{2,n_2+1}}^{k_{2,M_2}} dk_2 \right] \\
&\qquad\qquad \times \frac{-2\,\Psi_{12}(\mathbf{k},\mathbf{r})\, E(\mathbf{k}; k_2'; 0)\, \big(F(\mathbf{k}) - F(\mathbf{k}')\big)\, |\mathbf{k}'|^4}{|k_1|^2\, [|k_1|^2 + (k_3)^2]\, |\mathbf{k}|^2}\, \dot{\gamma}_{22}^{(\infty)\prime}(\mathbf{k}', n_1, n_2, n_3) \\
&\quad + \sum_{n_1=1}^{N_1-1} \sum_{n_3=1}^{N_3-1} \sum_{n_2=1}^{N_2-1} \int_{k_{1,n_1}}^{k_{1,n_1+1}} dk_1 \int_{k_{3,n_3}}^{k_{3,n_3+1}} dk_3 \left[\int_{k_{2,n_2}}^{k_{2,n_2+1}} dk_2 \int_{k_{2,n_2}}^{k_2} dk_2' + \int_{k_{2,n_2}}^{k_{2,n_2+1}} dk_2' \int_{k_{2,n_2+1}}^{k_{2,M_2}} dk_2 \right] \\
&\qquad\qquad \times \frac{\Psi_{12}(\mathbf{k},\mathbf{r})\, E(\mathbf{k}; k_2'; 0)\, |\mathbf{k}'|^2}{|k_1|\, |\mathbf{k}|^2}\, \dot{\gamma}_{12}^{(\infty)\prime}(\mathbf{k}', n_1, n_2, n_3) \qquad (4.78)
\end{aligned}$$

and

$$\begin{aligned}
&\int_{-\infty}^{0} dk_1 \int_{0}^{+\infty} dk_3 \int_{\mathbb{R}} dk_2\, \Psi_{11}(\mathbf{k},\mathbf{r})\, \dot{U}_{11}^{(\infty)}(\mathbf{k}) \\
&= \sum_{n_1=1}^{N_1-1} \sum_{n_3=1}^{N_3-1} \sum_{n_2=1}^{N_2-1} \int_{k_{1,n_1}}^{k_{1,n_1+1}} dk_1 \int_{k_{3,n_3}}^{k_{3,n_3+1}} dk_3 \left[\int_{k_{2,n_2}}^{k_{2,n_2+1}} dk_2 \int_{k_{2,n_2}}^{k_2} dk_2' + \int_{k_{2,n_2}}^{k_{2,n_2+1}} dk_2' \int_{k_{2,n_2+1}}^{k_{2,M_2}} dk_2 \right] \\
&\qquad\qquad \times \frac{2\,\Psi_{11}(\mathbf{k},\mathbf{r})\, E(\mathbf{k}; k_2'; 0)\, \big(F(\mathbf{k}) - F(\mathbf{k}')\big)^2\, |\mathbf{k}'|^4}{|k_1|^3\, [|k_1|^2 + (k_3)^2]^2}\, \dot{\gamma}_{22}^{(\infty)\prime}(\mathbf{k}', n_1, n_2, n_3) \\
&\quad + \sum_{n_1=1}^{N_1-1} \sum_{n_3=1}^{N_3-1} \sum_{n_2=1}^{N_2-1} \int_{k_{1,n_1}}^{k_{1,n_1+1}} dk_1 \int_{k_{3,n_3}}^{k_{3,n_3+1}} dk_3 \left[\int_{k_{2,n_2}}^{k_{2,n_2+1}} dk_2 \int_{k_{2,n_2}}^{k_2} dk_2' + \int_{k_{2,n_2}}^{k_{2,n_2+1}} dk_2' \int_{k_{2,n_2+1}}^{k_{2,M_2}} dk_2 \right] \\
&\qquad\qquad \times \frac{-2\,\Psi_{11}(\mathbf{k},\mathbf{r})\, E(\mathbf{k}; k_2'; 0)\, \big(F(\mathbf{k}) - F(\mathbf{k}')\big)\, |\mathbf{k}'|^2}{|k_1|^2\, [|k_1|^2 + (k_3)^2]}\, \dot{\gamma}_{12}^{(\infty)\prime}(\mathbf{k}', n_1, n_2, n_3) \\
&\quad + \sum_{n_1=1}^{N_1-1} \sum_{n_3=1}^{N_3-1} \sum_{n_2=1}^{N_2-1} \int_{k_{1,n_1}}^{k_{1,n_1+1}} dk_1 \int_{k_{3,n_3}}^{k_{3,n_3+1}} dk_3 \left[\int_{k_{2,n_2}}^{k_{2,n_2+1}} dk_2 \int_{k_{2,n_2}}^{k_2} dk_2' + \int_{k_{2,n_2}}^{k_{2,n_2+1}} dk_2' \int_{k_{2,n_2+1}}^{k_{2,M_2}} dk_2 \right]
\end{aligned}$$

$$\times \frac{2\,\Psi_{11}(\mathbf{k},\mathbf{r})\,E(\mathbf{k};k_2';0)}{|k_1|}\,\dot{\gamma}_{11}^{(\infty)\prime}(\mathbf{k}',n_1,n_2,n_3) \tag{4.79}$$

In the derivations of the above expressions, we have used the property of the characteristic functions to set the integral ranges and the partition of $\sum_{m_2=1}^{M_2-1} = \sum_{m_2=1}^{N_2-1} + \sum_{m_2=N_2}^{M_2-1}$. We have also employed the equality of

$$\begin{aligned}
&\sum_{m_2=2}^{N_2-1}\sum_{n_2=1}^{m_2-1}\int_{k_{1,n_1}}^{k_{1,n_1+1}} dk_1 \int_{k_{3,n_3}}^{k_{3,n_3+1}} dk_3 \int_{k_{2,m_2}}^{k_{2,m_2+1}} dk_2 \int_{k_{2,n_2}}^{k_{2,n_2+1}} dk_2' \Big[n_2\cdots\Big] \\
&= \sum_{n_2=1}^{N_2-2}\sum_{m_2=n_2+1}^{N_2-1}\int_{k_{1,n_1}}^{k_{1,n_1+1}} dk_1 \int_{k_{3,n_3}}^{k_{3,n_3+1}} dk_3 \int_{k_{2,m_2}}^{k_{2,m_2+1}} dk_2 \int_{k_{2,n_2}}^{k_{2,n_2+1}} dk_2' \Big[n_2\cdots\Big]
\end{aligned} \tag{4.80}$$

which can be proved through mathematical induction.

We employ Mathematica and the software package CUBA ([7], [8], [9]) to compute, respectively, the 1-dimensional integrals present in (4.71) through (4.73) and the 4-dimensional integrals present in (4.77) through (4.79). Specifically, we use the Mathematica function 'NIntegrate' to calculate the 1-dimensional integrals (with the default "Global Adaptive Strategy" and global error tolerance) and the CUBA algorithm 'Cuhre' to calculate the 4-dimensional integrals (with the default integration rule and accuracy). The Mathematica function 'Outer' is resorted to speed up the computations.

Matlab and the software package CVX/MOSEK ([4], [6]) are used to set up and solve the SOCP problem. Based on the above computed numerical data of the integrals, Matlab is employed to compute the coefficients of $\dot{\gamma}_{ij}^{(0)}(n_1,n_2,n_3)$ contained in the objective function and in the inequalities of (4.11) applied at the collocation points of (4.74) through (4.76). Next, CVX/MOSEK is used to set up and solve the SOCP problem (with the default tolerance levels), with $I_T^{\rm hom}(0)$ being maximized, subject to (4.70), the inequalities at the collocation points, and the global equality constraint. The constraints can be imposed selectively to test various effects.

4.5.1 Feasible Solutions

We explore feasible solutions of the SOCP problem first, since feasible solutions give us a great flexibility to select smaller supports for the control variables. From a computational perspective, such simulations can provide us useful information regarding the choice of the supports for the control and state variables and the meshes in the search of the optimal solution. Also, with the help of feasible solutions, we can resolve the issue whether $\sigma \in (0,1)$ is permissible within the second-order model. To this end, following the scheme sketched in Subsection 4.1, we adopt the supports of

$$\begin{aligned}
&\mathcal{D}_\gamma(0) = [-0.6,\,-0.3]\times[-0.2,\,0.4]\times[0.0,\,0.3], \\
&\mathcal{D}_U(0) = [-0.6,\,-0.3]\times[-0.2,\,1.8]\times[0.0,\,0.3]
\end{aligned} \tag{4.81}$$

Here, the use of $\max k_1 = -0.3$ implies that $K_0 \le |\max k_1|^2 = 0.09$ in (4.23).

In the numerical simulation, uniform mesh sizes along the directions of k_1, k_2 and k_3 are employed, respectively, to decompose the supports. Four meshes of $\mathcal{D}_\gamma(0)$ are tested which are listed in Table 4.1. The state variable support $\mathcal{D}_U(0)$ is decomposed with the same mesh

Table 4.1: Effects of $\mathcal{D}_\gamma(0)$ mesh sizes and inequality constraints on anisotropy tensor.

Test #	Mesh Elements (Size)	1D	1D & 2D & 3D
I	$3\times6\times3$ (0.1)	$(-0.2003,\ 0.0809,$ $-0.2282,\ 0.362\times10^{-3})$	NA
II	$6\times12\times6$ (0.05)	$(-0.2044,\ 0.0394,$ $-0.2133,\ 1.622\times10^{-3})$	$(-0.1889,\ 0.0471,$ $-0.2183,\ 1.239\times10^{-3})$
III	$12\times12\times6$	$(-0.2033,\ 0.0122,$ $-0.2056,\ 2.085\times10^{-3})$	$(-0.1947,\ 0.0085,$ $-0.2059,\ 1.770\times10^{-3})$
IV	$12\times24\times12$ (0.025)	$(-0.2001,\ 0.0135,$ $-0.2092,\ 2.747\times10^{-3})$	$(-0.1958,\ 0.0152,$ $-0.2110,\ 2.598\times10^{-3})$

sizes, along the k_j-directions, as those of $\mathcal{D}_\gamma(0)$. The objective $U_{kk}^{(\infty)}(\mathbf{0})$ of (4.18) is maximized, though other choices may be made. The four values in Columns 1D and 1D & 2D & 3D of the table represent, respectively, the components $b_{11}^{(\infty)}$, $b_{22}^{(\infty)}$ and $b_{12}^{(\infty)}$ of the anisotropy tensor and the turbulent fluctuation energy $U_{kk}^{(\infty)}(\mathbf{0})$. A few conclusions can be drawn from the numerical results.

1. If mesh sizes are large, only trivial solution of $\dot{\gamma}_{ij}^{(0)}(n_1, n_2, n_3) = 0$ is obtained which can satisfy all the constraints of inequality imposed. For example, in Test I the mesh sizes of $\delta k_1 = \delta k_2 = \delta k_3 = 0.1$ allow the imposition of Inequalities 1D. However, if Inequalities 2D and 3D are added, we get the trivial solution, as denoted by NA in the table. One reason is that, for the fixed support $\mathcal{D}_\gamma(0)$, larger mesh sizes lead to a less number of discrete control variables, these control variables can satisfy the number of constraints from 1D, they cannot, however, satisfy the greater number of constraints associated with 1D & 2D & 3D, without being trivial.

2. In all the four tests, we have $b_{11}^{(\infty)} < 0 < b_{22}^{(\infty)}$ or equivalently $U_{11}^{(\infty)}(\mathbf{0}) < U_{22}^{(\infty)}(\mathbf{0})$, which is incompatible with the experimental data [11]. This result can be attributed to the specific choice of $\mathcal{D}_\gamma(0)$ in (4.81), as suggested by Figure 4.3. The figure presents the contours of $\dot{\gamma}_{22}^{(\infty)}(\mathbf{k})$, $\dot{\gamma}_{12}^{(\infty)}(\mathbf{k})$ and $\dot{\gamma}_{11}^{(\infty)}(\mathbf{k})$ at the selected sections of $k_2 = -0.15$, 0, 0.1 and 0.2 in Test IV; The systematic dense contour line distributions in the subregions close to the boundaries of $k_1 = -0.3$ or $k_3 = 0.3$ indicate the great variations (normal to the boundaries) of the control variables in these subregions, since the control variables are set to zero on these two boundaries. Next, as k_2 increases, the dominant parts of the control variables shift toward the subregion close to the corner of $k_1 = -0.3$ and $k_3 = 0.3$. Thirdly, the contours at the section of $k_2 = -0.15$ are of significant values, implying the large changes the control variables undergo between the boundary of $k_2 = -0.2$ and the section. The selected boundaries of $k_1 = -0.3$, $k_2 = -0.2$ and $k_3 = 0.3$ play the role of blocking due to their smallness, as displayed in Fig. 4.3. It then follows that in the determination of the optimal solution we need to take $\max k_1$ close to 0, $\min k_2$ lower

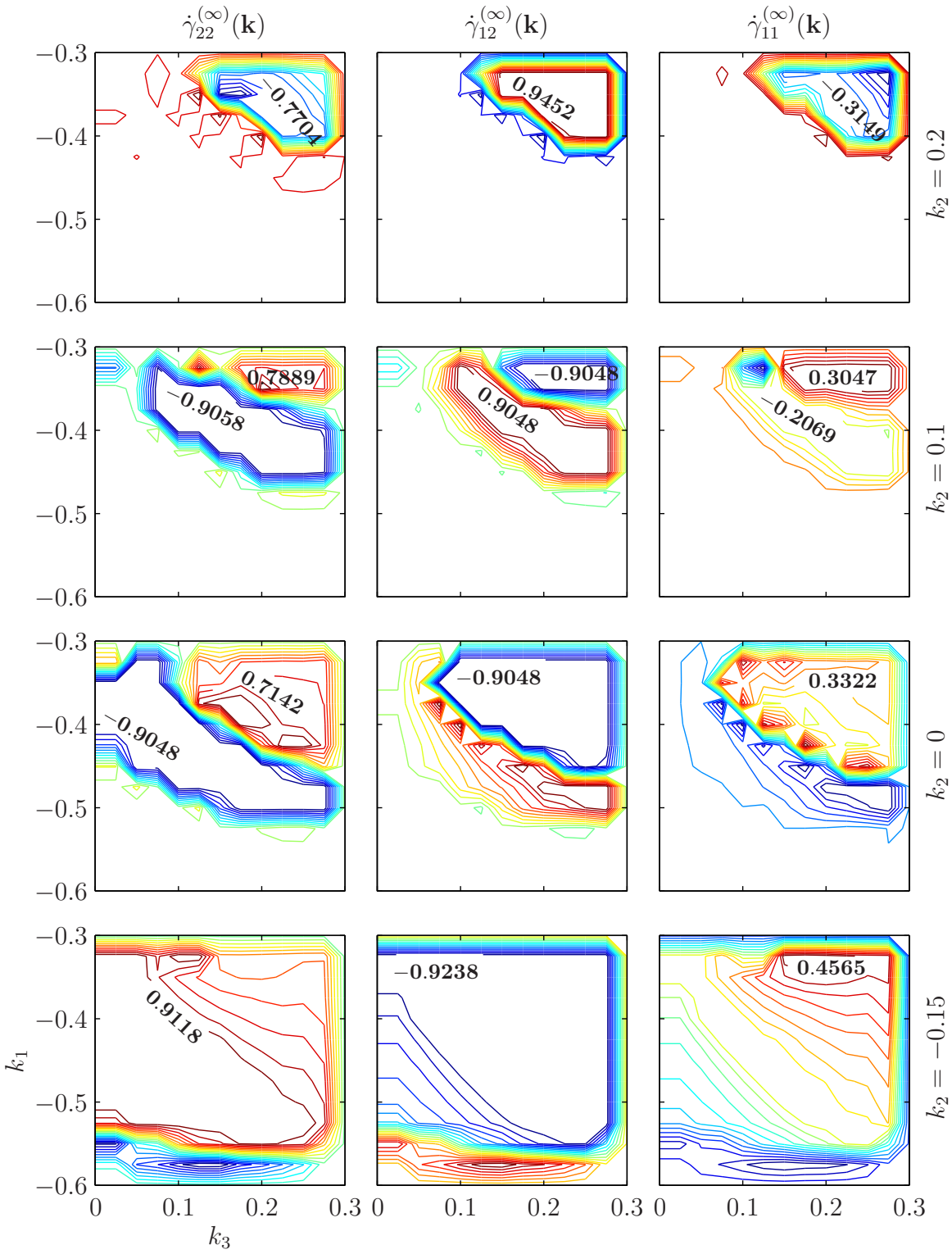

Figure 4.3: The contours of the control variables in the feasible solution at the selected sections of $k_2 = -0.15$, 0, 0.1 and 0.2 in Test IV under 1D & 2D & 3D. The four rows represent, respectively, the four sections of k_2 selected, as indicated by the right axis labels. The three columns display, respectively, the contours of $\dot{\gamma}_{22}^{(\infty)}(\mathbf{k})$, $\dot{\gamma}_{12}^{(\infty)}(\mathbf{k})$ and $\dot{\gamma}_{11}^{(\infty)}(\mathbf{k})$, as indicated by the top titles.

than -0.2, and $\max k_3$ greater than 0.3 in order to remove this blocking impact and be compatible with (4.52).

3. $\max k_2^U = 1.8$ is taken in (4.81), equivalent to $K_2 = 10$ in (4.62). This value is adequate to produce negligibly small $\left|\tilde{U}_{ij}^{(\infty)}(\mathbf{k})\right|_{k_2=K_2^U}$ and $\left|\overline{\tilde{\omega}_i\,\tilde{\omega}_j}^{(\infty)}(\mathbf{k})\right|_{k_2=K_2^U}$ in the orders of magnitude of 10^{-8} or less. This result suggests that, in the determination of the optimal solution, with an appropriate choice of $\mathcal{D}_\gamma(0)$, the coefficients of $E((k_1, K_{2U}^U, k_3); K_{2U}^\gamma; 0)$ in (4.59) through (4.61) are sufficiently small such that $K_{2U}^U = \max k_2^U$ need not be great to produce negligibly small $\left|\tilde{U}_{ij}^{(\infty)}(\mathbf{k})\right|_{k_2=K_{2U}^U}$ and $\left|\overline{\tilde{\omega}_i\,\tilde{\omega}_j}^{(\infty)}(\mathbf{k})\right|_{k_2=K_{2U}^U}$.

4. The tests imply that mesh sizes and Inequalities 2D and 3D have less impact on $b_{11}^{(\infty)}$ and $b_{12}^{(\infty)}$ than on $b_{22}^{(\infty)}$ (see Table 4.1). The turbulent energy increases as mesh sizes decrease. It is better to reduce the sizes further, say, to $24 \times 48 \times 24$ (0.0125) to have a better feasible solution for the supports of (4.81). The challenge is that it has taken seven days to run Test IV under 1D & 2D & 3D with the optimization code in Fujitsu's Celsius R570-2 Workstation.

5. Examining the values of $U_{kk}^{(\infty)}(\mathbf{0})$ listed in the table under various meshes and constraints, we notice that in the finer mesh of Test IV, the change of the objective value from 1D to 1D & 2D & 3D is 5.74%, compared with 30.9% of Test II and 17.8% of Test III. We may infer that, in the case of the finer mesh, the violation of the constraints of inequality outside the neighborhoods of the collocation points of (4.74) through (4.76) may be mild. We may further infer the existence of feasible solutions for the supports of (4.81) while σ is zero or σ has a value close to zero, say $|\sigma| < 0.09/50$ in (4.23), as argued in Subsection 4.1. We can then enlarge the specific supports of (4.81) to $\mathcal{D}_\gamma(\sigma) \supset \mathcal{D}_\gamma(0)$ and construct the feasible solutions which are identical to the above solution inside $\mathcal{D}_\gamma(0)$ and have the zero value in $\mathcal{D}_\gamma(\sigma)/\mathcal{D}_\gamma(0)$. Consequently, we have shown that the second-order model allows $\sigma > 0$ to occur.

4.5.2 Optimal Solutions

Guided by (4.52) and (4.64) and assisted with several simulation trials, we select the following supports for the control and the state variables in the search of optimal solutions,

$$\begin{aligned} \mathcal{D}_\gamma(0) &= [-0.71,\, -0.01] \times [-1.35,\, 1.25] \times [0.0,\, 0.8], \\ \mathcal{D}_U(0) &= [-0.71,\, -0.01] \times [-1.35,\, 1.65] \times [0.0,\, 0.8] \end{aligned} \tag{4.82}$$

In the numerical simulation, uniform mesh sizes along the directions of k_1, k_2 and k_3 are employed, respectively, to discretize the supports; Both supports have the same mesh size along the same direction. The mesh data of $\mathcal{D}_\gamma(0)$ and the corresponding representative data of the second order correlation of velocity fluctuations obtained are listed in Table 4.2. Specifically, the representative quantities are selected according to [11], their values are given in the third and fourth columns under two impositions of the constraints and arranged in the following order: the components $b_{11}^{(\infty)}$, $b_{22}^{(\infty)}$, $b_{33}^{(\infty)}$ and $b_{12}^{(\infty)}$ of the anisotropy tensor, the dimensionless ratio of turbulent energy over viscous dissipation ($(SK/\varepsilon)^{(\infty)} = -U_{kk}^{(\infty)}(\mathbf{0})/U_{12}^{(\infty)}(\mathbf{0})$), the dimensionless

ratio of $G = -\overline{w_i w_j}\, V_{i,j}$ over dissipation ($(G/\varepsilon)^{(\infty)} = -2\, U_{12}^{(\infty)}(\mathbf{0})/\overline{w_{j,k}\, w_{j,k}}^{(\infty)}(\mathbf{0})$) to characterize the extent of shear, and the turbulent energy ($U_{kk}^{(\infty)}(\mathbf{0})$). Here, the value of $U_{kk}^{(\infty)}(\mathbf{0})$ is included to indicate the effects of the mesh elements adopted and the constraints imposed. Also, for the purpose of comparison, the corresponding experimental data are presented in the bottom row of the table.

Table 4.2: Data from optimal solution simulations and the experiments listed in [11].

Test #	Mesh Elements (Size)	1D	1D & 2D & 3D
I	$7\times26\times8$ (0.1)	(0.3181, −0.2081, −0.1100, −0.1872, 5.343, 2.000, 3.453)	(0.3359, −0.2246, −0.1113, −0.1736, 5.762, 2.000, 2.999)
II	$14\times52\times16$ (0.05)	(0.3597, −0.2340, −0.1257, −0.1673, 5.978, 2.000, 4.929)	(0.3641, −0.2377, −0.1264, −0.1643, 6.086, 2.000, 4.807)
Experimental [11]:	$b_{11}^{(\infty)} = 0.203,\ b_{22}^{(\infty)} = -0.143,\ b_{33}^{(\infty)} = -0.06,$ $b_{12}^{(\infty)} = -0.156,\ (SK/\varepsilon)^{(\infty)} = 5.54,\ (G/\varepsilon)^{(\infty)} = 1.73$		

For the control variable and the state variable supports larger than the $\mathcal{D}_\gamma(0)$ and $\mathcal{D}_U(0)$ of (4.82), there is the concern of great number of discretized control variables and constraints to be involved under a finer mesh, because of the computing resources available. Also, the trial runs have shown the tendency that larger supports frequently lead to the problem of stall in MOSEK caused by scaling, and as a consequence, the SOCP problems are inaccurately solved to give near-optimal solutions. The adequacy of the supports in (4.82) is partially indicated by that the contours of the control variables in the tests do not display the kind severe blocking phenomenon in the subregions close to $\min k_1 = -0.71$ or $\max k_3 = 0.8$, in contrast to the case of the feasible solution presented above.

We have obtained the optimal and near-optimal solutions, respectively, under the two meshes of Test I and Test II, the associated values of the anisotropy tensor are listed in Table 4.2. We infer from the data that the values in Test II under 1D & 2D & 3D may be viewed as the representative, especially for the purpose to evaluate the limitations of the second-order model, though a finer mesh expectedly produces more accurate results, which will take much longer time to compute. It is relevant to notice that the values of the dimensionless quantities do not change significantly between Test I and Test II.

A few comparisons can be made between the computational and the experimental data. Firstly, the experimental data order of $b_{11}^{(\infty)} > 0 > b_{33}^{(\infty)} > b_{22}^{(\infty)}$ is produced in the simulations. Secondly, among the four nontrivial components of the anisotropy tensor, the calculated value of $b_{12}^{(\infty)} = -0.1643$ (Test II) is closer to the experimental value of $b_{12}^{(\infty)} = -0.156$. Thirdly, in the simulation, $(SK/\varepsilon)^{(\infty)}\, b_{12}^{(\infty)} = -1.000$ and $(G/\varepsilon)^{(\infty)} = 2.000$ are obtained, as dictated by (4.19) under $\sigma = 0$. Here, we have calculated the dissipation $\overline{w_{j,k}\, w_{j,k}}^{(\infty)}(\mathbf{0})$ and the correlation component $U_{12}^{(\infty)}(\mathbf{0})$ separately without resorting to (4.19), for the sake of partially checking the

computational adequacy of the codes. The experimental values of $(SK/\varepsilon)^{(\infty)}\, b_{12}^{(\infty)} = -0.864$ and $(G/\varepsilon)^{(\infty)} = 1.73$ may be attributed to the deviation from the asymptotic states of $\sigma = 0$ by the experiments and experimental errors. We notice that the predicted value of the anisotropy tensor $b_{ij}^{(\infty)}$ is much more anisotropic than the experimental (quantified by the extent of the component values away from zero), which may reflect the limitation of the second-order model itself — the model may catch the anisotropy caused by the mean shearing characterized by (2.1), it cannot satisfy the intrinsic constraint of equality (2.56) which plays the role of redistributing energy among the three components of $U_{\underline{ii}}^{(\infty)}(\mathbf{0})$. This constraint supposedly makes the anisotropy tensor have more isotropic values or the prediction closer to the experimental data, relative to the above results of the second-order model. Considering that the third-order model contains (2.56) and it has much less complexity and a much smaller computational size than the fourth-order model, we are carrying out the numerical simulation of the turbulence within the third-order model, in order to examine the issue further.

Acknowledgments

We thank the developer of the open-source package CUBA, and we thank CVX Research, Inc. for granting us a free academic license for CVX Professional to use MOSEK.

References

[1] P. S. Bernard and C. G. Speziale, *Bounded energy states in homogeneous turbulent shear flow - an alternative view*. ASME Journal of Fluids Engineering 114 (1992) 29-39.

[2] S. Boyd and L. Vandenberghe, *Convex Optimization*, Cambridge University Press, New York, 2004.

[3] A. J. Chorin, *Vorticity and Turbulence*, Springer-Verlag, New York, 1998.

[4] CVX Research, Inc. CVX: Matlab software for disciplined convex programming, version 2.0. http://cvxr.com/cvx, April 2011.

[5] P. A. Davidson, *Turbulence an Introduction for Scientists and Engineers*, Oxford University Press, New York, 2004.

[6] M. C. Grant and S. P. Boyd, *The CVX Users' Guide* Release 2.1. CVX Research, Inc. October 24, 2014.

[7] T. Hahn, *CUBA–a library for multidimensional numerical integration*. Computer Physics Communications 168 (2005) 78-95.

[8] T. Hahn, *The CUBA library*. Nuclear Instruments & Methods in Physics Research A559 (2006) 273-277.

[9] http://www.feynarts.de/cuba

[10] M. S. Lobo, L. Vandenderghe, S. Boyd and H. Lebret, *Applications of second-order cone programming*. Linear Algebra and its Applications 284 (1998) 193-228.

[11] J. Piquet, *Turbulent Flows. Models and Physics*, Springer, Berlin, 1999.

[12] P. Sagaut and C. Cambon, *Homogeneous Turbulence Dynamics*, Cambridge University Press, New York, 2008.

[13] L. Tao and M. Ramakrishna, *Multi-scale turbulence modelling and maximum information principle. Part 1*. arXiv:1009.1691v1 [physics.flu-dyn] 2010.

[14] L. Tao and M. Ramakrishna, *Multi-scale turbulence modelling and maximum information principle. Part 2*. arXiv:1307.4888v3 [physics.flu-dyn] 7 Jan 2014.

[15] L. Tao, *Multi-scale turbulence modelling and maximum information principle. Part 4*. arXiv:1509.06317v2 [physics.flu-dyn] 9 Dec 2015.

[16] L. Vandenberghe and S. Boyd, *Semidefinite programming*. SIAM Review 38 (1996) 49-95.

[17] J. Z. Wu, H. Y. Ma and M. D. Zhou, *Vorticity and Vortex Dynamics*. Springer, New York, 2006.